

DOCTORAL THESIS

The Roles of TIMELESS Protein and DNA Polymerase Epsilon in DNA Replication Initiation in Human Cells

Sameera Anant Vipat

TALLINN UNIVERSITY OF TECHNOLOGY
DOCTORAL THESIS
38/2025

The Roles of TIMELESS Protein and DNA Polymerase Epsilon in DNA Replication Initiation in Human Cells

SAMEERA ANANT VIPAT



TALLINN UNIVERSITY OF TECHNOLOGY
School of Science
Department of Chemistry and Biotechnology

This dissertation was accepted for the defense of the degree 06/05/2025

Supervisor: Prof Tatiana Moiseeva, PhD
Department of Chemistry and Biotechnology
Tallinn University of Technology
Tallinn, Estonia

Opponents: Prof Ivar Ilves, PhD
Faculty of Science and Technology
Institute of Technology
University of Tartu
Tartu, Estonia

Prof Logan Myler, PhD
University of Pittsburgh Medical Centre (UPMC)
Hillman Cancer Centre
University of Pittsburgh
Pittsburgh, USA

Defense of the thesis: 19/06/2025, Tallinn

Declar on:

Hereby I declare that this doctoral thesis, my original investigation and achievement, submitted for the doctoral degree at Tallinn University of Technology has not been submitted for doctoral or equivalent academic degree.

Sameera Anant Vipat

signature



European Union
European Regional
Development Fund



Investing
in your future

Copyright: Sameera Anant Vipat, 2025
ISSN 2585-6898 (publication)
ISBN 978-9916-80-309-7 (publication)
ISSN 2585-6901 (PDF)
ISBN 978-9916-80-310-3 (PDF)
DOI <https://doi.org/10.23658/taltech.38/2025>
Printed by Koopia Niini & Rauam

Vipat, S. A. (2025). *The Roles of TIMELESS Protein and DNA Polymerase Epsilon in DNA Replication Initiation in Human Cells* [TalTech Press]. <https://doi.org/10.23658/taltech.38/2025>

TALLINNA TEHNIKAÜLIKOOL
DOKTORITÖÖ
38/2025

TIMELESS valgu ja DNA polümeraas epsiloni rollid DNA replikatsiooni initsiatsioonis inimese rakkudes

SAMEERA ANANT VIPAT



Contents

List of publications	6
Author's contributions to the publications	7
Introduction	8
Abbreviations	9
1 Review of literature	10
1.1 DNA replication and its clinical relevance.....	10
1.2 DNA replication initiation and structure of the replication fork.....	11
1.3 TIMELESS protein in DNA replication.....	14
1.4 DNA polymerase epsilon and its non-catalytic regions in DNA replication	15
2 Aims of the study.....	17
3 Materials and methods.....	18
4 Results	19
4.1 Results obtained in III	19
4.2 Results obtained in I	19
4.3 Main points in II.....	19
5 Discussion	20
5.1 The role of TIMELESS protein in replication initiation	20
5.2 The non-catalytic roles of DNA polymerase epsilon domains in replication initiation	23
5.3 Future directions	25
6 Conclusions.....	27
List of figures	28
References.....	29
Acknowledgements	36
Abstract	37
Lühikokkuvõte	38
Appendix	39
Curriculum vitae	105
Elulookirjeldus.....	106

List of publications

The list of the author's publications, on the basis of which the thesis has been prepared:

- I. **S. Vipat***, D. Gupta*, S. Jonchhe*, H. Anderspuk, E. Rothenberg, and T. N. Moiseeva, '**The non-catalytic role of DNA polymerase epsilon in replication initiation in human cells**' *Nat Commun*, vol. 13, no. 1, p. 7099, Nov. 2022, doi: 10.1038/s41467-022-34911-4,
- I. **S. Vipat** and T. N. Moiseeva, '**The TIMELESS Roles in Genome Stability and Beyond**' *J Mol Biol*, vol. 436, no. 1, p. 168206, Jan. 2024, doi: 10.1016/j.jmb.2023.168206.
- II. **S. Vipat**, K. Shapovalovaite, A. Morgunov, R. Harolika, S. Vallo, T. Moiseeva, '**TIMELESS recruits the Fork Protection Complex to the replisome during DNA replication initiation in human cells**' (manuscript)

* contributed equally

Author's contributions to the publications

- I. **'The non-catalytic role of DNA polymerase epsilon in replication initiation in human cells'**
The author, SV, performed some experiments (DNA fibre analysis, cell line generation, and FACS), analyzed a part of the data, and participated in the review and editing of the manuscript.
- II. **'The TIMELESS Roles in Genome Stability and Beyond'**
The author, SV, did the literature review, and wrote the manuscript.
- III. **'TIMELESS recruits the Fork Protection Complex to the replisome during DNA replication initiation in human cells'**
The author, SV, designed and performed a majority of the experiments, analyzed the data, and wrote the manuscript.

Introduction

DNA replication is a very critical process in the cell cycle, necessary for equal distribution of the genome to daughter cells. In healthy cells, it is very tightly regulated, to ensure normal rates of cell division. In cancer, however, DNA replication is often misregulated, which is one of the factors that allows cancer cells to undergo uncontrolled cell division cycles. This is the reason why many anti-cancer therapies target DNA replication in modern times. The initiation of DNA replication is very tightly regulated, to ensure that it occurs once per round of cell division. Most studies about DNA replication have focused on model organisms like yeast and *Xenopus*, and there is a paucity of studies in the human system. A detailed mechanistic understanding of DNA replication initiation in humans, and of the functions of each protein involved, is most important in order to pave the way for devising new therapeutic strategies against cancer.

One of our two studies is focused on investigating the role of TIMELESS (TIM) protein in replication initiation in human cells. Our other study uncovers the non-catalytic role of DNA polymerase epsilon (POLE) in replication initiation in human cells. In both studies, we have employed a mini-auxin inducible degron-based strategy to create a conditional depletion system capable of rapid and complete degradation of the target protein. The presented work shows that TIM is required for efficient S phase entry, and for the loading of TIPIN, CLSPIN and PCNA during replication initiation. Additionally, our findings also show that POLE is dispensable for CMG assembly in humans, unlike in yeast. However, the non-catalytic domain of the catalytic subunit POLE1 can support very slow DNA synthesis in the absence of the full length POLE1.

The work presented in this thesis sheds light on the roles of TIM and POLE1 in DNA replication initiation in human cells. Such studies not only improve our understanding of this clinically relevant process, but also lay the foundation for developing future therapies against diseases that involve aberrant replication, such as cancer.

Abbreviations

3-IAA	Indole-3-acetic acid
5-pH-IAA	5-phenyl-indole-3-acetic acid
7-AAD	7-aminoactinomycin D
ATRi	Ataxia telangiectasia and Rad3-related protein inhibitor
aux	Auxin
CDK	Cyclin dependent kinase
CMG	CDC45-MCM-GINS complex
dox	Doxycycline
EdU	5-ethynyl-2'-deoxyuridine
FPC	Fork Protection Complex
HR	Homology regions
HU	Hydroxyurea
KI	Knock-in
mAID	Mini-auxin inducible degron
MCM	Mini-chromosome maintenance complex
ORC	Origin Recognition Complex
osTIR1	<i>Oryza sativa</i> Transport inhibitor response 1
PCNA	Proliferating-cell nuclear antigen
PIP	PCNA-interacting protein
polA	DNA polymerase alpha
POLD	DNA polymerase delta
POLE	DNA polymerase epsilon
RFC	Replication Factor C
RPA	Replication Protein A
ssDNA	Single-stranded DNA
TIM	TIMELESS protein
TIPIN	TIMELESS-interacting protein

1 Review of literature

1.1 DNA replication and its clinical relevance

DNA replication is a cellular process of generating two identical copies of the genome for their later distribution to each daughter cell during cell division. This process enables the generation of new cells from preexisting cells, and consequently the survival and propagation of the entire organism. This process must be carried out with extremely high fidelity [1] every single time, as errors occurring during DNA replication may cause DNA damage, and harmful mutations that could be inherited by the organism's offspring if such a mutation happens in germ cells [2]. Strikingly, dysregulated DNA replication [3], or somatic mutations during DNA replication [4], [5], may give rise to cancer, one of the most feared diseases that afflict mankind. Tightly controlled mechanisms are in all organisms from bacteria [6] to humans [7], [8], that ensure the fidelity and accuracy of DNA replication at every single round of cell division, as well as a single round of DNA replication per cell division.

The process of DNA replication is carried out by a large multi-protein complex known as the 'replisome.' The replisome complex assembles at the time of replication initiation, as cells transition from G1 phase to S phase of the cell cycle, at pre-marked sites in the genome called 'replication origins.' Replication is initiated from these origin sites in a process called 'origin firing.' Origin firing results in the establishment of replication forks, that then slide along DNA by unwinding the duplex, and synthesize new DNA using parental DNA strands as templates [9], [10]. The entire genome is duplicated during the S phase of the cell cycle. When converging forks meet, replication is terminated by coordinated disassembly of the replisome complex [11]. At the end of this phase, there are two full copies of the genome DNA present in cells, which marks the G2 phase of the cell cycle, with cells ready to divide. In subsequent mitosis phase the two duplicated copies of the genome are carefully distributed equally to the two daughter cells [12].

The development of an organism from conception through embryo state to adult depends upon regulated cellular division and proliferation. Failures or inadequacies in DNA replication, as happen in case of mutations in DNA replication genes, are known to be responsible for many types of developmental abnormalities or genetic diseases, as described in great details in excellent reviews [13], [14]. Meier Gorlin syndrome, characterized by dwarfism, small facial features, and hypoplasia of different tissues, and Seckel syndrome, characterized by microcephaly and mental retardation are classic examples. Other examples are conditions such as various skeletal and limb abnormalities, hypoplasia of reproductive organs, craniofacial abnormalities and short stature [14], [15], as also progeroid syndromes, characterized by accelerated ageing [16]. Recent advances in genome sequencing and whole exome sequencing are accelerating the identification of the huge repertoire of genes known to be associated with such conditions.

Mutations in replication proteins, especially in genes whose products are involved in DNA damage checkpoints and DNA repair pathways, are known to cause a heightened predisposition to cancer [17], [18], [19]. Mutations in the catalytic and proofreading domains of replicative polymerases, for instance, are known to cause mutagenesis and predisposition to cancer [20], [21], [22]. Among the different hallmarks of cancer, sustained proliferation and genomic instability are of prime importance. A variety of DNA repair and tumor suppressor mechanisms [23], [24], [25], have evolved in organisms, and have remained conserved in evolution, underlining their importance for maintaining

genomic stability and freedom from malignant transformation. Defects in DNA repair pathways cause great increases in the spontaneous mutation rate and DNA lesions [26], and this may be one of the mechanisms of how cancer arises in the first place.

Replication stress can, on the other hand, be exploited as an Achilles heel for targeting cancer cells using chemotherapy [27], [28], [29]. Different drugs that induce DNA damage [30] or compromise DNA repair pathways in cells [31], [32], are being used clinically or are being developed, as therapies against cancer. The strategy of targeting DNA replication for cancer therapy exploits the fact that cancer cells have high replication stress, are in greater need of active DNA repair pathways, and most of the times proliferate faster than normal cells, and thus aims to selectively target cancer cells and spare normal cells in the patient's body.

Interestingly, upregulation of DNA replication or repair-supportive proteins is a strategy commonly used by cancer cells to escape from drugs and continue unchecked proliferation. For instance, overexpressed TIM provides cancer cells with resistance to DNA damage-inducing drug cisplatin [33], while overexpressed CLASPIN promotes tumor progression [34]. Studies to expand our understanding of DNA replication on the molecular level are crucial to pave the way for new therapies for replication-related diseases.

1.2 DNA replication initiation and structure of the replication fork

The initiation of DNA replication is tightly controlled, to be allowed to happen once and only once per cell division. It is this step that is deregulated in many replication-related abnormalities that give rise to genome instability and even cancer [35], [36]. The process of DNA replication initiation involves a cascade of steps that begin in G1 phase of the cell cycle and lead to the entry of cells into S phase, as illustrated in Fig. 1.

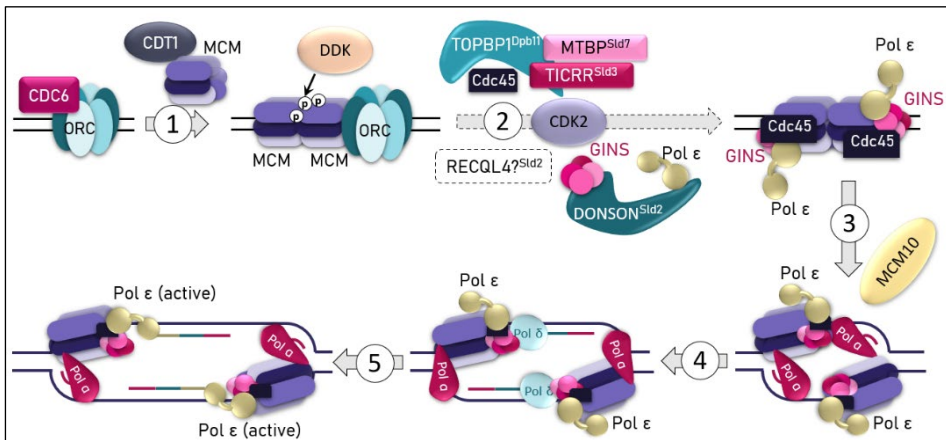


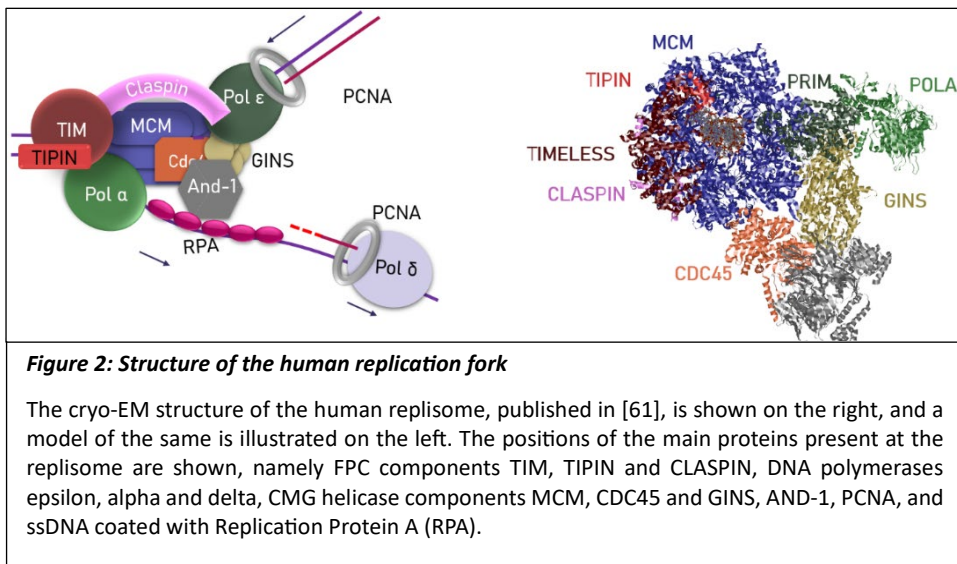
Figure 1: Steps in DNA replication initiation in human cells

Sequential steps in the process of DNA replication initiation are depicted. 1. Two MCM hexamers are loaded onto Origin Recognition complexes (ORC) present on various sites in the genome, and this step leads to the licensing of origins, some of which would fire later. 2. CDC45 and GINS load onto the MCMs, which leads to the assembly of the CMG helicase. This step requires CDK activity and the presence of accessory factors TOPBP1, TICRR, MTBP, RECQL4. After activation of CMG helicases via MCM-phosphorylation by CDC7-DBF4 kinase, the two CMG helicases begin to unwind DNA and start moving. Additionally, DONSON loads DNA polymerase epsilon to the CMG complex at this step. 3. Accessory factor MCM10 join the CMG complex, which assists in replication bubble formation and lagging strand ejection out of the CMG helicase. As the two CMG helicases continue to move, they bypass each other. Simultaneously, the DNA polymerase alpha-primase complex synthesizes RNA primers and a short stretch of DNA. 4. DNA polymerase delta joins the complex, and performs initial DNA synthesis at both the leading and the lagging strands. 5. DNA polymerase epsilon takes over the synthesis of the leading strand from DNA polymerase delta, in a 'polymerase switch' step. This leads to the establishment of two independent replication forks, moving in the opposite directions.

To begin the process of DNA replication, different positions in the genome are marked as potential replication origin sites in the G1 phase of the cell cycle, by loading of Origin Recognition Complex (ORC) [37] to these sites. Later during the course of G1 phase, the heterohexameric MCM complex, which is the primary constituent of the helicase complex that would later unwind DNA to begin DNA replication, loads to these ORC complexes [38], [39]. Two copies of the MCM hexamer meet each other on DNA as MCMs slide along DNA [39]. MCM loading 'licenses' origins so that they can be later activated for initiating replication. Many more origins are licensed during G1 phase than would actually fire later during replication initiation; cells keep a surplus of extra origins which would serve as alternative origins that would fire in case of replication stress [40]. A portion of the licensed origins fire to initiate replication, which marks the beginning of S phase. For origin firing, two critical proteins, CDC45 and GINS, are recruited to each of the two MCM hexamers positioned on DNA next to each other [41], [42]. MCM, CDC45 and GINS together form the active CMG helicase, capable of unwinding the two parental strands of DNA so that new daughter DNA strands can be synthesized on each parental

strand. Kinases CDC7-DBF4 (together known as DDK), CDK2 and CDK1 are important for CMG assembly in humans, their actions are reviewed in [43]. Additionally, accessory factors TOPBP1, Treslin, DUE-B and MTBP are required for CMG assembly in humans [44], [45], [46], [47], [48], reviewed in [43]. DNA polymerase epsilon, the leading strand DNA polymerase, is loaded at the same time as CMG assembly [49], [50], and in yeast also assists GINS loading [51].

CMG helicase is then activated and stabilized by phosphorylations of MCM by DDK and CDK2 kinases [41]. CMG assembly and phosphorylations activate the helicase and provide the stimulus for untwisting of the DNA double helix, to begin the process of DNA melting and separation of the two DNA strands [52]. After helicase activation, the accessory factor MCM10 loads to the CMG complex. The subsequent steps are not well understood in humans, and most of our understanding comes from yeast studies. Presumably, replication bubble formation due to separation of parental DNA strands is going on simultaneously, and MCM-10 assists the CMG helicase in ejecting the lagging strand from its pore. After this, each of the two CMG helicase molecules sits on one of the two parental strands, which becomes the respective leading strand for that CMG. The DNA polymerase alpha (polA)-primase complex also loads at this time, leading to the assembly of the full replisome [53]. RNA primers are synthesized by primase, to which PolA adds the first short stretch of DNA.



PCNA, the ring shaped molecule that encircles polymerases and ensures their processivity, is then loaded by Replication Factor C (RFC) onto these template-primer 3' end sites [54]. PCNA loading stimulates the loading of DNA polymerase delta (POLD) [55] [56], the main lagging strand polymerase. DNA polymerase delta takes over DNA synthesis from DNA polymerase alpha at each Okazaki fragment. The two CMG complexes start sliding towards each other and eventually bypass each other, which marks the beginning of two independent replication forks. As the CMG complexes move past one another, the initial DNA synthesis on both leading and lagging strands is performed by DNA polymerase delta [57]. DNA polymerase epsilon (POLE), the main leading strand DNA polymerase, which is already loaded at the time of CMG assembly,

then takes over leading strand DNA synthesis from DNA polymerase delta [58], in a 'polymerase switch' step. After this point of full replisome assembly, two replication forks, sliding away from each other, moving in opposite directions, are established, and the elongation phase of replication commences. Fig. 1 depicts the process of DNA replication initiation in humans, as per our current understanding, and Fig. 2 depicts the structure of the fully assembled replisome at the fork, based on recent structural studies [59], [60], [61].

Cancer cells initiate considerably more replication cycles compared to most normal cells in the body, and so the process of replication initiation is an attractive target for chemotherapy. This is also the reason why more studies are urgently needed to expand our understanding of the mechanistic details of the process of replication initiation in humans.

1.3 TIMELESS protein in DNA replication

TIMELESS protein (TIM) was initially discovered in *Drosophila*, named dTIM in *Drosophila*, where studies focused on its role in maintaining the rhythm of the circadian clock in flies. Mammalian TIM is functionally more similar to a homolog of dTIM found in flies – TIMEOUT [62]. TIM in mammals has well recognized roles in maintaining the integrity of the genome under conditions of replication stress or DNA damage, and loss of TIM causes severe replication stress [63].

TIM performs its replication-related roles in concert with its obligate binding partner TIPIN [63], [64]. TIM-TIPIN, together with a third replication-protective protein, CLASPIN, constitute the Fork Protection Complex (FPC) [65]. The FPC is believed, based on structural studies, to be positioned at the leading edge of the replication fork, ahead of MCM in the CMG helicase, and binding to and gripping the DNA double helix [59]. However, TIM-TIPIN are also revealed by biochemical studies to bind to and stimulate the activities of DNA polymerase epsilon [66], although it is hard to imagine how TIM which is positioned ahead of MCM could interact with DNA polymerase epsilon located behind MCM (Fig.2) Our study exploring the roles of TIM in supporting replication initiation, a part of this thesis, sheds some light on this enigma. TIM has mainly been studied in the context of protection of fork integrity at times when the fork has to move through genomic barriers, either intrinsic barriers such as G quadruplex regions, or extrinsic DNA lesions caused by genotoxic agents [67]. It is also known to sense DNA damage and engage cell cycle checkpoint pathways, such as the ATM pathway [68] and the ATR pathway [69]. The roles of TIM-TIPIN in protecting normal replication as well as replication under stress are reviewed in our recent review [70], a part of this thesis.

Much less is known about the possible role of TIM in supporting the initiation of DNA replication. Depletion of TIM is known to cause a defect in S phase entry, reducing the percentage of cells being able to successfully transition from G1 phase into S [71]. This indicates that TIM plays a role in this transition, or specifically, in DNA replication initiation. Exactly what role TIM plays in the cascade of origin firing has hardly been explored before, to the best of our knowledge. It has only been reported that loss of TIM leads to a shortened intra-origin distances in asynchronous cells, which is indicative of excessive origin firing [72], and is likely the consequence of slower replication forks.

Interestingly, overexpression of TIM is known to contribute to resistance of cancer cells to anti-cancer drugs. TIM upregulation in cancer cells results in their resistance to cisplatin, a DNA-damaging anti-cancer drug [73], [33]. The molecular mechanism behind this is as yet unestablished, but is presumably connected to TIM's role in protecting DNA

from extrinsic damage. Overexpression of TIM is associated with greater survival, proliferation and metastasis of cancer cells [74], as well as loss of differentiation of cells of different tissues [75].

Many details about TIM loading and role during replication initiation are not clearly understood. Firstly, its role in promoting S phase entry, and what step in replication initiation it may support, is not well studied. Secondly, at what point during origin firing TIM loads to DNA has hardly been investigated. Lastly, TIM's canonical position at the leading edge of the fork does not align with its biochemically observed function of coupling helicase and polymerase activities by physical interaction with both. Therefore, TIM's exact position at the fork needs to be investigated in more depth, especially in cell-based studies. Our study about the role of TIM in replication initiation, a part of this thesis, sheds some light on these questions.

1.4 DNA polymerase epsilon and its non-catalytic regions in DNA replication

DNA polymerase epsilon synthesizes DNA at the leading strand of the replication fork. This polymerase is one of the most accurate DNA polymerases in the cell for single base pair errors, due to its high intrinsic base selectivity [76]. Its exonuclease domain provides additional proofreading activity. However, it is not completely immune to making errors, and as expected, errors made by a DNA polymerase lead to mutations. Interestingly, in many forms of cancer, DNA polymerase epsilon is found to have mutations in its proofreading domain, which makes it error-prone, and causes a high number of mutations during DNA replication, known as 'ultramutation' [20].

Insufficiencies in this polymerase are found to cause syndromes characterized by hypoplasia of different tissues, immune insufficiency, adrenal dysfunction, genitourinary abnormalities and other signs characteristic of deficiencies of DNA replication-critical factors [77], [78], [79]. Mutations in the catalytic domain of the polymerase are relatively well studied, since they are associated with cancer-linked ultramutagenesis [20], however, consequences of mutations in the non-catalytic domain have not been widely explored, as they appear rarely in cancer cases. As with TIM, overexpression of DNA polymerase epsilon has been found to promote tumor progression in cancer [80].

DNA polymerase epsilon is a multisubunit complex comprising of four subunits: the catalytic subunit POLE1 in humans (pol2 in yeast), and three other subunits POLE2 (dpb2 in yeast), POLE3 (dpb3 in yeast) and POLE4 (dpb4 in yeast) [81], [82]. During replication initiation, DNA polymerase epsilon takes over leading strand DNA synthesis from DNA polymerase delta after initial DNA synthesis by POLD, as per findings in yeast [53], and then it functions as the main leading strand DNA polymerase in both yeast and humans. Both PCNA and the FPC are known to stimulate the its polymerase activity [66], [83], [84].

DNA polymerase epsilon is believed to have important non-catalytic functions in addition to its catalytic function during leading strand DNA synthesis. In yeast, DNA polymerase epsilon loads at the origins during the step of CMG assembly, and is essential for the loading of GINS [51]. In humans, however, the dependance of GINS loading on DNA polymerase epsilon has not been studied to the best of our knowledge. Moreover, DNA polymerase epsilon also functions to directly activate CMG helicase during origin firing, in yeast [85], and human studies about this function are lacking. The N-terminal catalytic domain of the catalytic subunit (POLE1 / pol2) of DNA polymerase epsilon is

dispensable for survival in yeast, but the C-terminal non-catalytic domain is essential [86]. The exact role of the non-catalytic domain has remained more enigmatic, in both yeast and humans. It is believed that this domain mediates interaction of the catalytic subunit with another subunit of the polymerase, POLE2. Our work on the role of the non-catalytic domain of POLE1 in humans, a part of this thesis, sheds some light on its function in replication initiation.

2 Aims of the study

The aim of the work performed in this doctoral thesis was to investigate the details of the roles of critical replication proteins TIMELESS and DNA polymerase epsilon in the process of DNA replication initiation. Specifically, the aims were as follows:

- To understand the role of TIMELESS protein in DNA replication initiation in human cells.
- To understand the non-catalytic role of DNA polymerase epsilon in DNA replication initiation in human cells, with emphasis on the role played by the C-terminal non-catalytic domain of subunit POLE1.
- To provide a comprehensive review of the roles played by TIMELESS protein in genome maintenance and various other cellular processes.

3 Materials and methods

The following methods were used in our studies, and are described in detail in our publication I and manuscript III:

- Molecular cloning (PCR- restriction enzyme-based and Gibson Assembly-based) – (I and III)
- Western blotting – (I and III)
- CRISPR-based homology-directed *knock-in* – (I and III)
- Mammalian cell culture – (I and III)
- Transfection – (I and III)
- Cell line generation with single cell cloning – (I and III)
- DNA fiber analysis and immunofluorescence-based staining – (I)
- Flow cytometry – (I and III)
- Protein mutant design – (I and III)
- Cell lysis, fractionation, insoluble chromatin isolation – (I and III)
- Cell synchronization – (I and III)

4 Results

4.1 Results obtained in III

‘TIMELESS recruits the Fork Protection Complex to the replisome during DNA replication initiation in human cells’

- TIMELESS (TIM) is required for normal S phase entry in human cells.
- TIM recruits TIPIN and CLASPIN to chromatin during replication initiation.
- The presence of TIM in G2 phase/mitosis is required for PCNA loading to chromatin at S phase entry.
- TIM, TIPIN and CLASPIN load to chromatin during replication initiation partially at the time of CMG assembly, and partially after DNA synthesis begins. Their loading partially depends on the activity of kinases CDK1, CDK2 and CDC7.
- TIM-MCM interaction is required for TIM, TIPIN and CLASPIN recruitment to chromatin during replication initiation.

4.2 Results obtained in I

‘The non-catalytic role of DNA polymerase epsilon in replication initiation in human cells’

- DNA polymerase epsilon (POLE) is not required for CMG assembly in human cells.
- In the absence of POLE1 catalytic domain, the C-terminal non-catalytic domain of POLE1 can support very slow forks.
- The POLE1 non-catalytic domain performs this function via its interaction with subunit POLE2.

4.3 Main points in II

‘The TIMELESS Roles in Genome Stability and Beyond’

- TIM is required to protect the integrity of DNA replication forks. It protects forks both under extrinsic replication stress and under normal replication conditions.
- TIM, as part of the Fork Protection Complex, plays critical roles in the repair of damaged DNA. It detects DNA damage and engages checkpoint responses and DNA repair pathways at damaged regions of the genome.
- TIM is also involved in multiple cellular processes other than DNA replication and repair, such as sister chromatid cohesion, mitosis, meiosis, recombination, transcription, and maintenance of circadian rhythm, among others.
- Upregulation of TIM is a strategy used by many different forms of cancer, and it is protumorigenic. It also confers upon cancer cells resistance to genotoxic cancer drugs.
- The molecular mechanisms behind TIM’s various functions are not well understood, and more studies need to focus on this.

5 Discussion

5.1 The role of TIMELESS protein in replication initiation

Most previous studies have focused on the role of FPC components in protecting forks from disintegration when faced with stressed DNA regions, or difficult-to-pass barrier regions in DNA. Not many studies have been devoted to the roles of the FPC in maintaining normal DNA replication under unstressed conditions, and even lesser efforts have been devoted to understanding their role at the step of replication initiation, a step very relevant for cancer as deregulation of this step is known to alter the frequency of replication.

Our work has explored the role of TIMELESS protein in the initiation of DNA replication in human cells. To study this, we have made use of a rapid and conditional TIM-depleting system, the mini-auxin inducible degron system [87], [88]. This system enabled us to deplete TIM in human cells to near-complete levels, and study the consequences of loss of TIM for replication initiation. The findings presented in this thesis show that the efficiency of S phase entry is compromised upon loss of TIM, with a higher proportion of cells being trapped in G1 phase and unable to transition into S phase, compared to control having normal levels of TIM. This indicated to us that a critical step in the initiation of DNA replication, which marks the beginning of S phase, could require the presence of TIM.

Replication initiation is in essence a cascade of steps, going from initial marking of replication origin sites on DNA, to assembly and activation of the CMG replicative helicase, to loading of leading and lagging strand polymerases and accessory factors, up to the establishment of two full replisomes sliding on DNA in opposite directions to synthesize daughter strands (illustrated in Fig. 1). To better understand what step in this replication initiation cascade might be supported by TIM, we studied the loading of replication initiation-critical proteins to chromatin in the absence of TIM. The presented data suggest that other components of the Fork Protection Complex, CLASPIN and TIPIN, are unable to load to chromatin in the absence of TIM. TIM is required for the loading of these two components, irrespective of whether their cellular levels are reduced or unaffected, indicating that TIM actually recruits, or at least stabilizes, these two proteins onto DNA during replication initiation. TIPIN is the obligate binding partner of TIM and interacts with TIM throughout S phase [72], so we believe that TIPIN may load to DNA bound to TIM. Whether TIM recruits CLASPIN to origins by physical association or whether it only stabilizes it in place as Claspin joins later, is not fully clear. We are inclined to think that CLASPIN may load to DNA after TIM, and simply be held in place by its TIM/TIPIN interaction. This is because, chromatin association of CLASPIN is known to increase specifically under replication stress, and TIM/TIPIN depletion affects CLASPIN loading, but CLASPIN depletion does not affect TIM/TIPIN loading [72], indicating that TIM-TIPIN loading may be independent of CLASPIN. Interestingly, it may be TIPIN rather than TIM that is required for CLASPIN loading [72], and the current work could not distinguish this as our system depletes both TIM and TIPIN.

Interestingly, our findings show that prolonged TIM depletion from G2 phase of the cell cycle as in our mAID1 TIM depletion system, but not a shorter TIM depletion from mid-G1 phase of the cell cycle as in our mAID2 system, delays the loading of polymerase processivity factor PCNA to chromatin during replication initiation. In mAID1, PCNA was found to load normally despite the absence of loaded TIM, TIPIN and CLASPIN. It has been reported that upon prolonged loss of TIM, levels of replication inhibitor p21 in the cell

rise, and cause a delay in CMG assembly [71]. Although no delay in CMG assembly was observed in our results, it is possible that an increase in p21 had other effects in our system. p21 has been shown to inhibit the loading of PCNA to DNA and its replication-supportive function [89], [90], [88]. We speculate that increased levels of p21 may be responsible for the PCNA loading defect in our mAID1 system. CLASPIN has a PIP-binding motif, and interacts with PCNA to support growth and DNA synthesis in cells [91]. TIM-TIPIN are also known to directly bind PCNA [92], [93]. Since the loss of these proteins on chromatin in our mAID2 system does not abrogate PCNA loading, we believe that these proteins may not be required for PCNA loading, but may only stabilize PCNA at the fork once it is loaded. If they are absent, one of PCNA's many other PIP-containing partners (such as CDC45) may perform the same function. This would explain the delay but not complete abrogation of PCNA loading in our case.

Details about the timing of loading of TIM/TIPIN and CLASPIN to chromatin have remained enigmatic so far. To understand the exact role of FPC components in replication initiation, it is imperative that we first have a clear understanding of when these proteins load to chromatin during replication initiation, and what processes are required for their loading. The only detail previously known about the timing of TIM loading is that it is recruited to chromatin at the same time as CDC45 [94]. The current work studied whether the loading of FPC proteins requires the activities of kinases CDK2, CDK1 and CDC7, and found that it only partially depends on their activities, and inhibition of these kinases suppresses S phase entry of cells. We propose that only a subset of FPC molecules require the activities of these kinases, and the rest may load independently of these kinases. However, more studies are necessary to elucidate this possibility, and to understand how this distinction is made at the molecular level. The presented findings, however, show that a combination treatment of CDK1 inhibitor + CDC7 inhibitor, which also completely abrogates CMG assembly, completely inhibits the loading of FPC proteins during replication initiation. This is interesting, as at the time of CMG assembly, the canonical position of TIM ahead of CMG helicase is not available, and two CMG helicases are positioned next to each other and facing each other with no space between them. And yet, loading of TIM at this time is observed in our experiments. At the moment, exactly what triggers the loading of FPC proteins cannot be pinpointed, as it is not entirely clear what roles each of these kinases play in human cells. Interestingly, the presented work found that the loading of FPC proteins also partially depends on DNA synthesis, as treatment with aphidicolin partially blocked the loading of these proteins with no effect on CDC45 recruitment. But the current work also separately showed that FPC proteins load at the same time as CMG assembly. Taken together, these observations suggest that during replication initiation, some molecules of FPC may load at the time of CMG assembly, and other molecules may load after DNA synthesis commences. Further investigations are necessary to understand how different FPC molecules may make this distinction of when to load. Ideally, future work should focus on elucidating exactly how many copies of FPC proteins are present per replication fork.

The canonical position of TIM ahead of the fork, bound to MCM and gripping DNA, as uncovered by structural studies (illustrated in Fig. 2), is inconsistent with its position indicated by biochemical studies, interacting with both MCM and polymerase epsilon. Structural studies sometimes do not align with actual events happening inside living cells, and may miss important interactions, especially those that involve difficult to crystallize protein complexes. The presented work was able to uncover some details of where TIM may actually be positioned at the fork *in cellulo*, and also where any additional molecules

of TIM, as predicted by our chromatin-binding studies, may be located at the fork. Using a split-Turbo ID based proximity labelling strategy, we identified that TIM is positioned in close proximity of TIPIN, CLASPIN, CHK1, CDC45, and DNA polymerases alpha and delta, suggesting some molecules of TIM may be located on the lagging strand, as illustrated in Fig. 3, also presented in our manuscript 1. TIM in its canonical position would be too far to interact with ORC6 which is present behind the fork where it functions in mismatch repair, and AND-1 which is present near polymerase epsilon, and this supports our belief that additional molecules of TIM would be associated with the lagging strand. As expected, two molecules of TIM were observed to come in close proximity to each other enough to biotinylate the above proteins, further supporting our proposition that there are additional molecules of TIM present at the fork, although at this point we do not exclude the possibility that this signal could come from TIMs present on two different forks. Future work should focus on stoichiometric studies to clarify how many molecules of TIM are present per replication fork.

Lastly, the current work presents studies on the significance of TIM-MCM interaction for TIM's ability to play a role in the initiation of DNA replication. TIM has been reported to interact with MCM not just at the beginning of S phase, but throughout all phases of the cell cycle [71]. We thus expected TIM to load at the same time as MCM, but the data from chromatin loading studies showed that TIM is recruited to chromatin after MCM loading. However, interaction with MCM was found to be critical for TIM chromatin loading, as a mutant of TIM whose interaction with MCM was abrogated, TIM-M*, was found to be unable to load to chromatin. These data suggest that TIM loads after MCM loading, by MCM interaction, and this interaction is critical for replication initiation. Indeed, the presented work illustrates that the expression of the TIM-M* mutant is unable to rescue the replication initiation defect of TIM-depleting cells. Cell lines expressing the TIM-M* mutant under the doxycycline-inducible promoter, generated on the background of our mAID1 TIM-depleting cell lines, were employed to study this. A concentration of doxycycline that did not deplete wt TIM but at the same time induced TIM-M* to levels comparable to the endogenous wild type TIM levels was used in these cells. The presence of TIM-M* mutant could not support the loading of CLASPIN, TIPIN and even PCNA in these cells, pointing towards a possible dominant negative effect of this mutant. Then, a concentration of doxycycline that completely depleted TIM-mAID-mCherry and expressed TIM-M* to high levels in cells was used. It was found that in spite of its high levels, the TIM-M* mutant could not rescue the defect in S phase entry in TIM-depleted cells. These findings underscore the importance of TIM-MCM interaction for its role in supporting replication initiation in human cells. A model of TIM's position and loading dynamics at the replication fork, based on our data, is illustrated in Fig. 3.

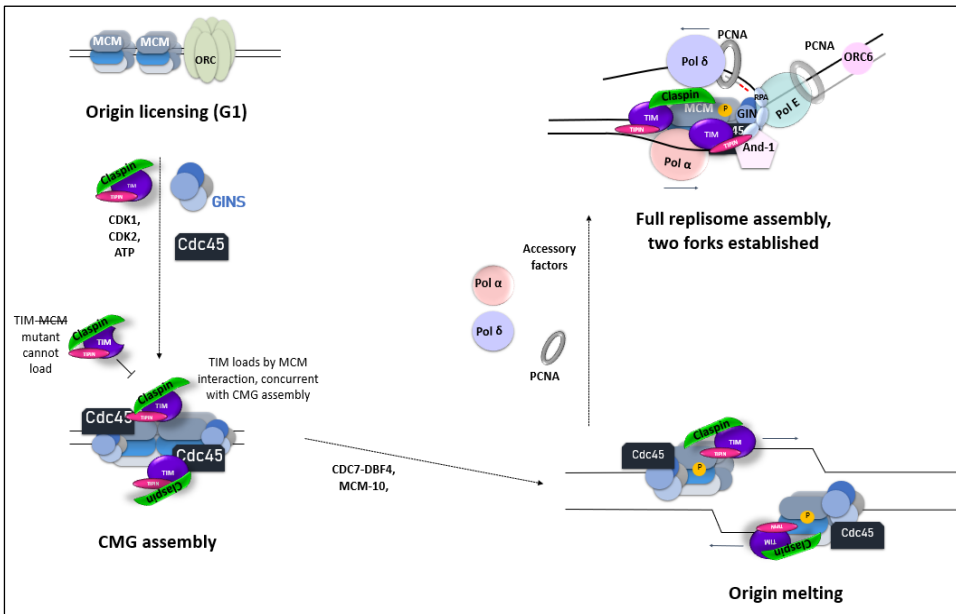


Figure 3: Proposed model of TIM position and loading dynamics at the replication fork

A model depicting the dynamics of loading of FPC components TIM, TIPIN and CLASPIN during the process of DNA replication initiation is shown, as suggested by our data. TIM, TIPIN and CLASPIN load to chromatin concurrently with the step of CMG assembly. FPC loading requires TIM-MCM interaction, and the inability to load of a TIM mutant unable to interact with MCM is indicated. As the canonical position of TIM at the leading edge of the CMG helicase becomes available after CMG bypass, the FPC is stabilized at this position by gripping DNA. Some molecules of TIM, TIPIN and Claspin are dependant on DNA synthesis, and are loaded after the establishment of the full replisome and the beginning of DNA synthesis. These molecules are positioned on the flexible lagging strand.

Overall, our studies show that TIM supports replication initiation in human cells by supporting the loading of other FPC components CLASPIN and TIPIN, and polymerase processivity factor PCNA to DNA during origin firing. TIM's interaction with MCM is critical for its role in replication initiation. The work presented in this thesis also provides evidence for the first time that more than one molecule of TIM may be present at the replication fork, and some molecules of TIM may load concurrently with CMG assembly and others, after the commencement of DNA synthesis.

5.2 The non-catalytic roles of DNA polymerase epsilon domains in replication initiation

DNA polymerase epsilon (POLE) is the leading strand DNA polymerase during DNA replication, and is positioned at the replication fork behind the MCM helicase on the leading strand (illustrated in Fig. 2). The role and catalytic activity of polymerase epsilon, conferred upon it by its catalytic subunit POLE1, have been very well studied in yeast as well as in humans. POLE additionally has important non-catalytic roles during DNA replication in yeast, including the recruitment of GINS during CMG assembly [51].

Structurally, it is the N-terminal catalytic domain of the catalytic subunit POLE1 of DNA polymerase epsilon that performs the catalysis during leading strand DNA synthesis. The smaller C-terminal domain of POLE1, which does not have any known catalytic activity, is very poorly studied, especially in human cells. In yeast, the catalytic domain is known to be dispensable for survival [86], [95], however the non-catalytic domain is required for survival and is able to support the assembly of a full but inefficient and error-prone replisome [96], [97], [98], [99], a fact underscores the importance of exploring the mechanistic details of the function of this domain. This also indicates that it is actually the non-catalytic function(s) of POLE that makes it an essential protein in cells. The non-catalytic domain of Pol2 in yeast not only supports the catalytic activity of DNA polymerase epsilon, but is also thought to play a role in replisome assembly [96]. Our studies explore and illuminate the role of this non-catalytic domain of POLE1 specifically, as well the non-catalytic roles performed by POLE holoenzyme in general, during the process of replication initiation in human cells.

The work presented in this thesis employed a conditional POLE-depleting system based on the mini-auxin inducible system (mAID1) [87], which allowed us to study the process of replication initiation with near-complete depletion of POLE in human cells. Contrary to observations in yeast, our work found that the absence of POLE does not affect CMG assembly (as judged by CDC45 and GINS loading in our chromatin protein loading experiments) or CMG activation (as judged by MCM hyperphosphorylation and the accumulation of ssDNA) in human cells. Importantly, GINS, which is recruited for CMG assembly by POLE in yeast, was found to load to chromatin during CMG assembly even in the absence of POLE in human cells. Furthermore, the current work shows using single molecule microscopy techniques that the absence of POLE does not actually lead to the disintegration of the assembled CMG, and MCM once loaded to DNA does not unload from DNA if POLE is absent. In short, our findings illustrate that unlike in yeast, POLE is not required for CMG assembly in humans. These findings highlight surprising evolutionary differences between lower eukaryotes and higher eukaryotes in highly conserved processes such as DNA replication, as systems evolve by exaptation of new roles by some proteins and loss of previous roles by other proteins.

The current work studied the effect of POLE depletion on the ability of cells to synthesize DNA, and it was found that loss of POLE slows down DNA synthesis at least 18–21 times compared to having normal levels of POLE. This is not surprising given the vital role of POLE in leading strand DNA synthesis during replication. Using mass spectrometry experiments to quantify levels of replication initiation proteins near newly synthesized DNA (IPOND-mass spectrometry, [100]), the presented work shows that levels of DNA polymerase delta (POLD) were at newly synthesized DNA were unaffected by loss of POLE. We speculate that in the absence of POLE, POLD may perform DNA synthesis at both leading and lagging strands, which presumably fails shortly after, at the time of expected POLD to POLE switch.

The presented work was aimed at studying what the essential role of the non-catalytic subunit of POLE1 might be in humans. To this end, we generated several truncation mutants of POLE holoenzyme, and studied their ability to rescue the replication defect of POLE-depleted cells, in order to pinpoint which regions of POLE are responsible for its role in supporting replication and replication initiation. As expected, expression of full length wild type POLE led to a full rescue of DNA synthesis in POLE-depleted cells, as judged by EdU-incorporation FACS studies. Expression of the mutant containing only the catalytic domain of POLE was unable to rescue the defect in DNA synthesis.

The expression of either the dcat mutant (a mutant containing only the C-terminal non-catalytic domain) or a catalytically dead mutant of POLE, however, was able to support a low-level DNA synthesis. Such an observation has been previously reported in yeast [97]. By generating and using cell lines stably expressing the dcat mutant on the background of our POLE-depleting cell lines, we studied the mechanism behind this low-level DNA synthesis. The presented DNA fibre analysis data indicate that this low-level DNA synthesis actually represents very slow-moving forks, which we estimated to be around 18-21 times slower than normal forks. Interestingly, the expression of the dcat/dzf mutant (mutant containing the non-catalytic domain but lacking the C-terminal-most zinc finger motifs responsible for the interaction of POLE1 with subunit POLE2) was unable to support such a low-level DNA synthesis. This indicates that the rescue in DNA synthesis and slow-moving forks supported by the non-catalytic subunit of POLE is done by its interaction with POLE2.

Our results support a model where POLE is dispensable for CMG assembly, but its absence leads to a failure of replication initiation at the step of POLE to POLD switch and processive DNA synthesis. The non-catalytic domain of POLE is necessary for maintaining normal speed of replication forks.

5.3 Future directions

The work presented in thesis shows that TIM is required for S phase entry and for loading of CLASPIN and TIPIN to DNA during replication initiation. It remains to be seen whether TIPIN and/or CLASPIN have roles to play in S phase entry as well. TIPIN depletion has been shown to negatively affect the ability of cells to continue replication under stressed conditions [72], however its role in supporting normal replication has not been studied, to the best of our knowledge. Although TIM and TIPIN perform most of their roles bound to each other as obligate partners, it is very likely that the smaller TIPIN has some specific roles to play that cannot be played by TIM alone. Such a possibility can be assessed using a conditional TIPIN depletion system.

CLASPIN is known to recruit CDC7 kinase necessary for MCM phosphorylation and CMG helicase activation during replication initiation [91]. Whether CLASPIN plays a role in any other steps of replication initiation remains a mystery. The current work also provides evidence that PCNA loading is delayed upon TIM depletion, and we believe that it may be CLASPIN rather than TIM that stabilizes PCNA on chromatin, via its PCNA-interacting PIP motif. Studies using a CLASPIN conditional depletion system and a PIP-deleted mutant of CLASPIN reported earlier [91], would help to uncover such a role. The mechanistic details of how components of the FPC promote PCNA recruitment remain an open question, and detailed investigations are necessary to understand such a significant role of the FPC. It is also possible in theory that it is not CLASPIN but TIM-TIPIN, whose additional molecules present on the lagging strand bind and stabilize PCNA at forks. Direct interaction between TIM and PCNA has not been reported, and such a possibility needs to be investigated further.

Our proposed model of the presence of more than one TIM molecule at the replication fork needs to be confirmed with stoichiometric studies. We think that the additional molecule(s) of TIM that were detected at replication forks may be bound at the lagging strand via the interaction of TIPIN with RPA on ssDNA. In such a case, TIPIN depletion should abrogate the binding of additional molecules of TIM at forks. Such a possibility can be assessed using a TIPIN depletion system. The presented work also shows that CLASPIN loads during replication initiation with the same dynamics as TIM-TIPIN. It is

unclear whether the additional molecules of TIM that we detected also have CLASPIN with them, forming the full FPC, or not, and this would be interesting to know.

A question the current work has not answered is, how does TIM recruit CLASPIN to DNA? It is known that TIPIN bound to RPA on ssDNA is responsible for recruiting CLASPIN [101] during replication stress. Does TIPIN also recruit CLASPIN during normal conditions? Studies using a TIPIN depletion system would shed light on this. Do TIM-TIPIN interact with CLASPIN before S phase and physically bring it to DNA at replication initiation, or does CLASPIN load on its own and is simply stabilized on chromatin by TIPIN interaction? We are inclined to believe the latter, as CLASPIN loading is specifically known to increase under stress, however, more direct studies are necessary to answer this question. CLASPIN is also bound to TIM at the fork, and is presumably additionally stabilized by this interaction. What region(s) in TIM are responsible for CLASPIN binding is not well studied, however the converse (regions of CLASPIN important for TIM interaction) has been studied [91]. More studies are necessary to understand the roles played by different domains in the TIM protein.

An important question, that has hardly been acknowledged in the literature, is how is TIM recruited to DNA during replication initiation? TIM has been shown to interact with MCM throughout the cell cycle, however, our findings show that TIM loading during replication initiation happens after MCM loading. The presented work shows that TIM, TIPIN and CLASPIN load to chromatin with the same dynamics, and although TIM-TIPIN are bound together throughout the cell cycle, the findings have not excluded the possibility that the loading of these proteins during replication initiation is concurrent but independent. There is evidence to suggest that TIM to DNA is recruited by TIPIN [102] and PARP-1 [103] (in this case TIM is not bound to TIPIN) during replication stress. Urgent studies are needed to explore how TIM is loaded to DNA during replication initiation in case of normal unstressed replication.

The work presented in this thesis shows that DNA polymerase epsilon is necessary for steps of replication initiation occurring after CMG assembly, and that the non-catalytic domain of catalytic subunit POLE1 is necessary for maintaining normal fork speed during replication. The non-catalytic domain can support very slow forks in the absence of the catalytic subunit, via its C-terminal zinc finger motifs, which mediate its interaction with subunit POLE2. The exact details of the role played by this non-catalytic domain have, however, remained unclear, and should be the focus of future studies. Especially, it is interesting to speculate what could be the function of the remaining portion of the non-catalytic domain, other than the zinc finger motifs, since it has clearly been preserved during evolution. In yeast, the subunit corresponding to POLE2, *dpb2*, plays the role of interacting with and integrating the catalytic subunit *pol2*, into the replisome. The role played by human POLE2 is not well studied, and more studies should be directed into this. POLE3 and POLE4 subunits are even more poorly studied.

Disease cases with mutations in the non-catalytic subunit of POLE1 are rare, understandable given its essential nature. Non-lethal mutations may be discovered in the population now that cheaper whole genome sequencing is gaining rapid ground, and it would be interesting to study what phenotypes these mutations cause. Mutations and insufficiencies of POLE2 are documented, and are known to cause syndromes similar to those of POLE1.

Lastly, since overexpression of replication proteins is well known to provide anti-cancer drug resistance to cells, and in some cases to also promote tumorigenesis, it is imperative that more studies be directed into investigating the effects of overexpression of FPC components and POLE on DNA replication.

6 Conclusions

From the studies of this thesis on the role of TIM and POLE in DNA replication initiation, the conclusions can be briefly summarized as follows:

TIM is required for normal S phase entry of cells. During replication initiation, TIM recruits TIPIN and CLASPIN to DNA. TIM is also required for the timely recruitment of PCNA during replication initiation. TIM, TIPIN and CLASPIN load to DNA partially during CMG assembly and partially after DNA synthesis, and TIM-MCM interaction is required for these proteins to load to DNA. Our data suggests that there are additional molecules of TIM present at replication forks, positioned on the lagging strand.

DNA polymerase epsilon has important non-catalytic roles to play in replication initiation. Although dispensable for CMG assembly, POLE is required for DNA synthesis in this process. The non-catalytic domain of POLE catalytic subunit POLE1 can support replication in the absence of the catalytic subunit, however the resulting forks are very slow. This domain acts by maintaining the association of subunit POLE2 with the replisome.

List of figures

Figure 1 Steps in DNA replication initiation in human cells.....12

Figure 2 Structure of the human replication fork.....13

Figure 3 Proposed model of TIM position and loading dynamics at the replication
fork.....23

References

- [1] R. A. Ganai and E. Johansson, "DNA Replication—A Matter of Fidelity," *Molecular Cell*, vol. 62, no. 5, pp. 745–755, Jun. 2016, doi: 10.1016/j.molcel.2016.05.003.
- [2] C. D. Campbell and E. E. Eichler, "Properties and rates of germline mutations in humans," *Trends in Genetics*, vol. 29, no. 10, pp. 575–584, Oct. 2013, doi: 10.1016/j.tig.2013.04.005.
- [3] K. K. Tachibana, M. A. Gonzalez, and N. Coleman, "Cell-cycle-dependent regulation of DNA replication and its relevance to cancer pathology," *The Journal of Pathology*, vol. 205, no. 2, pp. 123–129, 2005, doi: 10.1002/path.1708.
- [4] E. D. Pleasance *et al.*, "A comprehensive catalogue of somatic mutations from a human cancer genome," *Nature*, vol. 463, no. 7278, pp. 191–196, Jan. 2010, doi: 10.1038/nature08658.
- [5] I. R. Watson, K. Takahashi, P. A. Futreal, and L. Chin, "Emerging patterns of somatic mutations in cancer," *Nat Rev Genet*, vol. 14, no. 10, pp. 703–718, Oct. 2013, doi: 10.1038/nrg3539.
- [6] M. L. Mott and J. M. Berger, "DNA replication initiation: mechanisms and regulation in bacteria," *Nat Rev Microbiol*, vol. 5, no. 5, pp. 343–354, May 2007, doi: 10.1038/nrmicro1640.
- [7] J. J. Blow and A. Dutta, "Preventing re-replication of chromosomal DNA," *Nat Rev Mol Cell Biol*, vol. 6, no. 6, pp. 476–486, Jun. 2005, doi: 10.1038/nrm1663.
- [8] H. Nishitani and Z. Lygerou, "Control of DNA replication licensing in a cell cycle," *Genes to Cells*, vol. 7, no. 6, pp. 523–534, 2002, doi: 10.1046/j.1365-2443.2002.00544.x.
- [9] S. J. Benkovic, A. M. Valentine, and F. Salinas, "Replisome-Mediated DNA Replication," *Annual Review of Biochemistry*, vol. 70, no. Volume 70, 2001, pp. 181–208, Jul. 2001, doi: 10.1146/annurev.biochem.70.1.181.
- [10] "Dynamics of human replication factors in the elongation phase of DNA replication | Nucleic Acids Research | Oxford Academic." Accessed: Mar. 25, 2025. [Online]. Available: <https://academic.oup.com/nar/article/35/20/6904/2401915>
- [11] J. M. Dewar and J. C. Walter, "Mechanisms of DNA replication termination," *Nat Rev Mol Cell Biol*, vol. 18, no. 8, pp. 507–516, Aug. 2017, doi: 10.1038/nrm.2017.42.
- [12] M. Sullivan and D. O. Morgan, "Finishing mitosis, one step at a time," *Nat Rev Mol Cell Biol*, vol. 8, no. 11, pp. 894–903, Nov. 2007, doi: 10.1038/nrm2276.
- [13] R. Bellelli and S. J. Boulton, "Spotlight on the Replisome: Aetiology of DNA Replication-Associated Genetic Diseases," *Trends in Genetics*, vol. 37, no. 4, pp. 317–336, Apr. 2021, doi: 10.1016/j.tig.2020.09.008.
- [14] M. O'Driscoll, "The pathological consequences of impaired genome integrity in humans; disorders of the DNA replication machinery," *The Journal of Pathology*, vol. 241, no. 2, pp. 192–207, 2017, doi: 10.1002/path.4828.
- [15] "Congenital Diseases of DNA Replication: Clinical Phenotypes and Molecular Mechanisms." Accessed: Mar. 25, 2025. [Online]. Available: <https://www.mdpi.com/1422-0067/22/2/911>
- [16] R. Burla, La Torre, Mattia, Merigliano, Chiara, Verni, Fiammetta, and I. and Saggio, "Genomic instability and DNA replication defects in progeroid syndromes," *Nucleus*, vol. 9, no. 1, pp. 368–379, Dec. 2018, doi: 10.1080/19491034.2018.1476793.

- [17] M. Lei, "The MCM Complex: Its Role in DNA Replication and Implications for Cancer Therapy," *Current Cancer Drug Targets*, vol. 5, no. 5, pp. 365–380, Aug. 2005, doi: 10.2174/1568009054629654.
- [18] A. Umar and T. A. Kunkel, "DNA-replication Fidelity, Mismatch Repair and Genome Instability in Cancer Cells," *European Journal of Biochemistry*, vol. 238, no. 2, pp. 297–307, 1996, doi: 10.1111/j.1432-1033.1996.0297z.x.
- [19] A. Falaschi, Abdurashidova, Gulnara, and G. and Biamonti, "DNA replication, development and cancer: a homeotic connection?," *Critical Reviews in Biochemistry and Molecular Biology*, vol. 45, no. 1, pp. 14–22, Feb. 2010, doi: 10.3109/10409230903365608.
- [20] X. Xing, N. Jin, and J. Wang, "Polymerase Epsilon-Associated Ultramutagenesis in Cancer," *Cancers*, vol. 14, no. 6, Art. no. 6, Jan. 2022, doi: 10.3390/cancers14061467.
- [21] E. Rayner *et al.*, "A panoply of errors: polymerase proofreading domain mutations in cancer," *Nat Rev Cancer*, vol. 16, no. 2, pp. 71–81, Feb. 2016, doi: 10.1038/nrc.2015.12.
- [22] E. Heitzer and I. Tomlinson, "Replicative DNA polymerase mutations in cancer," *Current Opinion in Genetics & Development*, vol. 24, pp. 107–113, Feb. 2014, doi: 10.1016/j.gde.2013.12.005.
- [23] B. D. Preston, T. M. Albertson, and A. J. Herr, "DNA replication fidelity and cancer," *Seminars in Cancer Biology*, vol. 20, no. 5, pp. 281–293, Oct. 2010, doi: 10.1016/j.semcancer.2010.10.009.
- [24] R. D. Wood, M. Mitchell, J. Sgouros, and T. Lindahl, "Human DNA Repair Genes," *Science*, vol. 291, no. 5507, pp. 1284–1289, Feb. 2001, doi: 10.1126/science.1056154.
- [25] K. Macleod, "Tumor suppressor genes," *Current Opinion in Genetics & Development*, vol. 10, no. 1, pp. 81–93, Feb. 2000, doi: 10.1016/S0959-437X(99)00041-6.
- [26] A. Mazouzi, G. Velimezi, and J. I. Loizou, "DNA replication stress: Causes, resolution and disease," *Experimental Cell Research*, vol. 329, no. 1, pp. 85–93, Nov. 2014, doi: 10.1016/j.yexcr.2014.09.030.
- [27] H. Kitao *et al.*, "DNA replication stress and cancer chemotherapy," *Cancer Science*, vol. 109, no. 2, pp. 264–271, 2018, doi: 10.1111/cas.13455.
- [28] T. Ubhi and G. W. Brown, "Exploiting DNA Replication Stress for Cancer Treatment," *Cancer Research*, vol. 79, no. 8, pp. 1730–1739, Apr. 2019, doi: 10.1158/0008-5472.CAN-18-3631.
- [29] M. R. Waarts, A. J. Stonestrom, Y. C. Park, and R. L. Levine, "Targeting mutations in cancer," *J Clin Invest*, vol. 132, no. 8, Apr. 2022, doi: 10.1172/JCI154943.
- [30] K. Cheung-Ong, G. Giaever, and C. Nislow, "DNA-Damaging Agents in Cancer Chemotherapy: Serendipity and Chemical Biology," *Chemistry & Biology*, vol. 20, no. 5, pp. 648–659, May 2013, doi: 10.1016/j.chembiol.2013.04.007.
- [31] J. Zhang, Q. Dai, D. Park, and X. Deng, "Targeting DNA Replication Stress for Cancer Therapy," *Genes*, vol. 7, no. 8, Art. no. 8, Aug. 2016, doi: 10.3390/genes7080051.
- [32] M. J. O'Connor, "Targeting the DNA Damage Response in Cancer," *Molecular Cell*, vol. 60, no. 4, pp. 547–560, Nov. 2015, doi: 10.1016/j.molcel.2015.10.040.
- [33] S.-L. Liu *et al.*, "TIMELESS confers cisplatin resistance in nasopharyngeal carcinoma by activating the Wnt/ β -catenin signaling pathway and promoting the epithelial mesenchymal transition," *Cancer Lett*, vol. 402, pp. 117–130, Aug. 2017, doi: 10.1016/j.canlet.2017.05.022.

- [34] C. Cai *et al.*, "Claspin Overexpression Promotes Tumor Progression and Predicts Poor Clinical Outcome in Prostate Cancer," *Genetic Testing and Molecular Biomarkers*, vol. 25, no. 2, pp. 131–139, Feb. 2021, doi: 10.1089/gtmb.2020.0226.
- [35] J. J. Blow and P. J. Gillespie, "Replication licensing and cancer — a fatal entanglement?," *Nat Rev Cancer*, vol. 8, no. 10, pp. 799–806, Oct. 2008, doi: 10.1038/nrc2500.
- [36] N. Donley and M. J. Thayer, "DNA replication timing, genome stability and cancer: Late and/or delayed DNA replication timing is associated with increased genomic instability," *Seminars in Cancer Biology*, vol. 23, no. 2, pp. 80–89, Apr. 2013, doi: 10.1016/j.semcancer.2013.01.001.
- [37] S. P. Bell, "The origin recognition complex: from simple origins to complex functions," *Genes Dev.*, vol. 16, no. 6, pp. 659–672, Mar. 2002, doi: 10.1101/gad.969602.
- [38] O. Hyrien, "How MCM loading and spreading specify eukaryotic DNA replication initiation sites," *F1000Res*, vol. 5, p. F1000 Faculty Rev-2063, Aug. 2016, doi: 10.12688/f1000research.9008.1.
- [39] T. D. Deegan and J. F. Diffley, "MCM: one ring to rule them all," *Current Opinion in Structural Biology*, vol. 37, pp. 145–151, Apr. 2016, doi: 10.1016/j.sbi.2016.01.014.
- [40] M.-N. Prioleau and D. M. MacAlpine, "DNA replication origins—where do we begin?," *Genes Dev.*, vol. 30, no. 15, pp. 1683–1697, Aug. 2016, doi: 10.1101/gad.285114.116.
- [41] M. E. Douglas, F. A. Ali, A. Costa, and J. F. X. Diffley, "The mechanism of eukaryotic CMG helicase activation," *Nature*, vol. 555, no. 7695, pp. 265–268, Mar. 2018, doi: 10.1038/nature25787.
- [42] S. Tanaka, R. Nakato, Y. Katou, K. Shirahige, and H. Araki, "Origin Association of Sld3, Sld7, and Cdc45 Proteins Is a Key Step for Determination of Origin-Firing Timing," *Current Biology*, vol. 21, no. 24, pp. 2055–2063, Dec. 2011, doi: 10.1016/j.cub.2011.11.038.
- [43] T. N. Moiseeva and C. J. Bakkenist, "Regulation of the initiation of DNA replication in human cells," *DNA Repair*, vol. 72, pp. 99–106, Dec. 2018, doi: 10.1016/j.dnarep.2018.09.003.
- [44] A. Kumagai, A. Shevchenko, A. Shevchenko, and W. G. Dunphy, "Direct regulation of Treslin by cyclin-dependent kinase is essential for the onset of DNA replication," *Journal of Cell Biology*, vol. 193, no. 6, pp. 995–1007, Jun. 2011, doi: 10.1083/jcb.201102003.
- [45] U. Schmidt, Y. Wollmann, C. Franke, F. Grosse, H.-P. Saluz, and F. Hänel, "Characterization of the interaction between the human DNA topoisomerase II β -binding protein 1 (TopBP1) and the cell division cycle 45 (Cdc45) protein," *Biochemical Journal*, vol. 409, no. 1, pp. 169–177, Dec. 2007, doi: 10.1042/BJ20070872.
- [46] A. Kumagai, A. Shevchenko, A. Shevchenko, and W. G. Dunphy, "Treslin Collaborates with TopBP1 in Triggering the Initiation of DNA Replication," *Cell*, vol. 140, no. 3, pp. 349–359, Feb. 2010, doi: 10.1016/j.cell.2009.12.049.
- [47] D. Boos, M. Yekezare, and J. F. X. Diffley, "Identification of a Heteromeric Complex That Promotes DNA Replication Origin Firing in Human Cells," *Science*, vol. 340, no. 6135, pp. 981–984, May 2013, doi: 10.1126/science.1237448.
- [48] A. Chowdhury *et al.*, "The DNA unwinding element binding protein DUE-B interacts with Cdc45 in preinitiation complex formation," *Mol Cell Biol*, vol. 30, no. 6, pp. 1495–1507, Mar. 2010, doi: 10.1128/MCB.00710-09.

- [49] Z. F. Pursell and T. A. Kunkel, "DNA Polymerase ϵ : A Polymerase of Unusual Size (and Complexity)," in *Progress in Nucleic Acid Research and Molecular Biology*, vol. 82, P. M. Conn, Ed., Academic Press, 2008, pp. 101–145. doi: 10.1016/S0079-6603(08)00004-4.
- [50] S. Ahmad, S. Zhang, and X. Meng, "A conserved thumb domain insertion in DNA polymerase epsilon supports processive DNA synthesis," *Nucleic Acids Research*, vol. 53, no. 5, p. gkaf190, Mar. 2025, doi: 10.1093/nar/gkaf190.
- [51] S. Muramatsu, K. Hirai, Y.-S. Tak, Y. Kamimura, and H. Araki, "CDK-dependent complex formation between replication proteins Dpb11, Sld2, Pol (epsilon), and GINS in budding yeast," *Genes Dev*, vol. 24, no. 6, pp. 602–612, Mar. 2010, doi: 10.1101/gad.1883410.
- [52] J. S. Lewis *et al.*, "Mechanism of replication origin melting nucleated by CMG helicase assembly," *Nature*, vol. 606, no. 7916, pp. 1007–1014, Jun. 2022, doi: 10.1038/s41586-022-04829-4.
- [53] J. Walter and J. Newport, "Initiation of Eukaryotic DNA Replication: Origin Unwinding and Sequential Chromatin Association of Cdc45, RPA, and DNA Polymerase α ," *Molecular Cell*, vol. 5, no. 4, pp. 617–627, Apr. 2000, doi: 10.1016/S1097-2765(00)80241-5.
- [54] G.-L. Moldovan, B. Pfander, and S. Jentsch, "PCNA, the Maestro of the Replication Fork," *Cell*, vol. 129, no. 4, pp. 665–679, May 2007, doi: 10.1016/j.cell.2007.05.003.
- [55] W. C. Drosopoulos, D. A. Vierra, C. A. Kenworthy, R. A. Coleman, and C. L. Schildkraut, "Dynamic Assembly and Disassembly of the Human DNA Polymerase δ Holoenzyme on the Genome In Vivo," *Cell Rep*, vol. 30, no. 5, pp. 1329–1341.e5, Feb. 2020, doi: 10.1016/j.celrep.2019.12.101.
- [56] R. E. Georgescu *et al.*, "Mechanism of asymmetric polymerase assembly at the eukaryotic replication fork," *Nat Struct Mol Biol*, vol. 21, no. 8, Art. no. 8, Aug. 2014, doi: 10.1038/nsmb.2851.
- [57] "Evidence that DNA polymerase δ contributes to initiating leading strand DNA replication in *Saccharomyces cerevisiae* | Nature Communications." Accessed: Sep. 04, 2023. [Online]. Available: <https://www.nature.com/articles/s41467-018-03270-4>
- [58] "CMG–Pol epsilon dynamics suggests a mechanism for the establishment of leading-strand synthesis in the eukaryotic replisome | PNAS." Accessed: Sep. 04, 2023. [Online]. Available: <https://www.pnas.org/doi/full/10.1073/pnas.1700530114>
- [59] M. L. Jones, Y. Baris, M. R. G. Taylor, and J. T. P. Yeeles, "Structure of a human replisome shows the organisation and interactions of a DNA replication machine," *EMBO J*, vol. 40, no. 23, p. e108819, Dec. 2021, doi: 10.15252/embj.2021108819.
- [60] M. Jenkyn-Bedford *et al.*, "A conserved mechanism for regulating replisome disassembly in eukaryotes," *Nature*, vol. 600, no. 7890, pp. 743–747, Dec. 2021, doi: 10.1038/s41586-021-04145-3.
- [61] M. L. Jones, V. Aria, Y. Baris, and J. T. P. Yeeles, "How Pol α -primase is targeted to replisomes to prime eukaryotic DNA replication," *Molecular Cell*, vol. 83, no. 16, pp. 2911–2924.e16, Aug. 2023, doi: 10.1016/j.molcel.2023.06.035.
- [62] C. Benna *et al.*, "*Drosophila timeless2* Is Required for Chromosome Stability and Circadian Photoreception," *Current Biology*, vol. 20, no. 4, pp. 346–352, Feb. 2010, doi: 10.1016/j.cub.2009.12.048.
- [63] A. L. Gotter, C. Suppa, and B. S. Emanuel, "Mammalian TIMELESS and Tipin are evolutionarily conserved replication fork-associated factors," *J Mol Biol*, vol. 366, no. 1, pp. 36–52, Feb. 2007, doi: 10.1016/j.jmb.2006.10.097.

- [64] A. L. Gotter, "Tipin, a novel timeless-interacting protein, is developmentally co-expressed with timeless and disrupts its self-association," *J Mol Biol*, vol. 331, no. 1, pp. 167–176, Aug. 2003, doi: 10.1016/s0022-2836(03)00633-8.
- [65] M. Bando *et al.*, "Csm3, Tof1, and Mrc1 form a heterotrimeric mediator complex that associates with DNA replication forks," *J Biol Chem*, vol. 284, no. 49, pp. 34355–34365, Dec. 2009, doi: 10.1074/jbc.M109.065730.
- [66] W.-H. Cho, Y.-H. Kang, Y.-Y. An, I. Tappin, J. Hurwitz, and J.-K. Lee, "Human Tim-Tipin complex affects the biochemical properties of the replicative DNA helicase and DNA polymerases," *Proceedings of the National Academy of Sciences*, vol. 110, no. 7, pp. 2523–2527, Feb. 2013, doi: 10.1073/pnas.1222494110.
- [67] "Frontiers | Approaching Protein Barriers: Emerging Mechanisms of Replication Pausing in Eukaryotes." Accessed: Mar. 25, 2025. [Online]. Available: <https://www.frontiersin.org/journals/cell-and-developmental-biology/articles/10.3389/fcell.2021.672510/full>
- [68] X. Yang, P. A. Wood, and W. J. M. Hrushesky, "Mammalian TIMELESS is required for ATM-dependent CHK2 activation and G2/M checkpoint control," *J Biol Chem*, vol. 285, no. 5, pp. 3030–3034, Jan. 2010, doi: 10.1074/jbc.M109.050237.
- [69] M. G. Kemp *et al.*, "Tipin-Replication Protein A Interaction Mediates Chk1 Phosphorylation by ATR in Response to Genotoxic Stress," *J Biol Chem*, vol. 285, no. 22, pp. 16562–16571, May 2010, doi: 10.1074/jbc.M110.110304.
- [70] S. Vipat and T. N. Moiseeva, "The TIMELESS Roles in Genome Stability and Beyond," *J Mol Biol*, vol. 436, no. 1, p. 168206, Jan. 2024, doi: 10.1016/j.jmb.2023.168206.
- [71] X. Xu, J.-T. Wang, M. Li, and Y. Liu, "TIMELESS Suppresses the Accumulation of Aberrant CDC45-MCM2-7-GINS Replicative Helicase Complexes on Human Chromatin," *J Biol Chem*, vol. 291, no. 43, pp. 22544–22558, Oct. 2016, doi: 10.1074/jbc.M116.719963.
- [72] N. Yoshizawa-Sugata and H. Masai, "Human Tim/Timeless-interacting Protein, Tipin, Is Required for Efficient Progression of S Phase and DNA Replication Checkpoint *," *Journal of Biological Chemistry*, vol. 282, no. 4, pp. 2729–2740, Jan. 2007, doi: 10.1074/jbc.M605596200.
- [73] J. Zhou *et al.*, "Aberrantly Expressed Timeless Regulates Cell Proliferation and Cisplatin Efficacy in Cervical Cancer," *Hum Gene Ther*, vol. 31, no. 5–6, pp. 385–395, Mar. 2020, doi: 10.1089/hum.2019.080.
- [74] W. Zhang *et al.*, "Aberrant TIMELESS expression is associated with poor clinical survival and lymph node metastasis in early-stage cervical carcinoma," *Int J Oncol*, vol. 50, no. 1, pp. 173–184, Jan. 2017, doi: 10.3892/ijo.2016.3784.
- [75] T. Colangelo *et al.*, "Loss of circadian gene Timeless induces EMT and tumor progression in colorectal cancer via Zeb1-dependent mechanism," *Cell Death Differ*, vol. 29, no. 8, pp. 1552–1568, Aug. 2022, doi: 10.1038/s41418-022-00935-y.
- [76] D. A. Korona, K. G. LeCompte, and Z. F. Pursell, "The high fidelity and unique error signature of human DNA polymerase ϵ ," *Nucleic Acids Research*, vol. 39, no. 5, pp. 1763–1773, Mar. 2011, doi: 10.1093/nar/gkq1034.
- [77] J. Pachlopnik Schmid *et al.*, "Polymerase ϵ 1 mutation in a human syndrome with facial dysmorphism, immunodeficiency, livedo, and short stature ('FILS syndrome')," *J Exp Med*, vol. 209, no. 13, pp. 2323–2330, Dec. 2012, doi: 10.1084/jem.20121303.
- [78] C. V. Logan *et al.*, "DNA Polymerase Epsilon Deficiency Causes IMAGE Syndrome with Variable Immunodeficiency," *Am J Hum Genet*, vol. 103, no. 6, pp. 1038–1044, Dec. 2018, doi: 10.1016/j.ajhg.2018.10.024.

- [79] J. B. Sweasy, J. M. Lauper, and K. A. Eckert, "DNA Polymerases and Human Diseases," *Radiation Research*, vol. 166, no. 5, pp. 693–714, Nov. 2006, doi: 10.1667/RR0706.1.
- [80] H. Tang *et al.*, "Increased DNA Polymerase Epsilon Catalytic Subunit Expression Predicts Tumor Progression and Modulates Tumor Microenvironment of Hepatocellular Carcinoma," *J Cancer*, vol. 13, no. 9, pp. 2740–2750, Jun. 2022, doi: 10.7150/jca.64765.
- [81] Q. He, F. Wang, N. Y. Yao, M. E. O'Donnell, and H. Li, "Structures of the human leading strand Pole–PCNA holoenzyme," *Nat Commun*, vol. 15, no. 1, p. 7847, Sep. 2024, doi: 10.1038/s41467-024-52257-x.
- [82] Z. Yuan, R. Georgescu, G. D. Schauer, M. E. O'Donnell, and H. Li, "Structure of the polymerase ϵ holoenzyme and atomic model of the leading strand replisome," *Nat Commun*, vol. 11, no. 1, p. 3156, Jun. 2020, doi: 10.1038/s41467-020-16910-5.
- [83] S. H. Lee, Z. Q. Pan, A. D. Kwong, P. M. Burgers, and J. Hurwitz, "Synthesis of DNA by DNA polymerase epsilon in vitro," *Journal of Biological Chemistry*, vol. 266, no. 33, pp. 22707–22717, Nov. 1991, doi: 10.1016/S0021-9258(18)54626-3.
- [84] E. M. Boehm, M. S. Gildenberg, and M. T. Washington, "Chapter Seven - The Many Roles of PCNA in Eukaryotic DNA Replication," in *The Enzymes*, vol. 39, L. S. Kaguni and M. T. Oliveira, Eds., in DNA Replication Across Taxa, vol. 39, Academic Press, 2016, pp. 231–254. doi: 10.1016/bs.enz.2016.03.003.
- [85] P. Zegerman, "DNA Replication: Polymerase Epsilon as a Non-catalytic Converter of the Helicase," *Current Biology*, vol. 23, no. 7, pp. R273–R276, Apr. 2013, doi: 10.1016/j.cub.2013.03.008.
- [86] R. Dua, D. L. Levy, and J. L. Campbell, "Analysis of the essential functions of the C-terminal protein/protein interaction domain of *Saccharomyces cerevisiae* pol epsilon and its unexpected ability to support growth in the absence of the DNA polymerase domain," *J Biol Chem*, vol. 274, no. 32, pp. 22283–22288, Aug. 1999, doi: 10.1074/jbc.274.32.22283.
- [87] T. Natsume, T. Kiyomitsu, Y. Saga, and M. T. Kanemaki, "Rapid Protein Depletion in Human Cells by Auxin-Inducible Degron Tagging with Short Homology Donors," *Cell Reports*, vol. 15, no. 1, pp. 210–218, Apr. 2016, doi: 10.1016/j.celrep.2016.03.001.
- [88] A. Yesbolatova *et al.*, "The auxin-inducible degron 2 technology provides sharp degradation control in yeast, mammalian cells, and mice," *Nat Commun*, vol. 11, p. 5701, Nov. 2020, doi: 10.1038/s41467-020-19532-z.
- [89] J. Chen, P. K. Jackson, M. W. Kirschner, and A. Dutta, "Separate domains of p21 involved in the inhibition of Cdk kinase and PCNA," *Nature*, vol. 374, no. 6520, pp. 386–388, Mar. 1995, doi: 10.1038/374386a0.
- [90] V. N. Podust, L. M. Podust, F. Goubin, B. Ducommun, and U. Hübscher, "Mechanism of inhibition of proliferating cell nuclear antigen-dependent DNA synthesis by the cyclin-dependent kinase inhibitor p21," *Biochemistry*, vol. 34, no. 27, pp. 8869–8875, Jul. 1995, doi: 10.1021/bi00027a039.
- [91] C.-C. Yang *et al.*, "Claspin recruits Cdc7 kinase for initiation of DNA replication in human cells," *Nat Commun*, vol. 7, p. 12135, Jul. 2016, doi: 10.1038/ncomms12135.
- [92] X. H. Yang, B. Shiotani, M. Classon, and L. Zou, "Chk1 and Claspin potentiate PCNA ubiquitination," *Genes Dev*, vol. 22, no. 9, pp. 1147–1152, May 2008, doi: 10.1101/gad.1632808.
- [93] X. H. Yang and L. Zou, "Dual Functions of DNA Replication Forks in Checkpoint Signaling and PCNA Ubiquitination," *Cell Cycle*, vol. 8, no. 2, pp. 191–194, Jan. 2009.

- [94] A. R. Leman, C. Noguchi, C. Y. Lee, and E. Noguchi, "Human Timeless and Tipin stabilize replication forks and facilitate sister-chromatid cohesion," *Journal of Cell Science*, vol. 123, no. 5, pp. 660–670, Mar. 2010, doi: 10.1242/jcs.057984.
- [95] T. Kesti, K. Flick, S. Keränen, J. E. Syväoja, and C. Wittenberg, "DNA Polymerase ϵ Catalytic Domains Are Dispensable for DNA Replication, DNA Repair, and Cell Viability," *Molecular Cell*, vol. 3, no. 5, pp. 679–685, May 1999, doi: 10.1016/S1097-2765(00)80361-5.
- [96] T. Handa, M. Kanke, T. S. Takahashi, T. Nakagawa, and H. Masukata, "DNA polymerization-independent functions of DNA polymerase epsilon in assembly and progression of the replisome in fission yeast," *Mol Biol Cell*, vol. 23, no. 16, pp. 3240–3253, Aug. 2012, doi: 10.1091/mbc.E12-05-0339.
- [97] P. Goswami *et al.*, "Structure of DNA-CMG-Pol epsilon elucidates the roles of the non-catalytic polymerase modules in the eukaryotic replisome," *Nat Commun*, vol. 9, no. 1, p. 5061, Nov. 2018, doi: 10.1038/s41467-018-07417-1.
- [98] M. A. Garbacz, P. B. Cox, S. Sharma, S. A. Lujan, A. Chabes, and T. A. Kunkel, "The absence of the catalytic domains of *Saccharomyces cerevisiae* DNA polymerase ϵ strongly reduces DNA replication fidelity," *Nucleic Acids Res*, vol. 47, no. 8, pp. 3986–3995, May 2019, doi: 10.1093/nar/gkz048.
- [99] K. Shikata, T. Sasa-Masuda, Y. Okuno, S. Waga, and A. Sugino, "The DNA polymerase activity of Pol ϵ holoenzyme is required for rapid and efficient chromosomal DNA replication in *Xenopus* egg extracts," *BMC Biochemistry*, vol. 7, no. 1, p. 21, Aug. 2006, doi: 10.1186/1471-2091-7-21.
- [100] B. M. Sirbu, F. B. Couch, and D. Cortez, "Monitoring the spatiotemporal dynamics of proteins at replication forks and in assembled chromatin using isolation of proteins on nascent DNA," *Nat Protoc*, vol. 7, no. 3, pp. 594–605, Mar. 2012, doi: 10.1038/nprot.2012.010.
- [101] A. R. Leman and E. and Noguchi, "Local and global functions of Timeless and Tipin in replication fork protection," *Cell Cycle*, vol. 11, no. 21, pp. 3945–3955, Nov. 2012, doi: 10.4161/cc.21989.
- [102] E. Noguchi, "Division of labor of the replication fork protection complex subunits in sister chromatid cohesion and Chk1 activation," *Cell Cycle*, vol. 10, no. 13, pp. 2059–2058, Jul. 2011, doi: 10.4161/cc.10.13.15805.
- [103] L. M. Young *et al.*, "TIMELESS Forms a Complex with PARP1 Distinct from Its Complex with TIPIN and Plays a Role in the DNA Damage Response," *Cell Reports*, vol. 13, no. 3, pp. 451–459, Oct. 2015, doi: 10.1016/j.celrep.2015.09.017.

Acknowledgements

I would like to express my heartfelt gratitude towards my PhD supervisor, Prof. Tatiana Moiseeva, for not only her academic mentorship but also for her encouragement during difficult times, from the beginning until the end of my PhD journey. Her rigorous training and the intellectually stimulating environment in her group has truly shaped me as a researcher. I am additionally particularly grateful to the Director of the Department of Chemistry and Biotechnology Dr. Pirjo Spuul, the Head of the Division of Gene Technology Prof. Indrek Koppel and the Programme Director of Chemistry and Gene Technology Dr. Cecilia Sarmiento, for their unwavering support at various stages of my course, and for the welcoming environment they created for students at the institute. I extend my thanks to the Department of Chemistry and Biotechnology at Tallinn University of Technology, whose resources and positive environment have been invaluable to me. Additionally, I would like to acknowledge the generous financial support from the funding source that supported my work, Estonian Research Council (research grant PRG1477).

Abstract

The roles of TIMELESS protein and DNA polymerase epsilon in DNA replication initiation in human cells

DNA replication initiation is a rate-limiting step that determines the frequency of replication, as only a single round of replication must occur per cell division. This important process has been understudied in humans compared to the model organism yeast. Our current studies have been carried out in the human system, with the goal of improving our understanding of this very central molecular biological process in humans. Less is known about the role of TIMELESS (TIM) protein, a component of the Fork Protection Complex (FPC), in replication initiation, other than the fact that loss of TIM impairs S phase entry. Similarly, the catalytic functions of DNA polymerase epsilon (POLE) are well studied, but its non-catalytic roles have remained underexplored. We employed a conditional mini-auxin inducible degron- based depletion system to study the consequences of the loss of both these proteins on replication initiation, in order to decipher their roles in this process. The findings presented in this thesis provide evidence that TIM supports S phase entry by recruiting TIPIN and CLASPIN, and supporting the timely recruitment of PCNA, during replication initiation. The current findings also suggest that the non-catalytic domain of the catalytic subunit POLE1 of POLE supports replication initiation by maintaining normal speed of replication forks. Overall, our studies have uncovered a new previously unrecognized role of TIM protein, as well as an important non-catalytic role of POLE, in supporting the initiation step of DNA replication in the human system. Our work improves the mechanistic understanding of the process of DNA replication in humans, and is expected to have a broader impact in paving the way for development of future therapies.

Lühikokkuvõte

TIMELESS valgu ja DNA polümeraasi epsiloni rollid DNA replikatsiooni initsiatsioonis inimese rakkudes

DNA replikatsiooni initsiatsioon on selle protsessi kiirust piirav etapp, mis määrab replikatsiooni toimumise sageduse, kuna ühe raku-jagunemise kohta peab toimuma ainult üks replikatsioonisündmus. Replikatsioonikahvli kaitsekompleksi (FPC) komponendi TIMELESS (TIM) rollist initsiatsioonis on teada vaid asjaolu, et TIM-i kadumine kahjustab S-faasi sisenemist. Samamoodi on DNA polümeraasi epsiloni (POLE) katalüütilised funktsioonid hästi uuritud, kuid mittekatalüütilised rollid jällegi on võrdlemisi alauuritud. Mõlema valgu rolli uurimiseks replikatsiooni initsiatsioonil kasutasime tingimuslikku auksiin-indutseeritava degroni tehnoloogiat, mille abil on võimalik tingimuslikult kaotada uuritava valgu avaldumine rakkudes. Leidsime, et TIM toetab S-faasi sisenemist, värvates valgukompleksi TIPIN ja CLASPIN valgud ning toetades PCNA õigeaegset värbamist replikatsiooni initsiatsiooni ajal. Samuti leidsime, et POLE katalüütilise alaühiku mittekatalüütiline domeen POLE1 toetab initsiatsiooni, säilitades normaalse replikatsioonikahvli kiiruse. Kokkuvõttes on käesoleva töö tulemustena leitud TIM-i ja POLE olulisi ja varem tundmatuid funktsioone inimese rakkude replikatsiooni initsiatsioonis. DNA replikatsiooni on inimestel võrreldes mudelorganismi pärmiga alauuritud ja inimsüsteemi uuringud on hädavajalikud mitte ainult selleks, et parandada meie arusaamist sellest väga kesksest molekulaarbioloogilisest protsessist, vaid ka selleks, et panna alus tulevastele ravimeetoditele.

Appendix

Publication I

S. Vipat, D. Gupta, S. Jonchhe, H. Anderspuk, E. Rothenberg, and T. N. Moiseeva, 'The non-catalytic role of DNA polymerase epsilon in replication initiation in human cells', *Nat Commun*, vol. 13, no. 1, p. 7099, Nov. 2022, doi: 10.1038/s41467-022-34911-4.

The non-catalytic role of DNA polymerase epsilon in replication initiation in human cells

Received: 1 April 2022

Accepted: 10 November 2022

Published online: 19 November 2022

Sameera Vipat^{1,3}, Dipika Gupta^{2,3}, Sagun Jonchhe^{2,3}, Hele Anderspuk¹, Eli Rothenberg² & Tatiana N. Moiseeva¹✉

DNA polymerase epsilon (PoE) is an enzyme essential for DNA replication. Deficiencies and mutations in PoE cause severe developmental abnormalities and cancers. Paradoxically, the catalytic domain of yeast PoE catalytic subunit is dispensable for survival, and its non-catalytic essential function is linked with replicative helicase (CMG) assembly. Less is known about the PoE role in replication initiation in human cells. Here we use an auxin-inducible degron system to study the effect of POLE1 depletion on replication initiation in U2OS cells. POLE1-depleted cells were able to assemble CMG helicase and initiate DNA synthesis that failed shortly after. Expression of POLE1 non-catalytic domain rescued this defect resulting in slow, but continuous DNA synthesis. We propose a model where in human U2OS cells POLE1/POLE2 are dispensable for CMG assembly, but essential during later steps of replication initiation. Our study provides some insights into the role of PoE in replication initiation in human cells.

The core mechanisms of the initiation of DNA replication are conserved from yeast to mammals. Heterohexameric MCM helicase is a central element of the replication complex. MCM is loaded on the chromatin during origin licensing in G1 phase of the cell cycle and serves as a platform for recruiting all other replication components. MCM is activated by its binding partners CDC45 and GINS (forming the CMG helicase) and DDK- and CDK-dependent phosphorylations, while CTF4 brings together the CMG helicase and polymerase alpha/primase complex¹. After CMG activation, two heterohexameric MCM complexes start moving toward each other, bypassing each other^{2–4}. After priming by DNA polymerase alpha (POLA), the initial DNA synthesis during CMG bypass is performed by DNA polymerase delta (POLD), with DNA polymerase epsilon (POLE) taking over the leading strand synthesis after the initial bypass of polymerases past one another^{2,5}. After this “polymerase switch” step, two replication forks, each with its own leading and lagging strands, are established.

DNA polymerase epsilon (POLE) is a major DNA polymerase, responsible for synthesizing the leading strand during DNA

replication⁶. In yeast, polymerase epsilon (PoE) is recruited to MCM helicase together with GINS complex, playing a critical role in replisome assembly and activation^{7–9}. Surprisingly, the N-terminal catalytic domain of PoE catalytic subunit (Pol2 in yeast, POLE1 in humans) is dispensable for cell survival in yeast^{10,11}. Since this phenomenon was first observed^{10,11}, many studies have been conducted to elucidate the non-catalytic role of Pol2 in DNA synthesis and the mechanism allowing cells to survive in the absence of the catalytic domain of PoE^{9,12–15}. In the absence of the catalytic N-terminal domain, the C-terminal domain of Pol2 is necessary and sufficient to assemble a full helicase and support replication *in vitro*¹⁶. According to structural and biochemical data^{13,17}, DNA synthesis of both leading and lagging strands in the absence of Pol2 catalytic domain is performed by POLD. In this case, DNA synthesis is slower due to slower DNA unwinding by the CMG helicase¹⁷, suggesting suboptimal CMG activation in these cells. Systems that lack the catalytic domain of Pol2 have proven to be invaluable tools to study the mechanism of replication initiation in eukaryotes.

¹Department of Chemistry and Biotechnology, Tallinn University of Technology, Tallinn 12618, Estonia. ²Department of Biochemistry and Molecular Pharmacology, New York University School of Medicine, New York, NY 10016, USA. ³These authors contributed equally: Sameera Vipat, Dipika Gupta, Sagun Jonchhe. ✉e-mail: Tatiana.Moiseeva@taltech.ee

To our knowledge, no studies have been performed to clarify whether the non-catalytic role of DNA polymerase epsilon is conserved in human cells. In this study, we aimed to identify the essential domains of POLE1, test whether the non-catalytic C-terminal domain of human POLE is sufficient for DNA synthesis, and establish the role of DNA polymerase epsilon in the initiation of DNA replication in human cells.

We have created a cell line in which POLE1 is tagged with mAID (auxin-inducible degron), allowing rapid and efficient depletion of this protein in human U2OS cells without causing a G1 arrest. Surprisingly, POLE1 depletion did not prevent CMG assembly or MCM phosphorylation during ATR inhibition-induced origin firing, indicating that replisome assembly in POLE-deficient cells proceeds to a late stage before DNA replication fails. Indeed, we were able to observe some residual EdU incorporation that was sensitive to aphidicolin, in POLE1-depleted cells.

Using the POLE1-mAID cell line, we show that the C-terminal non-catalytic domain of POLE1 can support DNA replication in human cells in the absence of a full-length protein, although DNA synthesis in such cells is slower. We propose that polymerase delta substitutes for polymerase epsilon in cells expressing the POLE1 C-terminal domain, but is unable to support DNA synthesis in the absence of POLE1/POLE2 due to a failure of the replication initiation, probably at the step of polymerase switching.

POLE insufficiency is known to cause developmental abnormalities in humans^{18–20}, and drive replication stress and genomic instability in mice and *C. elegans*^{21,22}, which is generally attributed to insufficient origin firing. However, no specific molecular mechanism has been established to date. Our study provides mechanistic insight into the effects of POLE1 depletion and the role of POLE in DNA replication initiation in human cells.

Results

Development and characterization of mAID-tagged POLE1 in U2OS cells

We used an auxin-inducible degron system (mAID) to be able to study the role of DNA polymerase epsilon in replication initiation in human cells. This system is derived from plants and allows rapid depletion of the mAID-tagged protein after it is efficiently ubiquitinated by E3 ligase recruited by F-box protein osTIR1 only in presence of the plant hormone auxin (in this study we used indole-3-acetic acid or 3-IAA)²³. Following the approach described by Natsume et al.²⁴, we used CRISPR/Cas9 to knock-in (KI) osTIR1 under a doxycycline-inducible promoter into the AAVS1 “safe harbor” locus, and added a mAID-mCherry tag at the C-terminus of endogenous POLE1 using either one HR template (containing hygromycin resistance gene) or two HR templates (one containing neomycin resistance marker and the other with the hygromycin resistance marker—to increase the probability of homozygous knock-ins). After single-cell cloning, the clonal lines were tested by PCR to ensure homozygous KI of the mAID-mCherry tag (Supplementary Fig. 1a, b). Several homozygous KI clones were identified. Two of the homozygous KI clones—clones 16 (resistant to both neomycin and hygromycin) and 1.6 (sensitive to neomycin)—were treated with 2 µg/ml doxycycline (dox) to induce osTIR1 expression and 500 µM auxin (aux) to promote POLE1 degradation. 24 h treatment with doxycycline alone slightly reduced the level of POLE1 (Fig. 1a). POLE1 level was greatly decreased after the 24 h incubation with both chemicals, confirming the efficiency of the system (Fig. 1a). mAID-mCherry tagging also notably changed the electrophoretic mobility of the POLE1 protein, additionally confirming the absence of the endogenous untagged POLE1 in the tested clones.

In order to test the effect of POLE1 depletion on cell growth we seeded equal numbers of clone 16, clone 1.6, or U2OS cells and treated them with DMSO or dox/aux for 72 h, and counted the cells every 24 h (Fig. 1b). Untreated knock-in cells grew slightly slower compared to the wild-type U2OS cells, however, the addition of dox/aux completely

stopped proliferation of clones 16 and 1.6, in agreement with the essential role of POLE1 protein in the cell cycle. Dox/aux treatment also slightly decreased the growth of U2OS cells, as has been previously observed²⁵.

The effect of short-term POLE1 depletion on replication and cell cycle was evaluated by treating cells with doxycycline for 16 h to induce osTIR1 expression, followed by auxin treatment for 1–8 h. Western blot analysis showed that 1 h of auxin treatment was enough to greatly decrease the level of POLE1 in clone 16 cells (Fig. 1c). EdU incorporation analyses showed that while cells slowed down replication within 1 h of auxin addition, the most dramatic effect was seen after 3 h of auxin treatment, resulting in a strong block of EdU incorporation by S-phase cells (Supplementary Fig. 1c, gating strategy shown on Supplementary Fig. 1o). 16 or 24 h treatment with doxycycline alone (required for osTIR1 induction) visibly reduced levels of POLE1, resulting in EdU incorporation decrease (Supplementary Fig. 1d) and possibly creating stress even before the auxin addition. Therefore, to avoid potential difficulties interpreting results from such experiments, we decided to adhere to 16–24 h concurrent treatments with dox/aux in this study.

In order to ensure that the C-terminal tagging of POLE1 with mAID-mCherry did not have any significant effects of replication dynamics in U2OS cells, we performed a series of experiments comparing U2OS, clone 16, and clone 1.6 (Supplementary Fig. 1e–i). Our data show that POLE1 C-terminal tagging did not significantly affect POLE1 levels (Supplementary Fig. 1e), overall EdU incorporation (Supplementary Fig. 1f), the number of cells in S-phase (Supplementary Fig. 1g), or replication fork speed in U2OS cells (Supplementary Fig. 1h, i).

In order to evaluate the effect of POLE1 depletion on replication and cell cycle, we treated wild-type U2OS cells, clone 16, or clone 1.6 cells with dox/aux for 24 h, followed by a 30 min EdU pulse. Flow cytometry analysis of EdU incorporation and DNA content showed a dramatic decrease in EdU-positive cells after POLE1 depletion (Fig. 1d, e, gating is shown on Supplementary Fig. 1j). Similar results were observed with clone 1.6 (Supplementary Fig. 1k). Surprisingly, there was no notable G1 arrest after 24 h of treatment (Fig. 1f), indicating that POLE1 depletion did not prevent cells from entering S-phase.

Cell line instability is caused by TetR promoter methylation

In EdU incorporation FACS data, we noticed a subpopulation of POLE1-mAID cells that are resistant to dox/aux treatment and keep EdU incorporation at near-normal level. While the experiments shown above are done using early passages of clone 16, after a few weeks in culture this subpopulation grew, and after 2 months in culture (2m), nearly 100% of cells did not respond to treatment (Supplementary Fig. 1l). Similarly, treating clone 16 with dox/aux for 10 days selected a population (10d) that was fully resistant to dox/aux treatment (Supplementary Fig. 1m). In order to check that these resistant cells still express mAID-tagged POLE1 and osTIR1, we treated cells with DMSO or dox/aux for 16 h, followed by cell lysis and western blot analysis (Supplementary Fig. 1n). 2m and 10d cells still expressed mAID-mCherry-tagged POLE1, however, they failed to express osTIR1, which explained failure to deplete POLE1.

Inactivation of the doxycycline-inducible transgenes is a known problem that has been attributed to the methylation of the tetR promoter²⁶. In order to confirm that methylation is the reason for doxycycline resistance in our clones, we treated cells with demethylating agent 5-azacytidine (5AC) for 48 h before adding dox/aux for 16 h, and tested POLE1 and osTIR1 levels by western blot. Our data showed that demethylation restored osTIR1 expression and POLE1 degradation in response to dox/aux, thus confirming promoter methylation as the primary reason for the acquired doxycycline resistance (Supplementary Fig. 1n). Although we did not see an increase of Chk1 phosphorylation in our experiment, 5AC is a known

DNA damaging agent²⁷, and we therefore chose not to use it in the DNA replication experiments. For the data in this paper, we used early passages of the clones 16 and 1.6, disregarding the resistant population when possible. In the experiments where it was not possible to disregard the resistant population (i.e., western blots), the low POLE1 signal seen in dox/aux treated samples is likely coming from the wild-type levels of POLE1 in the resistant population (~10–20%) and does not indicate insufficient depletion of POLE1 in the vast majority of the cells.

ATRi-induced replication initiation in POLE1-depleted cells
ATR inhibitors (ATRi) have been shown to induce massive origin firing within minutes of treatment resulting in replication proteins' recruitment into the nuclease insoluble chromatin fraction, MCM4 hyperphosphorylation and an increase in EdU incorporation by replicating cells^{28,29}. In order to check if ATRi-induced replication initiation is blocked by POLE1 depletion, we treated clone 16 or clone 1.6 cells with DMSO or dox/aux combination for 16 h, added DMSO or 5 μ M ATRi (AZD6738) for the last 1 h, and isolated nuclease-insoluble chromatin

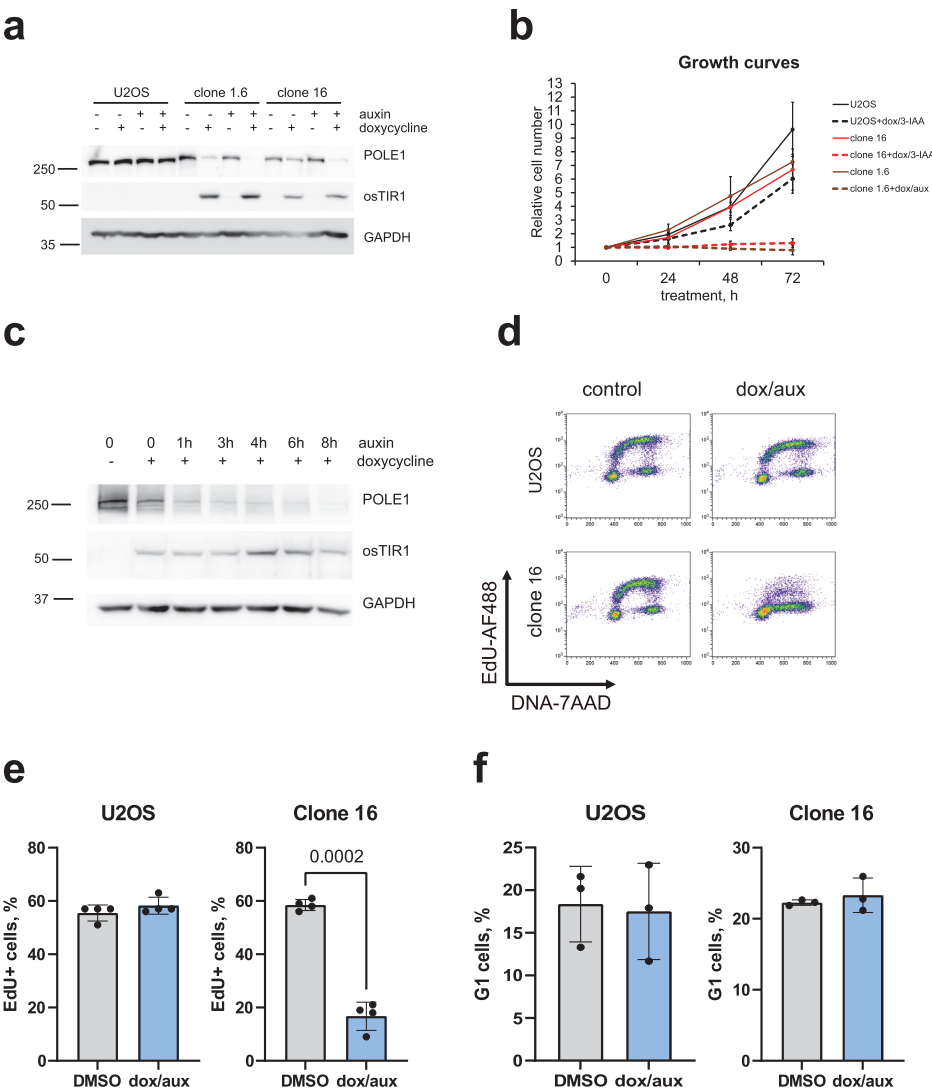


Fig. 1 | Creating and characterizing a cell line expressing mAID-tagged POLE1.
a Wild-type U2OS, homozygous mAID-KI clones 16 and 1.6 were treated for 24 h with doxycycline, auxin, or both, as indicated, western blots of total cell lysates are shown. **b** Equal numbers of wild-type U2OS, or homozygous mAID-KI clones 16 or 1.6, were seeded on 60 mm dishes and treated with DMSO or dox/aux for 72 h. The data are depicted as mean \pm SD from $n = 3$ independent experiments. **c** Clone 16 was treated with doxycycline overnight (16 h), auxin was added for the indicated times; western blots of total cell lysates are shown. **d–f** Wild-type U2OS, homozygous

mAID-KI clone 16 were treated for 24 h with DMSO or dox/aux, 10 μ M EdU was added for the last 30 min of treatment. **d** Flow cytometry plots showing EdU incorporation and DNA content (7-AAD staining) are shown. **e, f** Quantification of the flow cytometry data is shown—mean \pm SD from $n = 3$ independent experiments. Paired t-test was used for statistical analyses, p values are shown where they are statistically significant. **e** EdU+ cells were quantified based on EdU signal being above G1 and G2 levels. **f** Cells were assigned to G1 based on DNA content of 2n and being EdU negative. Source data are provided as a Source data file.

fraction (Fig. 2a, b, Supplementary Fig. 2a–d). Our experiment showed that while dox/aux treatment strongly depleted POLE1 both on chromatin and in the soluble protein lysate, it did not prevent MCM4 hyperphosphorylation or CDC45 recruitment to chromatin. In yeast the role of polymerase epsilon in CMG assembly is thought to be in the recruitment of GINS⁸. Therefore, we also studied the recruitment of SLD5 subunit of GINS to the nuclease insoluble chromatin in POLE1-depleted cells in response to ATR. Chromatin SLD5 levels, which increased with ATR-induced origin firing, were not suppressed by POLE1 depletion (Fig. 2a, b, Supplementary Fig. 2a–d), suggesting that GINS can be recruited to the sites of replication initiation in response to ATR in the absence of POLE1 in human cells.

To further investigate CMG helicase assembly in POLE1-depleted cells, we synchronized U2OS, clone 16, and clone 1.6 cells using thymidine-nocodazole block, and added dox/aux to all the cells during the last 8 h of nocodazole treatment (Fig. 2c). Cells were collected 0 (mitosis), 3, 9, and 12 h following the release from nocodazole into dox/aux containing medium, and the levels of MCM, CDC45, and SLD5 on chromatin were analyzed. All three cell lines have mostly completed mitosis by 3 h, and U2OS cells were in S-phase during the 9 h and 12 h timepoints (Supplementary Fig. 2e). POLE1-depleted clones 16 and 1.6, as expected, could not significantly progress through S-phase due to the lack of efficient DNA synthesis, however, these cells were capable of loading MCM on chromatin in G1 and recruiting CDC45 and GINS to chromatin 9–12 h after the release from nocodazole (Fig. 2c, Supplementary Fig. 2f–h). These data support our hypothesis that POLE1 is not required for CMG assembly in U2OS cells.

In order to test if the ATR-induced replisome assembly in the absence of POLE1 resulted in increased EdU incorporation, we added ATRi to the clone 16 or clone 1.6 cells after POLE1 depletion, followed by EdU-labeling of ongoing replication. Flow cytometry analysis showed a significant increase in EdU incorporation by S-phase cells even after POLE1 depletion (Fig. 2d, e, Supplementary Fig. 2i). These data indicate that ATR signaling actively suppressed DNA synthesis in POLE1-depleted cells, probably through the same mechanism as during normal, POLE-proficient replication²⁸.

Western blot with an antibody against CHK1 phosphorylated on serine-345, the canonical ATR-dependent phosphorylation site, confirmed that POLE1 depletion causes ATR activation, probably due to replication stress (Fig. 2a, Supplementary Fig. 2b–d). Accordingly, we observed an increase in ssDNA in POLE1-depleted cells by immunofluorescent detection of CldU under native conditions (Fig. 2f, Supplementary Fig. 2j).

Aberrant DNA synthesis in POLE1-depleted cells

In the ATRi EdU incorporation experiments (Fig. 2d), we observed a shift in EdU incorporation for the subpopulation of cells that we originally considered EdU negative. In order to verify that these seemingly EdU-negative cells after POLE1 depletion, in fact, do incorporate EdU, just at a slower rate, we depleted POLE1 in clone 16 or clone 1.6 by 16 h dox/aux treatment followed by incubations with EdU for 1–7 h instead of 30 min used in the standard setup (Fig. 3a–c). This experiment confirmed a slow EdU incorporation by POLE1-depleted cells, and allowed us to estimate that POLE1 depletion slows down EdU incorporation ~18–21 times, compared to wild-type levels of POLE1. Slow DNA synthesis by POLE1-depleted cells was sensitive to aphidicolin (Fig. 3d, Supplementary Fig. 3a), implying that a B-family DNA polymerase was responsible for this slow DNA synthesis.

Next, to test whether the cells could complete replication without POLE1, we treated control and POLE1-depleted cells with nocodazole—the inhibitor of microtubule polymerization—for 8 h to induce G2/M arrest (Supplementary Fig. 3b): while in the control sample the majority of the cells accumulated in G2 after nocodazole treatment, POLE1-depleted cells were barely affected by the nocodazole, indicating that these cells did not enter G2 during the time of treatment.

One possible explanation of such slow DNA synthesis is a low number of replication forks, limited by the availability of POLE1. Therefore, we assessed the effect of POLE1 depletion on replication dynamics by performing DNA fiber analysis on vehicle- or dox/aux-treated clone 16 or clone 1.6 cells. POLE1-depleted cells demonstrated “dotty” DNA fibers with an overall lower level of nucleotide incorporation (Fig. 3e, Supplementary Fig. 3c). Some “normal”-looking fibers, observed in dox/aux treated samples can be attributed to the dox-resistant cells or to the leftover POLE1. Since “dottiness” is a common artifact of DNA fiber and DNA combing experiments, quantitative analysis of purely “dotty” patterns can’t be reliable. To test if the “dots” represent extremely slow replication forks, we tried labeling ongoing DNA synthesis in POLE1-depleted cells for 60 min (Supplementary Fig. 3d), however, the phenotype did not change and we did not observe any tracks that could indicate continuous DNA synthesis. One possible explanation of such “dotty” phenotype is excessive origin firing with replication failure shortly after.

In order to identify the proteins involved in DNA synthesis after POLE1 depletion, we performed an iPOND experiment³⁰ on clone 16 cells with and without dox/aux treatment for 16 h. As expected, the amount of nascent DNA and proteins in the samples from cells treated with dox/aux, was lower than in the control samples (Supplementary data 1). In order to compare the protein composition of the replisome with and without POLE1, we performed two alternative normalizations: (1) normalization to the signal of five major histones (intended to normalize to the amount of the DNA in the sample), (2) normalization to the signal of MCM subunits (intended to normalize to the number of replication forks in the sample). After normalization to the histones (Fig. 3f, Supplementary Fig. 3e), we observed a strong decrease of MCM subunits, subunits of all three replicative polymerases and all RPA subunits. After normalization to MCM subunits (Fig. 3g, Supplementary Fig. 3f, Supplementary Table 1), we still observed a strong decrease in both POLE1 and POLE2 subunits, implying that there existed a subset of active replication complexes that included MCM helicase, but lacked polymerase epsilon. POLE3 and POLE4 subunits’ signals were very weak, and we therefore did not include them in the quantifications. We were also able to observe a decrease in POLA1 (polymerase alpha catalytic subunit), but DNA polymerase delta subunits showed no change relative to MCM after POLE1 depletion. This suggests that after POLE1 depletion there may exist a subset of active replication complexes that lack POLE, and possibly POLA. No other replication proteins showed a strong change in abundance relative to MCM after POLE1 depletion. No specialized polymerases were detected in the experiment. Overall, our data pointed to POLA/POLD-dependent DNA synthesis in the absence of POLE1.

POLE1 depletion does not lead to MCM unloading from failed replication forks

A decrease in MCM signal compared to nascent DNA (histones) (Fig. 3f) could indicate CMG helicase unloading upon failure of replication in the absence of POLE—in this case nascent DNA would not be associated with an active helicase anymore. CUL2 and p97/VCP have been shown to control CMG disassembly during S-phase in mammalian cells³¹, therefore we studied the signal for VCP/p97 in the iPOND data (CUL2 signal was insufficient for quantification). We observed an increase in VCP/p97 abundance in the iPOND pulldown, relative to MCM (Supplementary Fig. 4a), indicating possible active unloading of CMG through p97-mediated mechanism upon replication failure in the absence of POLE1. However, POLE1 depletion did not lead to a decrease of MCM7 on chromatin by FACS (Fig. 4a, b).

In order to study the presence of MCM at the sites of DNA replication more directly, we turned to single-molecule localization microscopy (SMLM) and analyzed EdU, PCNA, and MCM signals in replicating cells in high resolution (Fig. 4c). While EdU cluster density did not change after dox/aux treatment of clone 16 cells

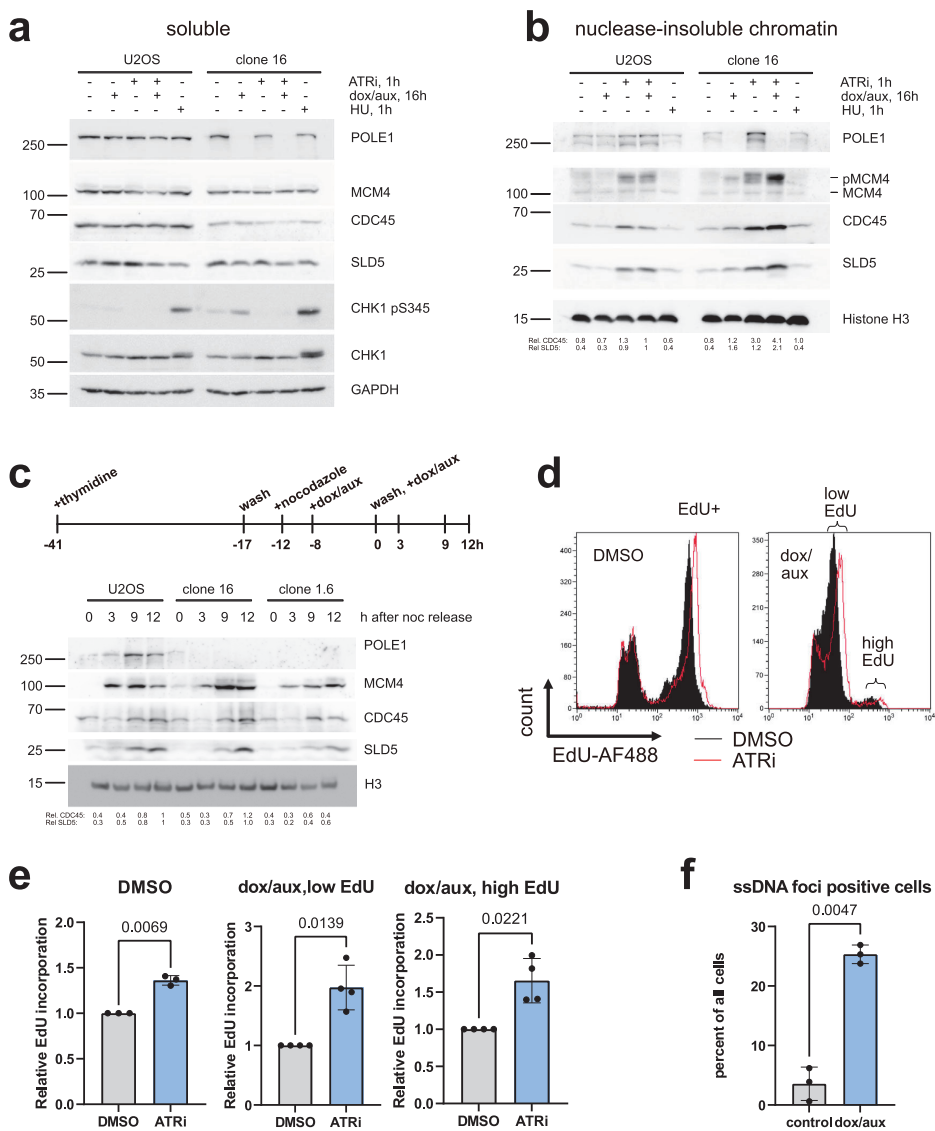
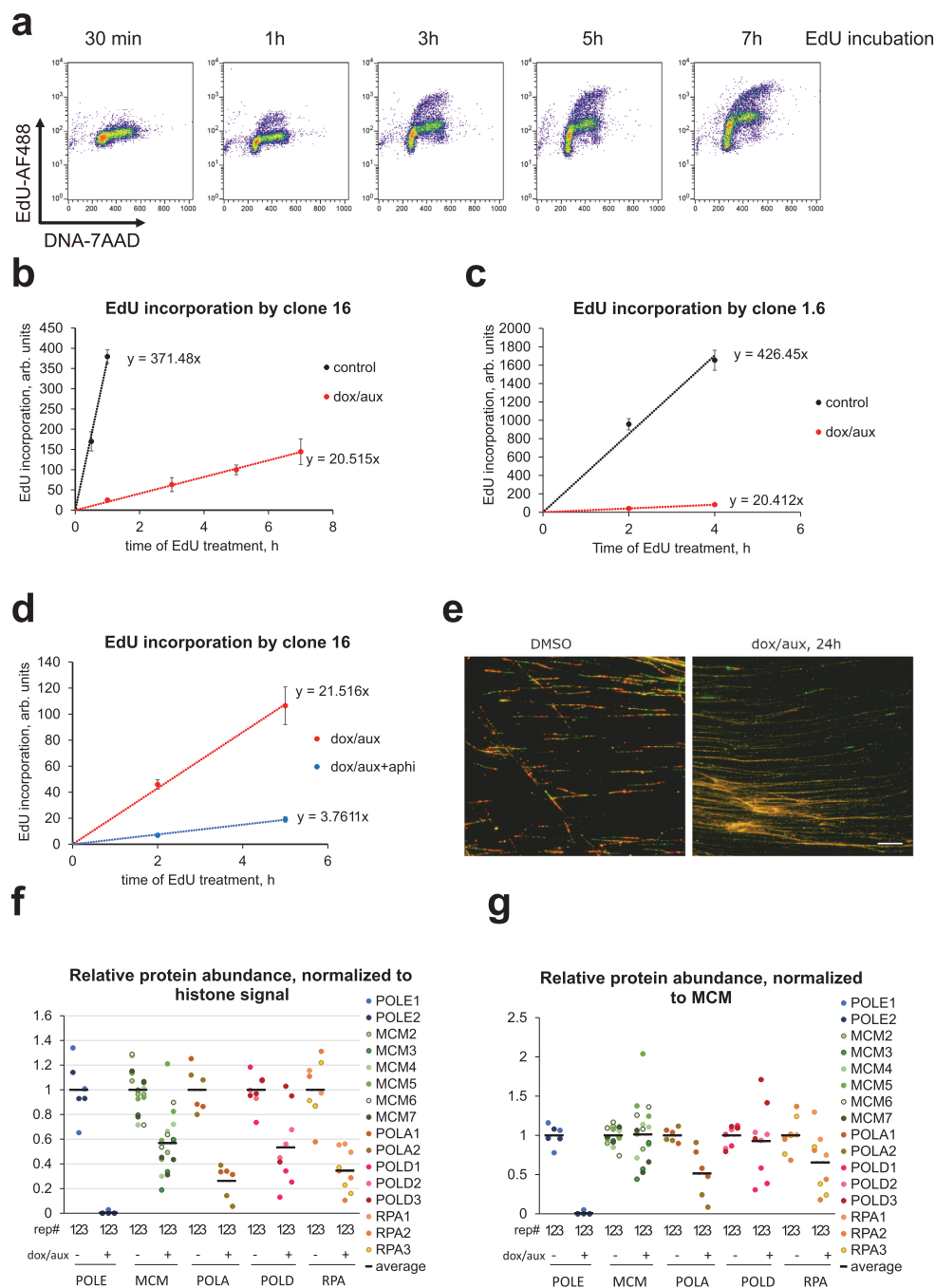


Fig. 2 | Origin firing in POLE1-depleted cells. a, b Wild-type U2OS or homozygous mAID-KI clone 16 were treated for 16 h with DMSO or dox/aux, 5 μ M ATRi was added to the indicated samples for 1 h, followed by cell lysis and the isolation of the insoluble chromatin fraction. Equal amounts of protein were loaded. Western blot of the soluble lysates (**a**) and insoluble chromatin fraction (**b**) is shown. 1 h hydroxyurea (HU, 2 mM) treatment was used as a positive control for replication stress. The second band on POLE1 blot (**b**) likely represents partially degraded protein. Specific signals of SLD5 and CDC45 were quantified by Fiji/ImageJ. **c** Indicated cell lines were synchronized by thymidine/nocodazole blocks and treated with dox/aux as indicated. Western blot analysis of chromatin from the cells collected at the indicated timepoints is shown. Equal amounts of protein were loaded. Specific signals of SLD5 and CDC45 were quantified by Fiji/ImageJ.

d, e Clone 16 cells were treated for 16 h with DMSO or dox/aux as indicated, DMSO or 5 μ M ATRi was added to the indicated samples for 60 min before harvest, 10 μ M EdU was added for the last 30 min of treatment. Flow cytometry plots showing EdU incorporation histograms (**c**) and relative EdU incorporation, normalized to the samples without ATRi, are shown (**d**)—mean \pm SD from $n = 3$ (DMSO) or $n = 4$ (dox/aux) independent experiments. Paired t-test was used for statistical analyses, p values are shown. **f** Clone 16 cells were incubated with 10 μ M CldU for 48 h, DMSO or dox/aux were added for the last 16 h of treatment. After CSK extraction, cells were fixed and stained with anti-CldU antibodies under native conditions. Quantification of ssDNA-positive cells is shown—mean \pm SD from $n = 3$ independent experiments. Paired t-test was used for statistical analyses, p value is shown. Source data are provided as a Source data file.



(Supplementary Fig. 4b), the amount of EdU per focus (Fig. 4d) and the average EdU density around PCNA (Supplementary Fig. 4c) significantly dropped after dox/aux treatment, confirming slow and inefficient DNA synthesis by POLE1-depleted cells. In contrast to EdU, both MCM cluster density (Supplementary Fig. 4d) and the amount of MCM per focus (Fig. 4e) were not affected by dox/aux treatment.

These data indicate that the failed origin firing in the absence of POLE1 does not lead to MCM unloading.

Interestingly, SMLM analysis of PCNA foci in POLE1-depleted cells showed that both PCNA cluster density (Fig. 4f) and the amount of PCNA per focus (Fig. 4g) slightly decreased in response to POLE1 depletion, while the overall PCNA signal remained

Fig. 3 | The effect of POLE1 depletion on DNA synthesis. **a–d** Clone 16 (**a, b, d**) or clone 1.6 (**c**) cells were treated for 16 h with dox/aux, followed by 10 μ M EdU additional for the indicated times. For (**d**) 2 μ M aphidicolin was added 1 h before the start of the EdU pulses. Flow cytometry plots showing EdU incorporation and DNA content (**a**) or EdU incorporation quantifications (**b–d**) are shown. Quantification is based on four (**b**) or three (**c, d**) independent experiments, means and standard deviations are shown, dox-resistant population was disregarded for the quantification. **e** Clone 16 cells were treated for 24 h with DMSO or dox/aux. Ongoing

replication was labeled with 10 min pulse of CldU (red) followed by 20 min pulse of IdU (green) and visualized using DNA fiber analysis, as described in “Methods”. Scale bar is 10 μ m. **f, g** Clone 16 cells were treated for 16 h with DMSO or dox/aux, followed by 10 min EdU pulse and iPOND isolation of protein, associated with nascent DNA, and mass-spectrometry. The signal was normalized to average signal of histones (**f**) or MCM subunits (**g**) in each sample, and to respective DMSO-treated samples. The means from $n = 3$ experimental replicates for each group are shown as horizontal black lines. Source data are provided as a Source data file.

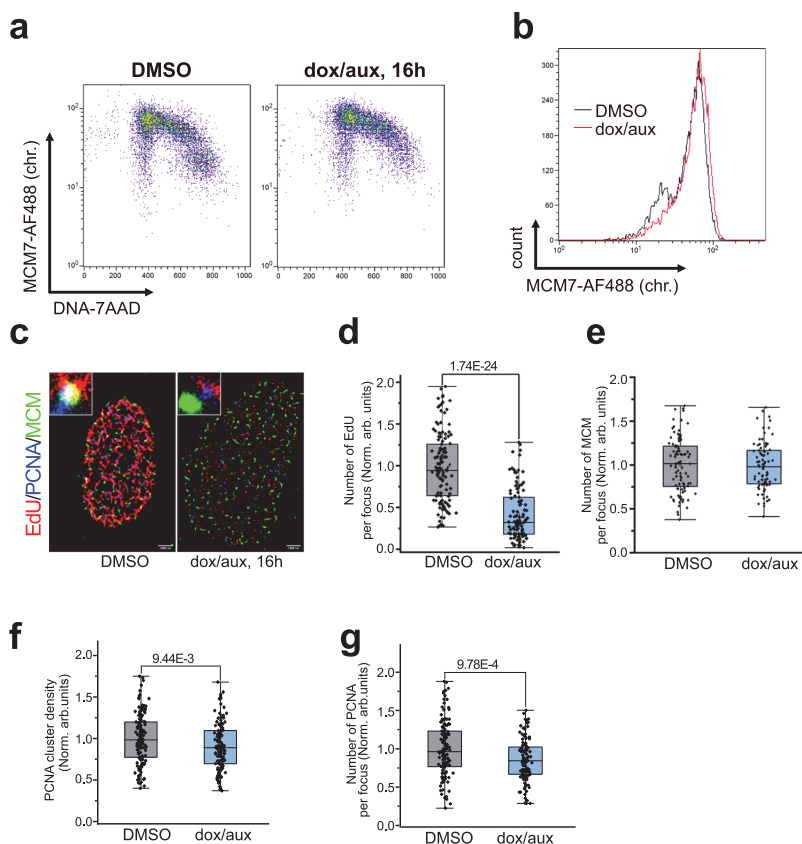


Fig. 4 | MCM on chromatin after POLE1 depletion. **a, b** Clone 16 cells were treated for 16 h with DMSO or dox/aux, followed chromatin extraction and MCM7 immunostaining. Flow cytometry plots of DNA/MCM7 staining (**a**) or MCM7 histograms (**b**) are shown. **c–g** Clone 16 cells treated for 16 h with DMSO or dox/aux were pulse labeled with thymidine analog EdU for 15 min prior to processing for super-resolution imaging. Representative multicolor super-resolution images (**c**) of PCNA (blue), MCM (green), and extent of EdU (red) incorporation in S-phase nuclei. Scale bar, 1500 nm. Quantitation of EdU (**d**) and MCM (**e**) detected per focus normalized

to DMSO-treated clone 16 control, based on at least 3 independent experiments (For EdU per focus, $n = 131, 109$, and for MCM per focus $n = 95, 83$ for DMSO and dox/aux treated clone 16 cells. Student's t-test was used for analyses, mean + SD and the p values are shown. Quantitation of PCNA detected per focus (**f**) and PCNA clusters (**g**), normalized to DMSO-treated clone 16 cells based on at least 2 independent experiments. (PCNA per focus, $n = 126, 106$; PCNA cluster density, $n = 139, 120$; student's t-test was used for analyses, mean + SD and p values are shown). Source data are provided as a Source data file.

unchanged (Supplementary Fig. 4e). Lower number of PCNA molecules per fork is consistent with failure to establish lagging strand synthesis that normally harbors the majority of PCNA molecules.

The C-terminal part of POLE1 supports DNA synthesis in the absence of the full-length protein

Previous studies in yeast have demonstrated that the non-catalytic C-terminal domain of POLE1 is sufficient for cell viability in the absence of

the full-length protein, implying that the essential function of POLE1 in replication initiation is not its catalytic function^{5,12}. In agreement with this, in *Xenopus laevis* egg extracts, the C-terminal non-catalytic domain of DNA polymerase epsilon was also able to partially restore DNA synthesis after the depletion of the endogenous protein³². In order to validate this model in human cells, we created several truncation mutants of POLE1 (Fig. 5a). Wild type and catalytically dead POLE1 were N-terminally tagged with FLAG-HA; N-terminal catalytic domain of POLE1 (cat), C-terminal domain (Δ cat), and Δ cat missing the

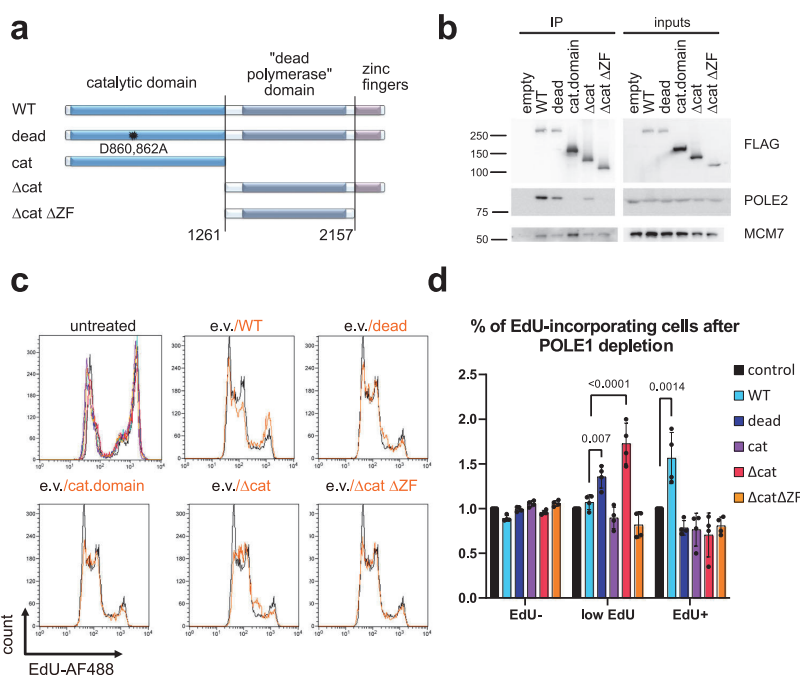


Fig. 5 | C-terminal non-catalytic part of POLE1 is critical for replication initiation. **a** Schematic representation of POLE1 constructs used in the study: wild-type protein, catalytically dead protein with mutations D860A, D862A, catalytic domain of POLE1 (aa1–1261), C-terminal half of POLE1 (without the catalytic domain, aa 1262–2305), C-terminal part of POLE1 without the zinc-finger domain (aa 1261–2151). **b** 293FT cells were transfected with an empty vector or the constructs described in panel a, fused to FLAG tags at their N termini. 48 h later cells were lysed and FLAG-tagged proteins were immunoprecipitated using M2 agarose beads, followed by elution with FLAG peptide. Western blots of the eluted protein and input samples are shown. **c**, **d** Clone 16 cells were transfected with indicated constructs. 32 h later dox/aux or DMSO was added to the cells for 16 h. 10 μ M EdU was

added for the last 30 min. Flow cytometry histograms of the EdU incorporation are shown (c). The first panel shows the transfected untreated samples, colors match the legend on 2D, the other panels represent samples treated with dox/aux for 16 h. Comparisons of samples transfected with indicated constructs (orange) to the sample transfected with an empty vector (black) are shown (c). **d** Quantification of the percent of cells in the dox/aux treated cells, corresponding to the indicated fractions, normalized to the empty vector control, are shown. Fractions were gated as indicated in Fig. S2. The quantification is based on $n = 4$ independent experimental repeats (means + SD and p values are shown where they are significant. One-way ANOVA was used for statistical analyses). Source data are provided as a Source Data file.

very C-terminal part containing zinc fingers (Δ cat Δ ZF) were N-terminally tagged with myc-FLAG tags.

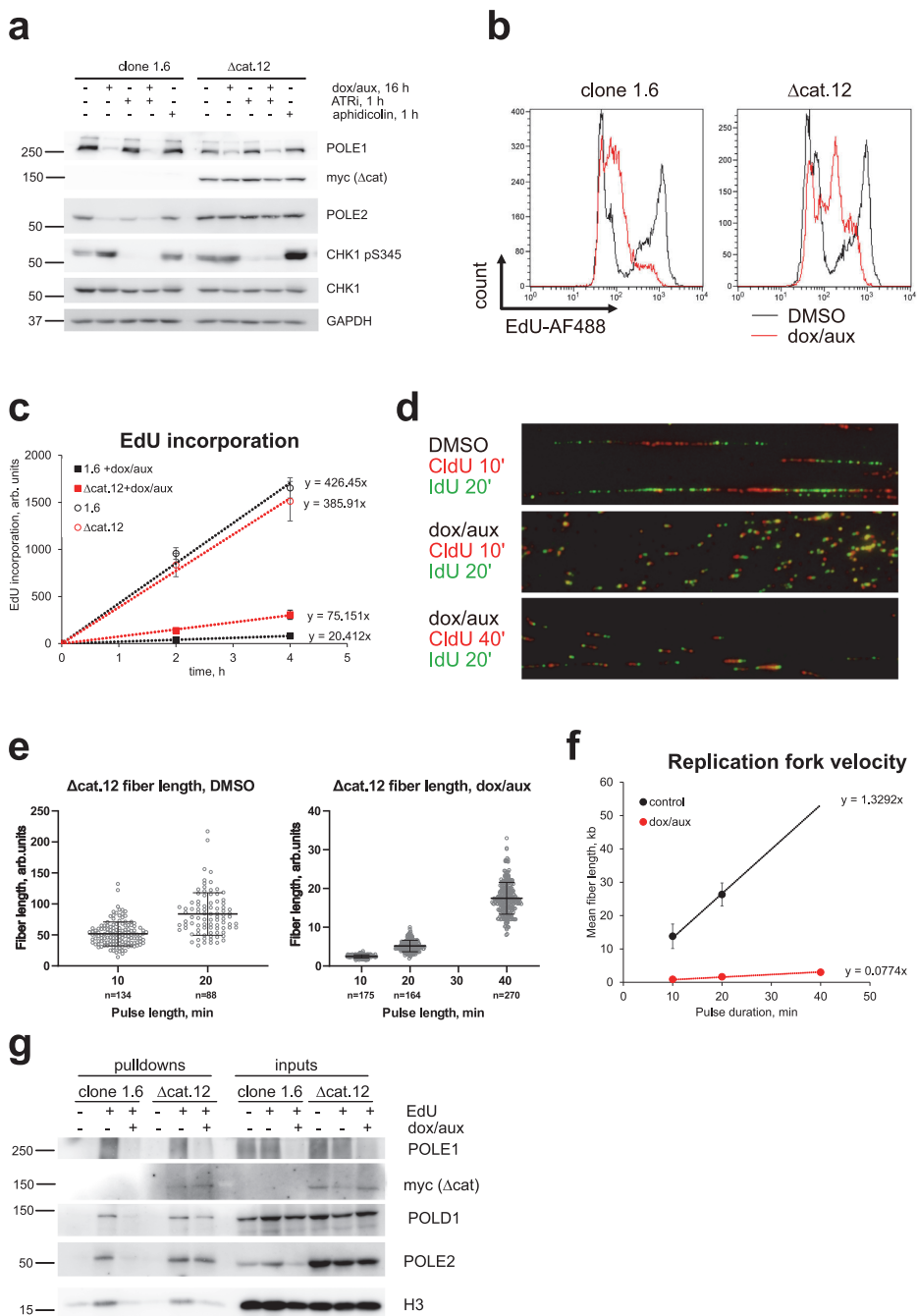
In order to check if the mutations and deletions affected the interactions of POLE1 with other replication proteins, we expressed the constructs in 293FT cells, followed by immunoprecipitation with FLAG-M2 beads, elution with FLAG peptide, and western blotting with antibodies against POLE2 and MCM7 (Fig. 5b). Previous studies³³ have shown that the C-terminal zinc-finger region binds the second DNA polymerase epsilon subunit POLE2. In agreement with these data, we found that cat (1–1261) and Δ cat Δ ZF (1262–2157) constructs were unable to pull down POLE2. However, all the POLE1 constructs retained the ability to co-precipitate with MCM complex.

We then proceeded to test if any of the POLE1 constructs could rescue DNA synthesis after POLE1 depletion. 32 h after transfection of the clone 16 cells with the described POLE1 constructs, we treated cells with DMSO or doxycycline/auxin for 16 h followed by labeling of ongoing replication with EdU for 30 min, and FACS analysis. Our experiment showed that expressing POLE1 or its truncation mutants in the absence of dox/aux treatment did not affect the percentage of EdU-positive cells or the level of EdU incorporation (Fig. 5c). However, cells transfected with POLE1 mutants after the depletion of the endogenous POLE1, displayed differences in EdU incorporation profile (Fig. 5c, d). As expected, the expression of the WT construct led to the increase in the cells incorporating EdU at the level of untreated S-phase

cells, confirming that the WT protein can fully restore replication. The expression of the N-terminal catalytic domain of POLE1 had no effect on EdU incorporation by dox/aux treated cells, but the expression of the C-terminal domain of POLE or the catalytically inactive POLE1 led to an increase in the fraction of cells with low level EdU incorporation ("low EdU", gating is shown on Supplementary Fig. 5a). This fraction did not increase with the expression of the Δ cat Δ ZF fragment of POLE1. The quantification of the three fractions—EdU-negative cells, cells incorporating low levels of EdU, and cells incorporating normal (high) levels of EdU, normalized to the control transfected with an empty vector—is shown in Fig. 5d. These data indicate that, in the absence of the full-length protein, the C-terminal zinc-finger region of POLE1, responsible for the interaction with POLE2, is essential for the partial rescue of DNA synthesis by Δ cat—the non-catalytic C-terminal domain of POLE1.

Slow DNA synthesis in presence of POLE1 C-terminal non-catalytic domain

In order to further investigate the DNA synthesis supported by Δ cat, we decided to develop a cell line that stably expressed Δ cat and could degrade the endogenous POLE1 after dox/aux treatment. Unfortunately, clone 16 could not be used, due to its resistance to multiple antibiotics, which made additional selection for adding Δ cat impossible. We therefore transfected clone 1.6 with a plasmid, expressing



Δ cat and a neomycin resistance marker, selected with G418, and performed single-cell cloning. We were able to identify two clones stably expressing Δ cat- Δ cat.12 and Δ cat.25 (Fig. 6a, Supplementary Fig. 6a). After the depletion of the endogenous POLE1 by dox/aux treatment, Δ cat cells showed EdU incorporation about 5 times lower than that of the POLE1-proficient cells, but still 4 times higher than POLE1-depleted clone 1.6 cells (Fig. 6b, c, Supplementary Fig. 6b). As the selection/

subcloning took some time, the dox-resistant population in Δ cat.12 and Δ cat.25 is relatively high even in the very early passages (Fig. 6a, b, Supplementary Fig. 6a).

One of the key properties of Δ cat is its ability to retain the interaction with POLE2 and MCM (Fig. 5b). Indeed, POLE1-depleted clone 1.6 showed a strong reduction in POLE2 level, indicating that POLE1 is necessary for POLE2 stability (Fig. 6a). Expressing Δ cat completely

Fig. 6 | DNA replication-dependent on the C-terminal non-catalytic domain of POLE1. **a–c** Clone 1.6 homozygous mAID-K1 cells (1.6) or clone 1.6 stably expressing myc-FLAG- Δ cat - clone 12 (Δ cat.12) were treated for 16 h with DMSO or dox/aux. **a** 5 μ M ATRi was added to the indicated samples for 1 h. Western blot of the whole cell lysates is shown. 1 h aphidicolin (2 μ M) treatment was used as a positive control for replication stress. **b, c** EdU was added for the last 30 min (**b**) or 2–4 h (**c**) of treatment, flow cytometry histograms of EdU incorporation (**b**) or EdU incorporation quantifications (**c**) are shown. Quantification is based on $n = 3$ independent experiments, means \pm SD are shown, dox-resistant population was disregarded for quantification. **d–f** Δ cat.12 cells were treated for 16 h with DMSO or

dox/aux. Ongoing replication was labeled with 10- or 40-min pulse of CldU followed by 20 min pulse of IdU and visualized using DNA fiber analysis, as described in “Methods”. Representative images (**d**), individual fiber lengths from a representative experiment (mean and SD) (**e**), and mean fiber lengths (based on $n = 3$ experimental repeats) and SD of the means (**f**), are shown. **g** Clone 1.6 and Δ cat.12 cells were treated for 16 h with DMSO or dox/aux, followed by 10 min EdU pulse (where indicated) and iPOND isolation of proteins, associated with nascent DNA. Western blot analyses of the inputs and pulldown samples are shown. Source data are provided as a Source data file.

rescued this effect, confirming that this C-terminal domain of POLE1 is sufficient for the interaction with and stabilization of POLE2 (Fig. 6a, Supplementary Fig. 6a).

Clones 16 and 1.6 exhibited ATR activation in response to POLE1 depletion (Figs. 2a, 6a, Supplementary Fig. 2b), however, Δ cat expression rescued this phenotype, indicating that using Δ cat in DNA replication did not lead to an accumulation of single-stranded DNA. ATRi treatment led to a modest increase in EdU incorporation in POLE1-depleted Δ cat-expressing cells, suggesting lower availability of unfired dormant origins (Supplementary Fig. 6c, d).

In order to assess the replication dynamics of cells relying on Δ cat in the absence of endogenous POLE1, we performed DNA fiber analysis (Fig. 6d–f, Supplementary Fig. 6e, f). Dox/aux treated Δ cat cells showed a very distinct phenotype of extremely short DNA fibers (Fig. 6d). Using longer CldU pulses we were able to measure replication fork velocity in such cells, which was about 18 times lower than the mean fork speed in POLE1-proficient cells (Fig. 6f). While we were not able to reliably measure inter-origin distances in dox/aux treated cells, it is clear from the imaging (Fig. 6d) that the inter-origin distances in such cells are shorter. Based on 5 \times lower EdU incorporation and 18 \times lower replication fork velocity compared to POLE1-proficient cells, and given that $\text{EdU} \sim \# \text{ of forks} \times \text{fork speed}$, we can expect about 3.6 \times more replication forks in dox/aux treated 1.6 + Δ cat cells. These data suggest that in U2OS cells the non-catalytic C-terminal domain of POLE1 is sufficient for DNA replication initiation, however, the resulting replication forks are extremely slow.

In the yeast system, in the absence of the catalytic domain of DNA polymerase epsilon, polymerase delta is thought to step in to synthesize the leading strand¹⁴. In order to check if this is true in human cells, we performed an iPOND experiment with clones 1.6 and Δ cat.12 (Fig. 6f). Our data confirmed, that POLE2, Δ cat, and POLD1 were present at the replication forks. These data are in agreement with the model where in the absence of POLE1 catalytic domain, its C-terminal non-catalytic domain was sufficient for the stabilization of POLE2 and DNA replication initiation, while POLD takes over the DNA synthesis at the leading strand.

In summary, our data indicate that in the absence of POLE1, replication origin firing in human cells proceeds past CMG assembly and activation, but fails at a later step. C-terminal non-catalytic domain of POLE1 is capable of rescuing this defect, resulting in continuous DNA synthesis, however, in this case replication forks are very slow.

Discussion

Origin firing in the absence of POLE1

In this study, we used an auxin-inducible degron system to establish rapid and efficient depletion of POLE1 in human cells. POLE1 knockdowns were previously used as controls in studies of other replication proteins^{34,35}. In the study by Ercilla et al.³⁵ POLE knockdown only slightly decreased EdU incorporation by S-phase cells, indicating that knockdown efficiency may have not been sufficient. While POLE4 knockout led to a decrease in POLE1 concentration²¹, the levels of POLE1 in the iPOND pulldowns were not affected by POLE4 knockout, confirming only partial depletion. In our study, the efficiency of rapid POLE1 depletion using an auxin-inducible degron system is confirmed

by its virtual absence in the iPOND pulldowns, which allowed us to observe and study defective replication origin firing in the absence of POLE1.

Here we show that while POLE1 depletion blocked any processive DNA synthesis, the number of active replication origins in POLE1-depleted cells was not limited by the level of POLE1, as additional origins were rapidly activated by ATR inhibition, which can be observed by the recruitment of the replication proteins to the chromatin fraction, phosphorylation of MCM4, and the increase in EdU incorporation (Fig. 2a, b, d). CMG assembly on chromatin was also observed during S-phase entry of POLE1-depleted cells (Fig. 2c).

One possible explanation of these data is that the scarce POLE transiently associates with pre-RCs, ensuring replication initiation, and quickly dissociates, moving on to the next pre-RC. This would agree with the absence of POLE1 in the iPOND pulldowns, but it would contradict a recent study³⁶ showing that yeast DNA polymerase epsilon has a very low exchange rate at the replication fork in vitro and this rate only goes down with the decrease of the concentration of polymerase epsilon. An alternative explanation is that POLE1 is not required for the initial steps of DNA replication initiation, but DNA synthesis stalls quickly after origin firing.

In yeast estimated the initial DNA synthesis at the origins (~180 bp) is performed by DNA polymerase delta², after which polymerase epsilon takes over. We propose that the DNA synthesis that we observe in the absence of POLE1 is the initial POLA/POLD-dependent synthesis that fails at the polymerase switch step (Fig. 7)—one notable structural rearrangement after the initial helicase activation. While further biochemical and structural studies are needed to confirm this model, it is supported by a “dotty” fiber pattern (Fig. 3e) and aphidicolin sensitivity of EdU incorporation by POLE1-depleted cells (Fig. 3d). Based on yeast data, we expected 100–200 bp tracks synthesized by POLD before the switch²⁴, however, at 2.59 kb/ μ m³⁷ 100 bp tracks would appear as 39 nm. This is below the resolution limit of our microscope, so we believe that such short DNA pieces appear as “dots” in the DNA fiber analysis.

Our data indicate that after DNA replication fails, MCM helicases are not unloaded and remain associated with chromatin (Fig. 4a–e). In addition, based on the accumulation of single-stranded DNA and ATR activation in POLE1-depleted cells (Fig. 2a, f), it is likely that MCM continues DNA unwinding for some time after DNA synthesis fails. It remains unclear what happens to these failed replication complexes, but being located far enough from the failed DNA synthesis could explain their decrease in the iPOND pulldown. As a standard response to ssDNA and replication stress, we would expect the recruitment of fork stabilization and remodeling proteins³⁸, but since proper replication forks are never established in the absence of POLE, the same mechanisms may not apply. No pathway allowing activated MCMs to be re-loaded back onto double-stranded DNA has been described to date, so MCMs from failed replication initiation likely remain encircling one DNA strand each.

A recent series of publications^{31,39,40} demonstrated that the DNA strand excluded by MCM helicase masks the site on MCM required for its recognition by CUL2/LRR ubiquitin ligase, preventing the disassembly of CMG helicase. In our model, where replication can't be

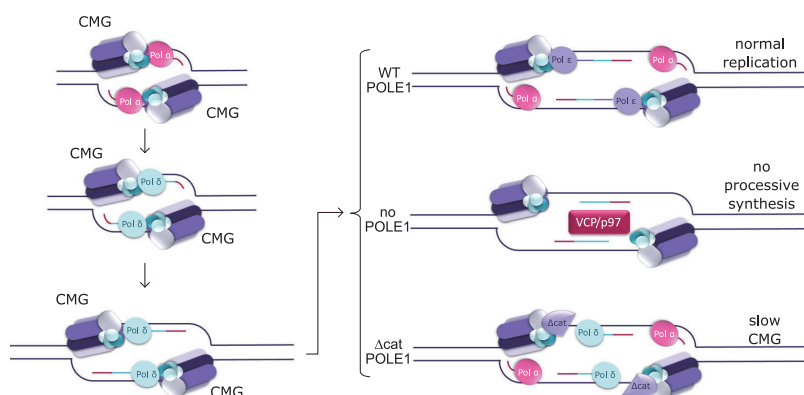


Fig. 7 | Proposed model of DNA replication initiation in human cells with and without POLE1, as well as in presence of Δ cat. POLE may be present at the early stages of origin firing, but according to our data it is not necessary. Under normal conditions, POLE replaces POLD as a leading strand polymerase. In the absence of

POLE, DNA synthesis fails at the polymerase switch step. Non-catalytic C-terminal domain of POLE1 is sufficient to proceed to replication elongation, in this case, POLD assumes the role of the leading strand polymerase, but the speed of DNA synthesis is much slower.

completed and MCM encircles one strand of DNA, allowing the excluded strand to prevent its disassembly, any unloading of the activated CMG from DNA is highly unlikely. A slight increase in p97 association with nascent DNA (Supplementary Fig. 4a) could be related to its recently proposed role in unloading excessive POLA/PRIM during origin firing⁴¹, but this requires further investigation.

DNA synthesis in the presence of C-terminal non-catalytic domain of POLE1

In U2OS cells that lack full-length POLE1, the expression of the C-terminal non-catalytic domain of POLE1 was sufficient for continuous albeit slow DNA synthesis (Fig. 6d, e). Similar observations have been previously made in yeast¹³, and our data suggest that the non-catalytic function of DNA polymerase epsilon is conserved in mammalian cells. Furthermore, in yeast, in the absence of the catalytic domain of Pol2, polymerase delta replicated both strands¹⁴. We observe a similar phenotype in U2OS cells expressing Δ cat in the absence of the full-length POLE1: POLD is associated with nascent DNA together with POLE2 and the C-terminal domain of POLE1 (Fig. 6f).

In the absence of POLE1 catalytic domain in U2OS cells, replication fork velocity was dramatically reduced (Fig. 6d, e). Nevertheless, such cells did not show any strong ATR activation, implying the absence of any significant replication stress caused by helicase/polymerase uncoupling. Therefore, the slow replication fork velocity is likely caused by slow DNA unwinding by the CMG helicase. Similar observations were previously made in a reconstituted yeast system¹⁷, confirming that the important role of the N-terminal catalytic domain of DNA polymerase epsilon catalytic subunit in full activation of the CMG helicase is conserved.

Protein-protein interactions of POLE1 and their role in origin firing in human cells

Our data demonstrate that the interaction between POLE1 and POLE2 was essential for supporting DNA synthesis: deleting the C-terminal zinc-finger region of Δ cat, responsible for the interaction with POLE2³³ (Fig. 5b), completely abolished its ability to support EdU incorporation in the absence of the full-length protein (Fig. 5c, d). Moreover, the expression of Δ cat was necessary and sufficient for POLE2 stability and recruitment to the replication fork (Fig. 6f). These data indicate that the essential role of POLE1 in replication initiation may include the stabilization and recruitment of POLE2. What makes POLE2 presence at

the replication initiation sites critical, remains to be elucidated. In yeast, the second subunit of DNA polymerase epsilon Dpb2 is essential for CMG assembly, and the expression of its N-terminal domain was sufficient to support cell viability, producing replisomes that lack DNA polymerase epsilon⁷. However, according to our data, POLE1 and POLE2 (which is destabilized in the absence of POLE1) are dispensable for CMG assembly and MCM phosphorylation on chromatin in response to ATRi in human cells (Fig. 2b, c). We therefore propose that POLE2 is critical at one of the later steps of replication initiation, possibly at the structural perturbations associated with the polymerase switch. According to a recent structural study⁴², human POLE2 binds the GINS-MCM junction of the CMG helicase, which could make POLE2 essential for the CMG stability during some conformational changes, such as the polymerase switch step. Further biochemical and structural studies are necessary to address this question.

We found that both N-terminal catalytic domain and C-terminal non-catalytic domain of POLE1 can co-precipitate with MCM (Fig. 5b). According to structural studies of yeast⁴³ and human⁴² replisomes, the PolE active conformation is connected to CMG solely through the C-terminal part of Pol2. However, the N-terminal domain of Pol2 participated in CMG binding in the inactive conformation⁵. In agreement with these findings, the N-terminal domain of Pol2 has recently been shown to play a role in mediating CMG-PolE interaction in yeast⁴⁴. Our data suggest a possibility for a similar mechanism in human cells.

Overall, our study provides some insights into the non-catalytic role of DNA polymerase epsilon in human cells. Since POLE1 mutations associated with multiple cancers and developmental diseases are often outside its catalytic domain, elucidating the non-catalytic functions of this protein may help shed a light on the molecular mechanisms behind these diseases.

Methods

Plasmids and cloning

For osTIRI K1 we used PX458-AAVS1 (a gift from Adam Karpf—Addgene plasmid # 113194) and pMK243-Tet-OsTIRI-PURO (a gift from Masato Kanemaki—Addgene plasmid # 72835) plasmids²⁴. For mAID K1 templates, homology arms were synthesized by Genscript in the pUC57 vector with stop codon substituted to BamHI site (TGCTCGGC TCAGCCTGGCCTCCTTGGCCTCCTCTGAGTGGACTGGGGTCTCAC TGTGCTGTATTATTCCTGCAGGTCTTCATGGAACAGATCGGAATATTC CGGAACATTGCCAGCACTACGGCATGTCGTACCTCCTGGAGACCT AGAGTGGCTGCTGCAGAAGAACCCACAGCTGGGCCATGGATCCCCAG

CCCCGGGCCCCGGGTGCCTCTGCGTCCGTGCCAGGCTCTGATGCC
AAGGCCACATCCCCGTCTCCAGTGACCAGACCACTGACCACCCTG
ACTGTCCAAACCTGTGACCCAGGCCAGGGAACGGGGAGGAAACCA
AAG).

Inserts from plasmids pMK293 (mAID-mCherry2-Hygro) and pMK292 (mAID-mCherry2-NeoR) (Addgene plasmids # 72831 and # 72830) were gifts from Masato Kanemaki²⁴ were cloned into the BamHI site of the synthesized plasmids. POLE1 C-terminus-targeting gRNA (GTCGUACCUCCUGGAGACCC) was expressed from pSpCas9 BB-2A-Puro (PX459) v2.0 plasmids (Genscript). POLE1 plasmid⁴⁵ was used as a template for creating the described deletion mutants, which were cloned into pCMV-AN-myc-DDK vector (Origene). Catalytically dead POLE1 was described previously⁴⁵.

Cell lines, cell culture, and transfections

U2OS (ATCC HTB-96) cells were grown in RPMI media (Lonza), supplemented with 10% FBS (GIBCO) and 1% penicillin-streptomycin (Invitrogen). For KI cells were transfected with corresponding gRNA and one or two (NeoR and HygroR for mAID-mCherry KI) HR templates. Growth medium was changed 8 h after transfection, 2.5 μ M DNAPK inhibitor was added for 48 h. KI cells were selected with G418, puromycin and/or hygromycin until the non-transfected control died, followed by single-cell cloning and KI validation by PCR and/or western blot. Transfections were carried out using Lipofectamine 2000 (ThermoFisher), according to manufacturer's instructions.

293FT cells (ThermoFisher #R70007) were grown in DMEM media (Lonza), supplemented with 10% FBS (GIBCO) and 1% penicillin-streptomycin (Invitrogen).

Cell lysis, insoluble chromatin isolation, and western blots

Cells were lysed in 50 mM Tris-HCl (pH 7.5), 150 mM NaCl, 50 mM NaF, 1% Tween-20, 0.5% Nonidet P-40, and protease inhibitors (Pierce #A32953) for 20 min on ice. Lysates were cleared by centrifugation, and soluble protein was used for immunoprecipitation or mixed with 2 \times Laemmli Sample Buffer (Bio-Rad) and incubated for 7 min at 96 °C and analyzed by Western blot. For nuclease insoluble chromatin, pellets were suspended in 150 mM Hepes (pH 7.9), 1.5 mM MgCl₂, 10% glycerol, 150 mM potassium acetate, and protease inhibitors containing universal nuclease for cell lysis (ThermoFisher, #88700) and incubated for 10 min at 37 °C on the shaker. Nuclease-insoluble chromatin was pelleted by centrifugation, washed with water, and dissolved in Laemmli Sample Buffer.

For western blot analyses, proteins were separated in 8–12% SDS-polyacrylamide gels in Running buffer (25 mM Tris, 192 mM glycine, 0.1% SDS), transferred onto PVDF membrane (BioRad, #1620177) in transfer buffer (25 mM Tris, 192 mM glycine, 10% ethanol), blocked with 5% non-fat milk (BioRad, #1706404) in TBST (ThermoFisher, #BP2471, 0.1% Tween-20), incubated with an appropriate dilution of the primary antibody overnight at 4 °C, washed with TBST buffer, incubated with secondary antibody for 1 h at room temperature, washed with TBST and developed using SignalFire™ Elite ECL Reagent (Cell Signaling, #12757P) and ImageQuant LAS 4000 imager (GE Healthcare). Quantification of western blots was performed using Fiji/ImageJ (version 1.53u).

Synchronizations and chromatin loading of CMG components

2 mM thymidine was added to ~25% confluent cells for 24 h. After thymidine removal, cells were washed once with warm PBS and allowed to recover in fresh medium for 5 h. Nocodazole was then added for 12 h to stop the cells in G2/M. Dox/aux were added 4 h after nocodazole to ensure the completion of DNA replication before POLE1 depletion. 8 h later, cells were released from nocodazole, washed once with warm PBS and incubated in pre-warmed medium with dox/aux for the indicated periods of time.

In order to assess the loading of the CMG components on chromatin, samples were collected by trypsinization at the indicated timepoints, pellets washed once with ice-cold PBS and kept at –80 °C, and processed the next day.

Thawed pellets were resuspended in CSK buffer (10 mM PIPES pH 7.0, 300 mM Sucrose, 100 mM NaCl, 3 mM MgCl₂, 0.5% Triton X-100, protease inhibitors (Pierce #A32953)), incubated for 5 min on ice, followed by a 5-min centrifugation (1000 \times g, 4 °C). The supernatant was collected as “soluble fraction”, the pellets were washed once more with CSK buffer, digested in CSK buffer with universal nuclease for cell lysis (ThermoFisher, #88700) for 10 min at 37 °C. Samples were mixed with 2 \times Laemmli Sample Buffer (BioRad) and boiled for 10 min before proceeding to western blot analysis.

Antibodies

POLE1 (Santa Cruz, #sc-390785, 1:500), osTIR1 (MBL International, #PD048, 1:1000), GAPDH (Santa Cruz, #sc-47724, 1:1000), pCHK1 (Cell Signaling, #2360S, 1:1000), Chk1 (Cell Signaling, #2348S, 1:1000), MCM4 (Cell Signaling, #3228S, 1:300), CDC45 (Santa Cruz, #sc-55569, 1:500), SLD5 (Santa Cruz, #sc-398784, 1:300), H3 (Santa Cruz, #sc-517576, 1:1000), MCM7 (Santa Cruz, #sc-9966, 1:1000), POLE2 (Santa Cruz, #sc-398582, 1:500), PCNA (Santa Cruz, #sc-56, 1:1000), FLAG (Sigma, F3165-1MG, 1:3000), myc (Cell Signaling, #2276, 1:1000).

Flow cytometry

For EdU FACS, cells were treated with 10 μ M EdU for 10 min, trypsinized, washed with PBS, and fixed with cold 70% ethanol on ice for 30 min to overnight. Cells were washed with PBS, and EdU staining was performed by using the EdU Click-iT kit (ThermoFisher, # C10632), according to the manufacturer's instructions. For DNA staining, we used 7-AAD (7-Aminoactinomycin D) (ThermoFisher, # A1310) or FxCycle™ PI/RNase Staining Solution (ThermoFisher, #F10797).

Chromatin association of MCM was assessed essentially as described⁴⁶: after trypsinization and PBS wash, cells were extracted with CSK buffer (10 mM PIPES pH 7.0, 300 mM Sucrose, 100 mM NaCl, 3 mM MgCl₂, 0.5% Triton X-100, protease inhibitors (Pierce #A32953), fixed with 4% paraformaldehyde, and blocked with 5% BSA followed by immunostaining with anti-MCM7 antibody (Santa Cruz, #sc-9966) at 1:200 dilution. 7-AAD (7-Aminoactinomycin D) (ThermoFisher, # A1310) was used for DNA staining.

Flow cytometry was performed on an FACSCalibur flow cytometer, and data were analyzed by using FCSalyzer software. Graph-Pad Prism 9 was used for statistical analyses.

Fiber analysis

DNA fiber analysis was performed essentially as in ref. 47. Briefly, ongoing DNA synthesis was labeled with the indicated nucleotide analogs, cells were washed with PBS, lysed with lysis buffer (0.5% SDS, 200 mM Tris-HCl (pH 7.4) and 50 mM EDTA) and spread on glass slides by tilting. After drying, the slides were fixed in methanol: acetic acid (3:1), dried, and rehydrated in PBS. DNA was denatured by incubating the slide in 2.5 N hydrochloric acid for 1 h. After neutralization in PBS, samples were blocked in blocking buffer (10% NGS in PBS), and stained with primary antibodies (Mouse Anti-BrdU Clone B44 (BD, #347580) for IdU, Abcam ab6326 for CldU, both 1:50 in the blocking buffer), washed with PBS-1%Tween20, incubated with fluorescently labeled secondary antibodies (Goat anti-mouse AlexaFluor 488 (Invitrogen, #A-11001), Goat anti-rat AlexaFluor 594 (Invitrogen, #A-11007), both 1:150 in blocking buffer). After extensive washes with PBS-Tween20 and PBS, slides were mounted with Prolong Diamond Antifade mounting medium (Invitrogen, #P36961). Samples were imaged using Olympus BX61 fluorescence microscope at 60 \times magnification; image analysis was performed using Fiji (ImageJ) software. At least 100 tracks per sample were analyzed.

PCR

For validations of the knock-ins, genomic DNA was isolated using genomic DNA miniprep kit (Zymo Research, # D3025). Primers: Endogenous allele (C-terminus of POLE coding region) Forward GACCAGCA TGCCGTGTACTG, Reverse CTCCTTCCTGTGACGTCTGAG; mAID KI Forward GACCAGCATGCCTGTGTACTG, Reverse GCGGCATGGACGAG CTGTACAA; osTIR1 endogenous allele (AAVS) Forward GGTCGGAGAG CTCAGCTAGT Reverse TGGTCCATCGTAAGCAAAC; primers to amplify tetR promoter (used for cloning) Forward: GGTACCGAGGAGA TCTGCCGCCGCGATCGCGCCCTGGTTTACATAAGCAAAGCTTATA, Reverse: ATCGTCGTCATCTTGTAAATCCAGGATATCGTCCAGTCTAGA CATGGAATTTCGATGATC.

IPOND

Nascent DNA pulldown was performed essentially as described³⁰. Four 150 mm dishes were used for each sample. Three independent experiments were performed. Briefly, ongoing DNA synthesis was labeled by incubation with 10 μ M EdU for 10 min, followed by washes and fixation with 1% formaldehyde, quenched with 0.125 M glycine, scraped off the plates and permeabilized with 0.25% Triton X-100 in PBS. After washes with PBS-0.5% BSA, click reaction was used to label EdU with biotin-azide (25 μ M azide-PEG3-biotin (Sigma # 762024), 10 mM sodium ascorbate, 2 mM copper sulfate). After washes with PBS-BSA cells were lysed in RIPA buffer (150 mM NaCl, 50 mM Tris-HCl pH 7.5, 1% Triton X-100, 0.1% SDS, protease inhibitor cocktail (Pierce #A32953) DNA was sheared using Bioruptor (Diagenode), 20 cycles of 30 s on/30 s off. After 15 min centrifugation (14,000 $\times g$, 15 min), supernatants were incubated with streptavidin agarose (Sigma Merck #S1638) overnight. After 3 washes with RIPA buffer, samples on agarose beads were stored at -80°C and transported to the Tartu University Proteomics Facility on dry ice. Alternatively, the beads were boiled with Laemmli Sample Buffer for 30 min, followed by western-blot analysis.

Proteomics sample preparation and LC/MS/MS analysis was performed at Proteomics core facility at the University of Tartu, Estonia, essentially as described previously⁴⁸, except that identification was carried out against [UniProt Homo sapiens reference proteome](#) with POLE1-mAID-mCherry addition. The detailed description is available alongside the deposited proteomics dataset with the ProteomeXchange ID PXD033757.

To assess the abundance of replication proteins we normalized the intensity of each protein of interest to the sum intensity of 6 MCM subunits or sum intensity of major histones (H1, H2A, H2B, H3, H4) in each sample, as indicated. Normalization approach was based on previously published method⁴⁹. In order to disregard the differences in intensities between proteins (as they largely depend on the protein's physical properties), we normalized the data for each protein to the average intensity of this protein in the control samples, focusing on the changes induced by treatments (except Supplementary Fig. 4a showing data for one protein only).

Single-stranded DNA staining

In order to assess the presence of ssDNA in the cells, cells were treated with 20 μ M CldU for 48 h, dox/aux were added to the indicated samples for the last 16 h of treatment. After two PBS washes, cells were briefly extracted with CSK buffer (10 mM PIPES pH 7.0, 300 mM Sucrose, 100 mM NaCl, 3 mM MgCl₂, 0.5% Triton X-100; 5 min on ice), followed by fixation with 4% paraformaldehyde for 10 min at room temperature. After washes with PBS, samples were blocked with 5% BSA and stained with anti-BrdU antibody (ab6326, 1:150) followed by the incubation with secondary antibody, goat anti-rat AlexaFluor 594 (Invitrogen #A-11007, 1:300). After extensive PBS washes, nuclei were stained with 0.1 μ g/ml Hoechst 33342 for 10 min and after a brief wash with PBS, samples were mounted using Prolong Diamond Antifade mounting medium (Invitrogen, #P36961). Samples were imaged using

Olympus BX61 fluorescence microscope at 60 \times magnification; cell containing over 5 bright ssDNA foci were considered ssDNA-positive.

Sample preparation, imaging, and image analysis for SMLM

Clone 16 cells were seeded onto glass coverslips (Fisher Scientific, 12-548-B) in a 6-well plate. At 50% cell confluence, cells were incubated with 2 μ g/ml doxycycline (dox) and 500 μ M auxin (aux) for 16 h to promote POLE1 degradation. Cells were incubated with 10 μ M EdU for 15 min prior to harvest to detect nascent DNA synthesis. Cells were then permeabilised with 0.5% Triton X-100 in ice-cold CSK buffer (10 mM Hepes, 300 mM Sucrose, 100 mM NaCl, 3 mM MgCl₂, pH 7.4) for 10 min at room temperature to remove a majority of the cytoplasmic and non-chromatin bound proteins followed by three PBS washes. Cells were fixed with 4% paraformaldehyde (Electron Microscopy Sciences, 15714) in PBS for 15 min, at room temperature. After washing twice with PBS, cells were washed with blocking buffer for 5 min, thrice (2% glycine, 2% BSA, 0.2% gelatine, and 50 mM NH₄Cl in PBS). Incorporated EdU was detected using the Click-iT Plus EdU Alexa Fluor 647 Imaging Kit (ThermoFisher, C10640). Cells were then washed with blocking buffer for 5 min, thrice followed by overnight incubation in blocking buffer at 4 $^{\circ}\text{C}$. Cells were then incubated with primary antibodies against MCM6, (Abcam ab236151, conjugated to IR750 – cat #1556-1, 1:2500) and PCNA (Santa Cruz Biotechnology, sc-56, 1:1000) in blocking buffer for 1 h, at room temperature. After three washes for 5 min each with blocking buffer, cells were incubated with mouse IgG, AF 488 (Invitrogen, A11029, 1:5000) in blocking buffer for 30 min, at room temperature. After three 5 min washes with blocking buffer, stained coverslips were mounted onto a glass microscope slide and freshly prepared imaging buffer (1 mg/mL glucose oxidase (Sigma, G2133), 0.02 mg/mL catalase (Sigma, C3155), 10% glucose (Sigma, G8270), 100 mM mercaptoethylamine (Fisher Scientific, BP2664100)) was flowed through just prior to imaging.

For SMLM-SR imaging, raw image stacks with a minimum of 2000 frames for each color, acquired at 33 Hz, were captured on a custom-built optical imaging platform based on a Leica DMI 300 inverted microscope with three laser lines, 488 nm (Coherent, Sapphire 488 LPX), 639 nm (Ultralaser, MRL-FN-639-1.2), and 750 nm (UltraLaser, MDL-III-750-500). Lasers were aligned and combined using dichroic mirrors and focused onto the back aperture of an oil immersion objective (Olympus, UApO N, 100 \times , NA = 1.49, TIRF) via multiband dichroic mirror (Semrock, 408/504/581/667/762-Di01). For multicolor imaging, fluorophores were sequentially excited using a Highly Inclined and Laminated Optical (HILO) illumination configuration. Corresponding emissions were expanded with a 2X lens tube, filtered using single-band pass filters in a filter wheel (Thorlabs, FW102C): IR750 (Semrock, FF02-809/81), AF488 (Semrock, FF01-531/40), AF647 (Semrock, FF01-676/37) and collected on a sCMOS camera (Photometrics, Prime 95B). A 405 nm laser line (MDL-III-405-150, CNI) was used to drive Alexa Fluor 647 fluorophores back to their ground state. Images were acquired using Micro-Manager (v2.0) software.

Precise localization of each collected single molecule was performed as described in refs. 50–53. For display purpose, the representative images were generated by rendering the raw coordinates into 10 nm pixel canvas, convolved with a 2D-Gaussian ($\sigma = 10$ nm) kernel and brightness/contrast of the individual color channels were adjusted for display purposes. Raw result tables of the localization coordinates for each fluorophore blinking within a $6 \times 6 \mu\text{m}^2$ square region of interest (ROI) were directly submitted to Auto-Pair-Correlation analyses^{54,55} to estimate the nuclear density of the fluorophores. Any artificial blinking events (one blinking event recorded multiple times in consecutive frames) were eliminated before the computation of cross-pair correlations.

A correlation profile was plotted as a function of the pair-wise distances and fit into a Gaussian model. The average molecular content and density within each focus was derived based on the computed

average probability of finding a given species around itself and the apparent average radius of the focus. This function estimated the nuclear density of EdU and MCM fluorophores within a nucleus, as well as average number of fluorophores within each EdU or MCM focus. For the Cross-PC analyses, the correlation profile was plotted as a function of the pair-wise distances between EdU and PCNA, and fitted into a Gaussian model to determine the cross EdU-PCNA pair correlation amplitude. Using this, we were able to estimate the average local density of EdU around each PCNA molecule within a given ROI.

Reporting summary

Further information on research design is available in the Nature Portfolio Reporting Summary linked to this article.

Data availability

The mass spectrometry proteomics data generated in this study have been deposited to the ProteomeXchange Consortium (<http://proteomecentral.proteomexchange.org>) via the iProX partner repository⁵⁶ with the dataset identifier [PXD033757](https://doi.org/10.1016/j.molcel.2018.10.019). The UniProt Homo sapiens reference proteome data used in this study for mass-spectrometry data analysis are available in the Uniprot database under Proteome ID [UP000005640](https://doi.org/10.1016/j.molcel.2018.10.019). Source data are provided with this paper.

References

- Moiseeva, T. N. & Bakkenist, C. J. Regulation of the initiation of DNA replication in human cells. *DNA Repair* **72**, 99–106 (2018).
- Zhou, Z.-X., Lujan, S. A., Burkholder, A. B., Garbacz, M. A. & Kunkel, T. A. Roles for DNA polymerase δ in initiating and terminating leading strand DNA replication. *Nat. Commun.* **10**, 3992 (2019).
- Aria, V. & Yeeles, J. T. P. Mechanism of bidirectional leading-strand synthesis establishment at eukaryotic DNA replication origins. *Mol. Cell* <https://doi.org/10.1016/j.molcel.2018.10.019> (2018).
- Garbacz, M. A. et al. Evidence that DNA polymerase δ contributes to initiating leading strand DNA replication in *Saccharomyces cerevisiae*. *Nat. Commun.* **9**, 858 (2018).
- Zhou, J. C. et al. CMG-Pol epsilon dynamics suggests a mechanism for the establishment of leading-strand synthesis in the eukaryotic replisome. *Proc. Natl Acad. Sci. USA* **114**, 4141–4146 (2017).
- Nick McElhinny, S. A., Gordenin, D. A., Stith, C. M., Burgers, P. M. J. & Kunkel, T. A. Division of labor at the eukaryotic replication fork. *Mol. Cell* **30**, 137–144 (2008).
- Sengupta, S., van Deursen, F., de Piccoli, G. & Labib, K. Dpb2 integrates the leading-strand DNA polymerase into the eukaryotic replisome. *Curr. Biol.* **23**, 543–552 (2013).
- Muramatsu, S., Hirai, K., Tak, Y.-S., Kamimura, Y. & Araki, H. CDK-dependent complex formation between replication proteins Dpb11, Sld2, Pol (epsilon), and GINS in budding yeast. *Genes Dev.* **24**, 602–612 (2010).
- Handa, T., Kanke, M., Takahashi, T. S., Nakagawa, T. & Masukata, H. DNA polymerization-independent functions of DNA polymerase epsilon in assembly and progression of the replisome in fission yeast. *Mol. Biol. Cell* **23**, 3240–3253 (2012).
- Dua, R., Levy, D. L. & Campbell, J. L. Analysis of the essential functions of the C-terminal protein/protein interaction domain of *Saccharomyces cerevisiae* pol epsilon and its unexpected ability to support growth in the absence of the DNA polymerase domain. *J. Biol. Chem.* **274**, 22283–22288 (1999).
- Kesti, T., Flick, K., Keränen, S., Syväoja, J. E. & Wittenberg, C. DNA polymerase epsilon catalytic domains are dispensable for DNA replication, DNA repair, and cell viability. *Mol. Cell* **3**, 679–685 (1999).
- Feng, W. & D'Urso, G. *Schizosaccharomyces pombe* cells lacking the amino-terminal catalytic domains of DNA polymerase epsilon are viable but require the DNA damage checkpoint control. *Mol. Cell. Biol.* **21**, 4495–4504 (2001).
- Goswami, P. et al. Structure of DNA-CMG-Pol epsilon elucidates the roles of the non-catalytic polymerase modules in the eukaryotic replisome. *Nat. Commun.* **9**, 5061 (2018).
- Garbacz, M. A. et al. The absence of the catalytic domains of *Saccharomyces cerevisiae* DNA polymerase ϵ strongly reduces DNA replication fidelity. *Nucleic Acids Res.* **47**, 3986–3995 (2019).
- Stepchenkova, E. I. et al. Compensation for the absence of the catalytically active half of DNA polymerase ϵ in yeast by positively selected mutations in CDC28. *Genetics* <https://doi.org/10.1093/genetics/iyab060> (2021).
- Witosch, J., Wolf, E. & Mizuno, N. Architecture and ssDNA interaction of the Timeless-Tipin-RPA complex. *Nucleic Acids Res.* **42**, 12912–12927 (2014).
- Yeeles, J. T. P., Janska, A., Early, A. & Diffley, J. F. X. How the eukaryotic replisome achieves rapid and efficient DNA replication. *Mol. Cell* **65**, 105–116 (2017).
- Logan, C. V. et al. DNA polymerase epsilon deficiency causes IMAGE syndrome with variable immunodeficiency. *Am. J. Hum. Genet.* **103**, 1038–1044 (2018).
- Pachlopnik Schmid, J. et al. Polymerase ϵ 1 mutation in a human syndrome with facial dysmorphism, immunodeficiency, livedo, and short stature ('FILS syndrome'). *J. Exp. Med.* **209**, 2323–2330 (2012).
- Frugoni, F. et al. A novel mutation in the POLE2 gene causing combined immunodeficiency. *J. Allergy Clin. Immunol.* **137**, 635–638.e1 (2016).
- Bellelli, R. et al. Pole instability drives replication stress, abnormal development, and tumorigenesis. *Mol. Cell* **70**, 707–721.e7 (2018).
- Bellelli, R. et al. Synthetic lethality between DNA polymerase epsilon and RTEL1 in metazoan DNA replication. *Cell Rep.* **31**, 107675 (2020).
- Nishimura, K., Fukagawa, T., Takisawa, H., Kakimoto, T. & Kanemaki, M. An auxin-based degron system for the rapid depletion of proteins in nonplant cells. *Nat. Methods* **6**, 917–922 (2009).
- Natsume, T., Kiyomitsu, T., Saga, Y. & Kanemaki, M. T. Rapid protein depletion in human cells by auxin-inducible degron tagging with short homology donors. *Cell Rep.* **15**, 210–218 (2016).
- Chou, H.-C. et al. The human origin recognition complex is essential for pre-RC assembly, mitosis, and maintenance of nuclear structure. *eLife* **10**, e61797 (2021).
- Gödecke, N. et al. Controlled re-activation of epigenetically silenced Tet promoter-driven transgene expression by targeted demethylation. *Nucleic Acids Res.* **45**, e147–e147 (2017).
- Kiziltepe, T. et al. 5-Azacytidine, a DNA methyltransferase inhibitor, induces ATR-mediated DNA double-strand break responses, apoptosis, and synergistic cytotoxicity with doxorubicin and bortezomib against multiple myeloma cells. *Mol. Cancer Ther.* **6**, 1718–1727 (2007).
- Moiseeva, T. N. et al. An ATR and CHK1 kinase signaling mechanism that limits origin firing during unperturbed DNA replication. *Proc. Natl Acad. Sci. USA* **116**, 13374–13383 (2019).
- Moiseeva, T. et al. ATR kinase inhibition induces unscheduled origin firing through a Cdc7-dependent association between GINS and And-1. *Nat. Commun.* **8**, 1392 (2017).
- Sirbu, B. M., Couch, F. B. & Cortez, D. Monitoring the spatiotemporal dynamics of proteins at replication forks and in assembled chromatin using isolation of proteins on nascent DNA. *Nat. Protoc.* **7**, 594–605 (2012).
- Villa, F. et al. CUL2LRR1, TRAP and p97 control CMG helicase disassembly in the mammalian cell cycle. *EMBO Rep.* **22**, e52164 (2021).
- Shikata, K., Sasa-Masuda, T., Okuno, Y., Waga, S. & Sugino, A. The DNA polymerase activity of Pol ϵ holoenzyme is required for rapid

- and efficient chromosomal DNA replication in *Xenopus* egg extracts. *BMC Biochem.* **7**, 21 (2006).
33. Baranovskiy, A. G. et al. Crystal structure of the human Pole B-subunit in complex with the C-terminal domain of the catalytic subunit. *J. Biol. Chem.* **292**, 15717–15730 (2017).
 34. Bellelli, R. et al. POLE3-POLE4 is a histone H3-H4 chaperone that maintains chromatin integrity during DNA replication. *Mol. Cell* **72**, 112–126.e5 (2018).
 35. Ercilla, A. et al. Physiological tolerance to ssDNA enables strand uncoupling during DNA replication. *Cell Rep.* **30**, 2416–2429.e7 (2020).
 36. Lewis, J. S. et al. Tunability of DNA polymerase stability during eukaryotic DNA replication. *Mol. Cell* **77**, 17–25.e5 (2020).
 37. Jackson, D. A. & Pombo, A. Replicon clusters are stable units of chromosome structure: evidence that nuclear organization contributes to the efficient activation and propagation of S phase in human cells. *J. Cell Biol.* **140**, 1285–1295 (1998).
 38. Bhat, K. P. & Cortez, D. RPA and RAD51: fork reversal, fork protection, and genome stability. *Nat. Struct. Mol. Biol.* **25**, 446–453 (2018).
 39. Deegan, T. D., Mukherjee, P. P., Fujisawa, R., Polo Rivera, C. & Labib, K. CMG helicase disassembly is controlled by replication fork DNA, replisome components and a ubiquitin threshold. *eLife* **9**, e60371 (2020).
 40. Low, E., Chistol, G., Zaher, M. S., Kochenova, O. V. & Walter, J. C. The DNA replication fork suppresses CMG unloading from chromatin before termination. *Genes Dev.* **34**, 1534–1545 (2020).
 41. Rodríguez-Acebes, S. et al. VCP/p97 extracts DNA polymerase α /Primase from chromatin to limit the activation of the replication stress response. Preprint at <https://doi.org/10.1101/2022.07.25.501345> (2022).
 42. Jones, M. L., Baris, Y., Taylor, M. R. G. & Yeeles, J. T. P. Structure of a human replisome shows the organisation and interactions of a DNA replication machine. *EMBO J.* **40**, e108819 (2021).
 43. Yuan, Z., Georgescu, R., Schauer, G. D., O'Donnell, M. E. & Li, H. Structure of the polymerase ϵ holoenzyme and atomic model of the leading strand replisome. *Nat. Commun.* **11**, 3156 (2020).
 44. Meng, X. et al. DNA polymerase ϵ relies on a unique domain for efficient replisome assembly and strand synthesis. *Nat. Commun.* **11**, 2437 (2020).
 45. Moiseeva, T. N., Gamper, A. M., Hood, B. L., Conrads, T. P. & Bakkenist, C. J. Human DNA polymerase ϵ is phosphorylated at serine-1940 after DNA damage and interacts with the iron-sulfur complex chaperones CIAO1 and MMS19. *DNA Repair* **43**, 9–17 (2016).
 46. Matson, J. P. et al. Intrinsic checkpoint deficiency during cell cycle re-entry from quiescence. *J. Cell Biol.* **218**, 2169 (2019).
 47. Mansilla, S. F. et al. Cyclin Kinase-independent role of p21CDKN1A in the promotion of nascent DNA elongation in unstressed cells. *eLife* **5**, e18020 (2016).
 48. Crowe-McAuliffe, C. et al. Structural basis for bacterial ribosome-associated quality control by RqcH and RqcP. *Mol. Cell* **81**, 115–126.e7 (2021).
 49. Wiśniewski, J. R., Hein, M. Y., Cox, J. & Mann, M. A “proteomic ruler” for protein copy number and concentration estimation without spike-in standards. *Mol. Cell. Proteom.* **13**, 3497–3506 (2014).
 50. Holden, S. J., Uphoff, S. & Kapanidis, A. N. DAOSTORM: an algorithm for high-density super-resolution microscopy. *Nat. Methods* **8**, 279–280 (2011).
 51. Huang, F., Schwartz, S. L., Byars, J. M. & Lidke, K. A. Simultaneous multiple-emitter fitting for single molecule super-resolution imaging. *Biomed. Opt. Express* **2**, 1377–1393 (2011).
 52. Huang, F. et al. Video-rate nanoscopy using sCMOS camera-specific single-molecule localization algorithms. *Nat. Methods* **10**, 653–658 (2013).
 53. Yin, Y., Lee, W. T. C. & Rothenberg, E. Ultrafast data mining of molecular assemblies in multiplexed high-density super-resolution images. *Nat. Commun.* **10**, 119 (2019).
 54. Sengupta, P. et al. Probing protein heterogeneity in the plasma membrane using PALM and pair correlation analysis. *Nat. Methods* **8**, 969–975 (2011).
 55. Veatch, S. L. et al. Correlation functions quantify super-resolution images and estimate apparent clustering due to over-counting. *PLoS ONE* **7**, e31457 (2012).
 56. Ma, J. et al. iProX: an integrated proteome resource. *Nucleic Acids Res.* **47**, D1211–D1217 (2019).

Acknowledgements

This work was supported by Estonian Research Council (research grant PRG1477 to T.N.M.). Research in E.R. lab is supported by NIH grants: R35 GM134947, AI153040, and CA247773 (E.R.), the V Foundation BRCA Research collaborative grant (E.R.) and by Pfizer (E.R.). We are grateful to Dr. Julieta Martino, Dr. Peter Ly, and Alison Guyer for advice on fiber spreading assay. We thank Dr. Sergo Kasvandik for the advice on the analysis of mass-spectrometry iPOND data.

Author contributions

T.N.M. conceived the project. T.N.M., D.G., S.J., and E.R. designed the experiments. S.V., H.A., and T.N.M. performed and analyzed all experiments except SMLM which were performed and analyzed by D.G. and S.J. T.N.M. wrote the manuscript with review and editing from S.V., D.G., S.J., H.A., and E.R.

Competing interests

The authors declare no competing interests.

Additional information

Supplementary information The online version contains supplementary material available at <https://doi.org/10.1038/s41467-022-34911-4>.

Correspondence and requests for materials should be addressed to Tatiana N. Moiseeva.

Peer review information *Nature Communications* thanks Huiqiang Lou and the other, anonymous, reviewer(s) for their contribution to the peer review of this work. Peer reviewer reports are available.

Reprints and permissions information is available at <http://www.nature.com/reprints>

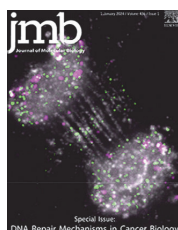
Publisher's note Springer Nature remains neutral with regard to jurisdictional claims in published maps and institutional affiliations.

Open Access This article is licensed under a Creative Commons Attribution 4.0 International License, which permits use, sharing, adaptation, distribution and reproduction in any medium or format, as long as you give appropriate credit to the original author(s) and the source, provide a link to the Creative Commons license, and indicate if changes were made. The images or other third party material in this article are included in the article's Creative Commons license, unless indicated otherwise in a credit line to the material. If material is not included in the article's Creative Commons license and your intended use is not permitted by statutory regulation or exceeds the permitted use, you will need to obtain permission directly from the copyright holder. To view a copy of this license, visit <http://creativecommons.org/licenses/by/4.0/>.

© The Author(s) 2022

Publication II

S. Vipat and T. N. Moiseeva, '**The TIMELESS Roles in Genome Stability and Beyond**', *J Mol Biol*, vol. 436, no. 1, p. 168206, Jan. 2024, doi: 10.1016/j.jmb.2023.168206.



The TIMELESS Roles in Genome Stability and Beyond

Sameera Vipat and Tatiana N. Moiseeva*

Department of Chemistry and Biotechnology, Tallinn University of Technology, Tallinn 12618, Estonia

Correspondence to Tatiana N. Moiseeva: Tallinn University of Technology, Akadeemia tee, 15, Tallinn 12618, Estonia. Tatiana.Moiseeva@taltech.ee (T.N. Moiseeva) [Tat1anaMoiseeva](https://doi.org/10.1016/j.jmb.2023.168206) (T.N. Moiseeva)

<https://doi.org/10.1016/j.jmb.2023.168206>

Edited by Eli Rothenberg

Abstract

TIMELESS protein (TIM) protects replication forks from stalling at difficult-to-replicate regions and plays an important role in DNA damage response, including checkpoint signaling, protection of stalled replication forks and DNA repair. Loss of TIM causes severe replication stress, while its overexpression is common in various types of cancer, providing protection from DNA damage and resistance to chemotherapy. Although TIM has mostly been studied for its part in replication stress response, its additional roles in supporting genome stability and a wide variety of other cellular pathways are gradually coming to light. This review discusses the diverse functions of TIM and its orthologs in healthy and cancer cells, open questions, and potential future directions.

© 2023 The Author(s). Published by Elsevier Ltd.

Introduction

DNA replication must be completed with exceptional fidelity in every cell cycle. Multiple mechanisms are in place to protect the cell from DNA replication errors, as consequences of such errors could be lethal to the cell, and potentially to the whole organism, if they lead to cancer. During replication, advancing forks encounter barriers arising either from repetitive or difficult-to-replicate regions, or from DNA damage. The protein TIMELESS (TIM), as part of the Fork Protection Complex (FPC), plays a central role in supporting efficient DNA replication and genome stability.

TIM was first discovered and studied in *Drosophila Melanogaster* for its circadian clock related functions. There are two paralogs of this gene in *Drosophila*: *dTIM* and *timeout*. *Drosophila* *dTIM* is a canonical clock protein, while *TIMEOUT* has roles in both maintenance of normal DNA metabolism and chromosome integrity.¹ In mammals, there is a single TIM gene, *TIMELESS*. Mam-

malian TIM shares sequence homology with both *dTIM* and *TIMEOUT*, however it is functionally orthologous to *TIMEOUT*. TIM is widely conserved across eukaryotes - from yeast homologs *Tof1* in *S. cerevisiae* and *Swi1* in *S. pombe*,² to TIM in *C. elegans* and *mTIM* in mouse.

The best studied role of mammalian TIM is in replication stress and DNA damage response, including cell cycle checkpoint regulation and replication fork stability.² However, in the absence of stress, TIM also supports DNA replication and smooth replication fork movement past genomic barriers such as repetitive regions, telomeres and DNA-protein complexes (DPCs).³ Further, it has been shown to regulate a diverse array of cell functions, including transcription,⁴ DNA repair,⁵ recombination,⁶ mitosis⁷ and meiosis.⁸ Some of these functions could be attributed to TIM's roles at stalled replication forks, but others are completely independent – for example, in some post-mitotic cells TIM is localized to the cytosol.⁹

As TIM overexpression has been detected in many types of tumors, where it supports cancer progression and provides resistance to certain genotoxic drugs, it may be an attractive target for cancer therapies. In this context, it is crucial to understand the exact roles of TIM in mammalian cells, as any potential therapeutic approach targeting this protein has to consider all the pathways that would be affected. However, mechanistic details for many of the TIM's functions are still unclear – from its position at the unstressed and stressed replication forks to its roles in transcription and circadian rhythm. In this review, we summarize our current understanding of the various functions of TIM and its orthologs in healthy and cancer cells and discuss open questions and possible future research directions.

TIM Structure and Interacting Partners

TIM is best known as a part of the replication fork protection complex composed of three proteins: TIM, TIPIN, CLASPIN and AND-1 in humans (Tof1, Csm3, Mrc1, and Ctf4 in *S. cerevisiae*) (Figure 1). TIM and TIPIN (TIMELESS-interacting protein, Csm3 in *S. cerevisiae* and Swi3 in *S. pombe*) form a stable heterodimer throughout the cell cycle,¹⁰ and they reach their highest level in S-phase, when they associate with replication forks.^{2,10} TIM and TIPIN are mutually required for each other's stability^{10,11} and regulation: TIM facilitates the nuclear localization of TIPIN,² and its binding to TIPIN prevents the formation of inactive TIM

multimers.¹² TIPIN has earlier been shown to bind a compact fold at the N terminal region of TIM,¹³ however recent structural studies indicate that TIPIN binds the middle region of TIM at the fork.^{14,15}

TIM interacts with CLASPIN (Mrc1 in *S. cerevisiae*), another part of the FPC, although the structure of CLASPIN is not fully understood to date – it is thought to be largely disordered.¹⁴ Depletion of TIM/TIPIN reduces CLASPIN levels in the cell under unperturbed conditions,¹⁶ and in the chromatin fraction specifically under replication stress.¹⁰ Coordinating CLASPIN is one of the key functions of TIM/TIPIN at the replication fork.¹⁷

Several regions of TIM have been shown to bind DNA, including DDT (DNA-binding homeobox and different transcription factors) domain (regions 342–376, 814–866 (or 816–954¹⁸), 1084–1144).¹⁹ Recent structure of the human replisome (PDB: 7PFO) showed TIM/TIPIN binding dsDNA ahead of the replication fork, this binding largely mediated by TIPIN-DNA contact, but also by TIM's Ω -loop as well as a short DNA-binding motif in its MCM-plugin region.¹⁵ Significant portions of TIM are not modeled in the 7PFO structure, presumably due to the abundance of flexible linkers between some small functional domains, including some covered by other structures.¹⁸ In order to better illustrate the full structure of TIM, we marked the known domains and interaction sites on the TIM structure predicted by AlphaFold^{20,21} (Figure 1(B)) (the part covered by 7PFO structure is shown in dark brown and the modeled domains are in beige or colored). The locations of the additional DNA-binding domains and the PARP-interacting site are consistent with

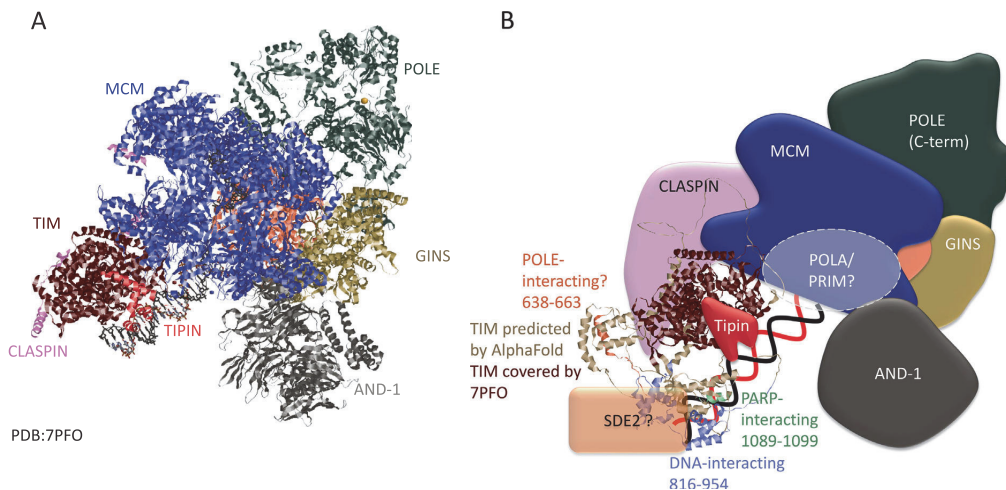


Figure 1. Position of TIM at the human replisome. A. According to PDB: 7PFO, TIM is located at the leading edge of the replisome, ahead of the replicative helicase. B. TIM structure is from the AlphaFold prediction (core region covered by 7PFO is shown in dark brown, predicted regions are in beige), the other proteins are shown as cartoons based on 7PFO or articles referenced in the text. Regions of TIM known to be involved in the interactions with other proteins or DNA are marked.

their possible role in sensing secondary structures and DNA damage ahead of the fork.²² The interaction between TIM and SDE2 protein²³ at the sites of DNA replication is mediated by the same region of TIM that has been previously reported to bind DNA,¹⁸ in agreement with SDE2 being involved in the stabilization of TIM/TIPIN binding to DNA.²⁴

TIM has also been biochemically shown to interact with MCM helicase, as well as DNA polymerases epsilon and delta directly²⁵ and with RPA via TIPIN.^{26,27} TIM-TIPIN were initially thought to be positioned between the MCM helicase and the DNA polymerases, physically connecting MCM with the polymerases.² This view was supported by the ability of the FPC to bind RPA on the ssDNA. However, the structure of active human replisome¹⁵ puts TIM-TIPIN at the leading edge of the fork, ahead of MCM. According to this structure, TIM could plausibly interact with DNA polymerase alpha and/or RPA on the lagging strand, but how it could directly interact with and stimulate DNA polymerase epsilon^{25,28} located on the opposite side of the MCM hexamer, is unclear (Figure 1(A,B)). The site marked as interacting with POLE on Figure 1(B) is based on the biochemical data from.²⁸

Table 1 lists known interaction partners of TIM, and the significance of these interactions for various functions of TIM.

Overall, some early-discovered roles and biochemical properties of TIM are not well-aligned

with its position at the leading edge of the replication fork, suggesting additional complexity in TIM/FPC localization, stoichiometry, and protein–protein interactions that requires further investigation.

TIM Is Essential for Normal Cell Cycle Progression and Genome Stability

TIM/TIPIN are crucial for normal cell cycle progression in unperturbed cells as well as during replication stress. TIM and its yeast counterparts are necessary for the cell viability, normal growth, and proliferation.^{16,23} Downregulation of TIM or Tof1 leads to replication fork slowing,^{23,29} and a global inhibition of DNA synthesis.¹⁶ TIM depletion caused an increase in dormant origin firing, accumulation of ssDNA,³⁰ spontaneous replication stress,^{2,23} DNA double-strand breaks,^{11,31} activation of ATR³⁰ and ATM,¹⁶ chromosome fragmentation,³² chromosomal translocation events, fusions³¹ and gaps,¹⁶ as well as abnormally high levels of sister chromatid exchanges.³¹ TIM or TIPIN depletion by siRNA resulted in accumulation of cells in late S¹⁰ or G2 phase of the cell cycle,^{10,16} indicating a defect in S phase progression, and an inability to complete DNA replication, and highlighting an essential role of TIM in maintaining genome stability

Table 1 Interaction partners of TIMELESS:

Interacting protein	Significance	Reference
TIPIN	Obligate binding partner of TIM	2,12,46
Csm3 in <i>S. cerevisiae</i>	Most of TIM's functions in DNA replication and fork protection are performed in complex with TIPIN	
Swi3 in <i>S. pombe</i>	TIPIN inhibits formation of inactive TIM homodimers	121–125
CLASPIN	Part of the FPC	26,122,126
Mrc1 in <i>S. cerevisiae</i>	Essential for optimal replication fork speed Maintains fork stability through difficult genomic regions Mediates CHK1 phosphorylation by ATR	
MCM helicase	TIM interacts with MCM at the fork TIM inhibits MCM helicase and couples the activities of MCM helicase and the polymerases	15,25,42
DNA polymerases (epsilon, alpha and delta)	Stimulates polymerases and couples MCM helicase and polymerases	25,28
SDE2	SDE2 may recruit TIM to the fork, enhance TIM stability, mediate protection of stalled forks	23,127
DDX11 helicase	Promotes sister chromatid cohesion, maintains fork progression under replication stress and G4 structures, promotes DNA repair	18,68,71
TRF1 and TRF2	Efficient DNA replication through telomeres	57
CUL2 ^{LLR1} ubiquitin ligase	Replisome disassembly at DNA replication termination	45,101
Estrogen receptor α	Enhances the transcriptional activity of this receptor	4
CRY2	Potentially couples circadian clock and cell cycle	64
RPA (Replication Protein A)	RPA recruits TIM-TIPIN to the stalled fork TIPIN in the TIM-TIPIN complex interacts with RPA to mediate ATR/CHK1 pathway activation	26,27
PARP1	DNA damage response signaling and DNA repair	5,22
ATR-ATRIP, CHK1	Mediates checkpoint activation. Possibly though CLASPIN. Not well studied.	64
Topoisomerase I (with yeast Tof1 only)	Fork slowdown at replication barriers	39–41
FACT nucleosome reorganizing complex (with yeast Tof1 only)	This histone chaperone reorganizes nucleosomes during replication	128

during S-phase even in the absence of external stress.

Replication Initiation

It has been long established that TIM and the FPC is a core part of the replisome, but how and at what point during replication initiation TIM is recruited to the sites of DNA replication is not well understood.

One possibility is that TIM is recruited to replication forks via its interaction with SDE2. SDE2-TIM interaction enhances the stability of TIM, while SDE2 depletion leads to accelerated degradation of TIM at the forks.²³ However, TIM is also known to interact with MCM even before origin licensing in G1,³³ which might indicate that it is loaded at the origins along with MCM. CLASPIN, another component of the FPC, has also been proposed to be loaded onto the origins of replication before the start of DNA synthesis in *Xenopus* egg extract system.³⁴ The roles of TIM/TIPIN in DNA damage response and their interaction with ssDNA allow for a model where more than one FPC per fork is present, and while ssDNA-bound FPC may be recruited/stabilized by SDE2, the leading edge FPC could be loaded on the chromatin alongside MCM. This model is difficult to reconcile with the MCM double hexamer (MCM-DH) structure,³⁵ indicating that perhaps the interaction surfaces between MCM and TIM are different before and after replication initiation. Further studies are needed to clarify the nature of interaction between MCM and TIM before the initiation of DNA replication.

It is not clear whether TIM depletion inhibits or supports the initiation of DNA replication, as there are very few studies exploring whether TIM plays any role in replication initiation. In both Tof1- and TIM-depleted cells, inter-origin distances appear to be shorter, indicating excessive origin firing,¹⁰ which is likely a result of the compensation for the slower replication fork speed or a dysfunction in the baseline ATR/CHK1 signaling.³⁶ However, TIM depletion caused S phase entry delay and a reduction in S phase cell population³³ after synchronization, indicating possible problems with the initiation of DNA replication. TIM depletion led to a decrease in chromatin-associated cyclin E in late G1 and persistently high levels of p21 and p27 suppressing CDK2 activity.³³ Additionally, the level of chromatin-bound CDC6, which is required for both MCM loading on chromatin, as well as chromatin recruitment and the activation of cyclin E-CDK2, was also reduced in TIM-depleted cells, resulting in compromised origin licensing. These data point to a possible role for TIM in G1 phase of the cell cycle, in promoting G1/S transition, while during S-phase TIM may not be necessary for efficient origin firing. Given the well-established function of TIM in mitosis (discussed below), chromosome missegregation and resulting DNA damage in TIM-

depleted cells could explain some of the observed phenotypes, however, the referenced study³³ did not detect any DNA damage in G1, so a possible role of TIM in G1/S transition should be further studied.

Interestingly, defective CMG helicase complexes were found on chromatin, both in S-phase and, abnormally, in G1-phase TIM-depleted cells.³³ Abnormal CMG complexes in S phase are most likely the ones that failed to unload after replication termination, indicating the role of TIM in the CMG unloading (discussed below). Assembled CMG in the absence of TIM in G1 could be left over from the previous cell cycle, or it could point to a possible role for TIM in the timing of CMG assembly.

Replication Elongation and Fork Progression

Both human TIM³² and *S. cerevisiae* Tof1³⁷ travel with the replication fork. TIM- or Tof1- deficient cells exhibit a slower replication fork progression. Both in yeast and in human reconstituted systems, FPC proteins are essential for optimal speed of replication fork.^{17,37} In yeast, it is Mrc1 and not Tof1 that is primarily responsible for this effect, and Tof1/Csm3 are responsible for maintaining the association of Mrc1 with the replisome.³⁸ Similarly, the interaction between TIM and CLASPIN is critical for the optimal replication fork progression in the reconstituted replication reaction with purified human proteins.¹⁷

Another way Tof1 facilitates fork progression is by recruiting topoisomerase I to its C-terminal region³⁹ to alleviate torsional stress,⁴⁰ and by inhibiting excessive fork rotation: Tof1 loss causes DNA precatenation that leads to DNA damage.⁴¹ To the best of our knowledge, this role of mammalian TIM has not yet been explored.

Several lines of evidence suggest that TIM and its orthologs support DNA replication by coupling together the helicase and the polymerase activities at the replication fork. *In vitro* biochemical studies with purified proteins showed that TIM directly interacts with the MCM helicase,^{25,42} and can inhibit the DNA unwinding and ATPase activities of the CMG complex.²⁵ Whether TIM physically interacts with any of the replicative polymerases is not clear. TIM position at the leading edge of the replisome ahead of the MCM helicase,¹⁵ allows for a possibility of TIM - DNA polymerase alpha interaction (Figure 1(B)), however DNA polymerase epsilon (POLE) located on the opposite side of the MCM hexamer is unlikely to form a direct interaction with TIM. The catalytic domain of POLE is connected to its non-catalytic domain via a flexible linker and could theoretically bend far enough to interact with TIM (Figure 2(A)), but this implies a sharp bend in the leading strand, which is not supported by any experimental evidence so far. Using biochemical approaches, direct

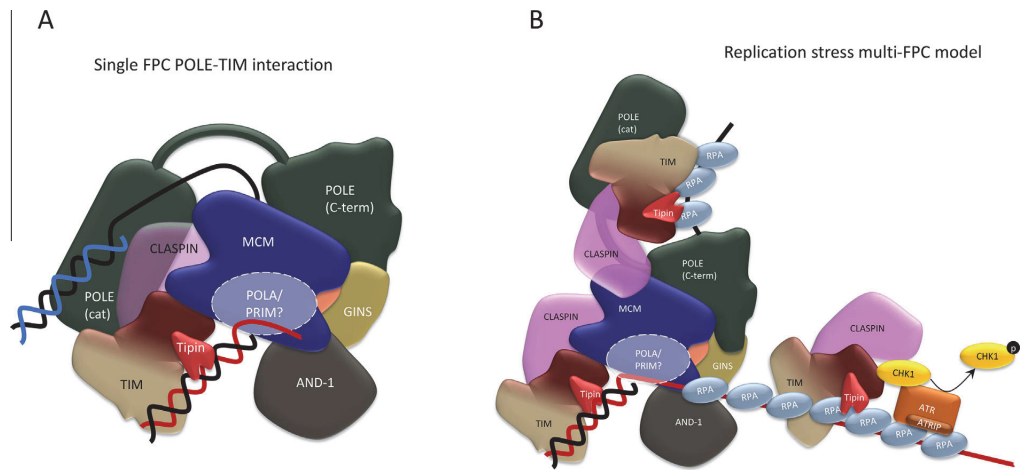


Figure 2. Proposed models. A. Sharp bend in the leading strand could allow TIM-POLE interaction. B. Multiple FPCs per fork could explain the binding of both dsDNA and ssDNA, the functions of TIM in cell cycle checkpoint activation, and the interaction with DNA polymerases.

interaction between TIM and POLE has been detected by some studies,²⁸ but not others,²⁵ with some evidence that TIM can also stimulate the polymerase activity of POLE.^{25,28} Given that CLASPIN is known to directly interact with POLE,⁴³ it could be the link that helps TIM coordinate POLE and MCM, however it would not explain TIM directly stimulating POLE in *in vitro* assays in the absence of CLASPIN. Interactions between TIM and DNA polymerases alpha and delta have not been detected by immunoprecipitation, however BiFC assays indicate that TIM either directly interacts with or is in close proximity with these polymerases.²⁵ Whether TIM is able to stimulate the activities of polymerase delta and alpha is unclear, with some evidence that it is,²⁵ but other evidence that it is not.²⁸ In summary, given the inconsistency of the data on TIM interaction with DNA polymerases, especially in mammalian cells, more research is needed to validate or clarify this model.

Replication Termination

The accumulation of aberrant catalytically defective CMG complexes on chromatin in TIM-deficient cells discussed above, indicated that TIM has a role in the disassembly or dissociation of CMG from chromatin after the completion of DNA replication.³³ Further studies confirmed this hypothesis. In *C. elegans*, TIM-TIPIN are required for CMG ubiquitylation during replication termination in early embryos, where they act by recruiting CUL-2^{LRR-1} ubiquitin ligase and stabilizing the association between CUL-2^{LRR-1} and CMG to stimulate the elongation of ubiquitin chains on CMG,⁴⁴ which leads to replisome disassembly by the p97/CDC-48

unfoldase. The interaction between LRR1 and TIM has now been demonstrated by structural studies in humans, suggesting that the role of TIM in recruiting CUL-2^{LRR-1} for replisome disassembly during termination is conserved.⁴⁵

Genome Stability at Difficult-to-replicate Genomic Regions

TIM and its orthologs are essential for efficient replication through various genomic barriers,⁴⁶ such as regions prone to forming secondary structures (ribosomal genes, centromeric and telomeric regions, tRNA genes, repeat regions (reviewed in⁴⁷), as well as covalent and non-covalent DNA-protein complexes (DPCs) (reviewed in³)

TIM supports replication through G-quadruplex (G4) structures by using its C-terminal DNA-binding domain (DBD) to recruit DDX11 helicase and stimulate its G4-unwinding activity.¹⁸ The role of DBD appears to be partially redundant with the PARP-binding domain of TIM in chicken DT-40 cells, indicating a possible role for PARP1 in helping replication fork progression through G4s.¹⁸

TIM orthologs act as molecular brakes, slowing down the forks at difficult to replicate regions. *S. cerevisiae* Tof1 promotes fork pausing at DPCs,⁴⁸ programmed pause sites in ribosomal DNA barriers, and accidental barriers like promoters of tRNAs or centromeres.⁴⁹ *S. pombe* Swi1 and Swi3⁵⁰ and human TIM have also been shown to pause replication forks at ribosomal DNA barriers.⁵¹ The Tof1-Csm3 complex recruits topoisomerase I to the replisome⁴⁰ via the 627 – 830 region of Tof1,³⁹ however whether it is required for the fork pausing at DPCs remains unclear.

FPC orthologs control the stability of repeat regions in the genome, suppressing their expansions or contractions. This role of TIM orthologs and other FPC components is linked to their function in fork stabilization and remodeling during replication stress: Tof1 or Mrc1 deficiency, for example, resulted in CAG repeat fragility and expansion.⁵² *S. cerevisiae* FPC is required to prevent the expansions of (CTG)₁₃ tracks, associated with myotonic dystrophy,⁵³ GAA repeats, linked with Friedreich's ataxia, as well as (ATTCT)_n, linked with spinocerebellar ataxia,⁵⁴ and the contractions of (CAG)₂₀ repeats,⁵² associated with Huntington's disease, myotonic dystrophy type 1 and several types of spinocerebellar ataxia.⁵³ Tof1-Csm3 also keep in check the expansions of minisatellite repetitive DNA sequences by regulating the LLR (large loop repair) pathway.⁵⁵ In human cells, loss of FPC components leads to increased instability of the trinucleotide repeat (CTG)_n·(CAG)_n in the 3' untranslated region (UTR) of the DMPK gene, which is associated with myotonic dystrophy type I.⁵⁶

Human TIM⁵⁷ and *S. pombe* Swi1⁵⁸ play a role in preserving telomere length in a telomerase-independent manner. TIM depletion led to telomere shortening, telomere specific DNA damage and telomere aberrations, and Swi1 depletion additionally resulted in more frequent amplification of telomeres and subtelomere regions. TIM⁵⁷ and Swi1⁵⁹ bind to Shelterin components TRF1 and TRF2, helping recruit important replication factors to telomeres, and prevent fork collapse by TIM's fork pausing activity. TIM/TIPIN also suppress telomeric clustering - a hallmark of ALT (alternative lengthening of telomeres) cancers - and the mitotic DNA synthesis, presumably via their fork protection function.⁶⁰

TIM orthologs are known to differentially modulate the recombination potential of replication fork barriers. *S. cerevisiae* Tof1-Csm3 control recombination positively or negatively, depending on whether it is provoked by polar fork arrest (blocking replication in one direction) or by transcription, respectively. Tof1-Csm3 promote recombination at *ter* sites, but inhibit recombination at the *HOT1* site, where recombination is stimulated by RNA polymerase I-dependent transcription and does not depend on fork arrest.⁶ Tof1 also suppressed excessive retro-mobility of a retrovirus-like transposable element Ty1 preventing genome instability.⁶¹ Similarly, the loss of *S. pombe* Swi1 increased recombination at tRNA genes, sup3-e and tRNAGLU,⁶² as well as in response to DNA damage,⁶³ but completely blocked recombination at the RTS1 element.⁶² The two independent roles of TIM orthologs in programmed fork arrest and the subsequent fork stabilization/remodeling could explain some of these phenotypes: they may be required to initiate the recombination by inducing the fork arrest/pausing

in some particular cases, but could also promote safe fork restart preventing recombination.

DNA Damage Response

The role of TIM/TIPIN and the FPC in the DNA damage response has been extensively studied. TIM/TIPIN binding to ssDNA and stabilizing CLASPIN at stalled replication forks, make FPC the central component in checkpoint signaling²⁹ and even some DNA repair processes at stalled forks and DSBs.⁵

Down-regulation of TIM⁶⁴ or TIPIN^{10,11} compromises both basal and DNA damage-induced ATR-dependent CHK1 phosphorylation and disrupts replication checkpoint signaling.⁶⁴ Mechanistically, TIM is thought to bring together ATR/ATRIP and CHK1 for efficient CHK1 phosphorylation.^{26,64} Given that CLASPIN also mediates ATR-dependent CHK1 phosphorylation,⁶⁵ and that TIM/TIPIN are required for CLASPIN stability and chromatin binding,¹⁶ especially in response to replication stress,¹⁰ the role of TIM/TIPIN in checkpoint regulation may be in part in the recruitment of CLASPIN: TIPIN-RPA interaction stabilizes FPC binding to RPA-coated ssDNA, promoting CLASPIN-mediated phosphorylation of CHK1 by ATR.²⁶ Interestingly, in the absence of DNA damage, TIM/TIPIN depletion resulted in CLASPIN-mediated CHK1 phosphorylation,¹⁶ indicating a possibility of TIM/TIPIN-independent replication stress checkpoint activation – at the stalled fork or post-replicatively.

Due to its possible role in circadian clock pathway, TIM may also coordinate the circadian clock-dependent control of ATR pathway: TIM-ATR interaction is time gated by CRY1 which temporally interacts with TIM and stimulates TIM-ATR interaction in a temporal manner.⁶⁶

Some data indicate that TIM/TIPIN may be also involved in the G2/M checkpoint after ionizing radiation¹¹; or doxorubicin treatment⁶⁷: TIM was required for ATM-dependent activation of CHK2 after doxorubicin treatment,⁶⁷ however the exact role of TIM in CHK2 activation remains to be uncovered.

Perhaps, at least in part due to its role in ATR-CHK1 pathway activation, TIM accumulates at stalled replication forks⁵ and is required for fork protection²³ and fork restart after HU treatment.⁶⁸ Additionally, together with CHK1, FPC facilitates PCNA ubiquitination after DNA damage by recruiting ubiquitin ligase RAD18 to single stranded DNA.^{69,70}

TIM/TIPIN are rapidly but transiently recruited to DNA damage sites induced by microirradiation, in both S phase and non-S phase cells, through TIM interaction with PARP1⁵ but independently of PARP catalytic activity²² and independently of TIM-TIPIN interaction,²² to promote homologous recombination repair of DSBs.⁵ TIM mediated the interaction

between PARP1 with some of its substrates,²² pointing to its potential role in DNA repair as a recruitment platform.

Reports indicating TIM/FPC recruitment to the sites of DNA damage or ssDNA, including that in non-S-phase cells,^{5,22} suggest a possibility that in addition to its location at the leading edge of the replication fork, FPC may bind ssDNA behind a stalled fork or at a resected DSB (Figure 2(B)). Interestingly, at the leading edge of the fork, TIPIN binds dsDNA before it is unwound by the CMG helicase,¹⁵ while in the event of replication stress it is known to also interact with ssDNA/RPA complex.^{27,29} Whether and how the same TIPIN molecule could accommodate both interactions at the same time, remains unclear. It is plausible that during replication stress more than one FPC per fork is present to support its functions in DNA damage signaling and replication fork stabilization described above. It is tempting to speculate that even during unperturbed replication, additional FPC complex (es) may bind ssDNA between Okazaki fragments or be recruited to forks passing difficult to replicate genomic regions. At the replication pause sites, one FPC could promote the fork arrest, while the other helps stabilize the fork and promote its restart. This hypothesis would also agree with the long-standing model of the FPC connecting CMG helicase to the replicative DNA polymerases. More research is needed to clearly establish the stoichiometry of FPC at the replication fork and its regulation in response to replication stress.

Mitosis and Meiosis

TIM-depleted HCT116 cells showed numerous mitotic defects including ineffective chromosome condensation, reduced sister chromatid cohesion (SCC), disorganized bipolar spindle formation, and abnormal accumulation of mitotic entry kinases.⁷ Some of these defects could be in part due to the problems with DNA synthesis, however, the role of TIM and its orthologs in SCC has been studied extensively.

TIM in human cells^{71,72} and in *Xenopus* egg extracts,⁷³ as well as *S. cerevisiae* Tof1-Csm3^{74,75} and *S. pombe* Swi1 and Swi3⁸ promote the association of cohesin with chromatin. Loss of TIM resulted in a strong increase in sister chromatid dis-cohesion.⁷⁶ Mechanistically, TIM interacts with DDX11 helicase, which helps transfer the pre-loaded cohesin rings to tether the two sister chromatids behind the moving replication fork.⁷² In addition to its role in SCC, TIM is thought to link replication termination to mitotic entry by participating in Polo-like Kinase 1 and Aurora A activation.⁷

In *S. cerevisiae*, Tof1 knockout causes uncoupling of DNA replication from the formation of double strand breaks (DSB), as well as a global delay in DSB formation in meiosis. Tof1 and Csm3 physically associate with DDK which is critical for

DSB formation, tethering it to the replisome, thus coupling replication with DSB formation.^{77,78} In the absence of Tof1, Mer2 phosphorylation by DDK is no longer coordinated with replication and occurs regardless of replication timing.⁷⁸

Miscellaneous Roles of TIM

TIM is essential for the normal development, and TIM knockouts are embryonically lethal by day 5 of embryonic development in mouse, indicating its critical role from the time of implantation.⁷⁹ Interestingly, during brain development, TIM is localized to the nucleus, but shifts to the cytoplasm (cell body, axons and dendrites) in mature cortical and hippocampal neurons, indicating a possible function unrelated to replication in non-dividing cells,⁹ perhaps in circadian rhythm. Studies on differentiating mouse embryonic stem cells showed that TIM depletion resulted in defects in apoptosis⁸⁰ required for cavitating of embryoid bodies. Given the critical importance of apoptosis in brain development, the cytoplasmic localization of TIM in neurons could be also related to its role in apoptosis regulation.

TIM and its orthologs are known to bind steroid receptors and co-activate them, leading to modulation of the expression of downstream target genes. Human TIM is a coactivator of estrogen receptor α (ER α) that binds ER α , enhances its transcriptional activity, and is recruited at GREB1 and Myc promoters together with ER α .⁴ Similarly, in *S. pombe*, Swi1, Swi2 and Swi3 were required for hormone-dependent transcriptional enhancement of yeast promoters linked to glucocorticoid response element sequences.⁸¹ It has been speculated that TIM may itself function as a transcription factor via its DDT domain,¹⁹ a domain that allows DNA binding and is commonly found in different transcription and chromatin remodeling factors,⁸² however this has not been clearly demonstrated. A recent study⁸³ identified the role of TIM in Pde4b transcription and cAMP signaling, modulating synaptic plasticity and cognitive function in mice, potentially linking the roles of TIM as a transcription modulator and a circadian clock protein.

In insects, the role of one of the TIM orthologs, dTIM, in maintaining a robust circadian rhythm is well established. dTIM is cyclically expressed and its protein levels oscillate over the circadian day.⁸⁴ dTIM levels affect behavioral rhythmicity,⁸⁵ pathogen resistance⁸⁶ and photoperiodic functions⁸⁷ in insects. However, as mammalian TIM is more orthologous to *Drosophila* TIMEOUT than to dTIM, it has long been controversial whether these circadian rhythm related roles of dTIM are conserved in mammals. TIM depletion in human and mouse cells shortens the circadian period by 1 hour.⁸⁸ Gamma irradiation and other genotoxic agents cause an advancing of the phase in the circadian clock in cultured cells, but loss of TIM diminishes this DNA

damage-dependent phase advancing.⁸⁸ Human TIM interacts with canonical clock protein CRY2, and could be the link connecting the circadian clock and cell cycle in humans.^{64,66}

In rat, TIM mRNA oscillates⁸⁹ in suprachiasmatic nucleus (SCN), the site of the master circadian clock, and TIM loss abolished the endogenous rhythm of neuronal firing,⁹⁰ indicating that TIM could be involved in maintenance of circadian rhythmicity in mammals as well. Downregulation of TIM negatively affected the levels of dedicated clock proteins Per1, Per2, Per3, and led to disrupted clock regulation.^{64,90} In humans, a heterozygous mutation in TIM is known to cause advanced sleep phase, as this mutated TIM remains in the cytoplasm and destabilizes the negative regulators of the circadian clock PER2 and CRY2.⁹¹ This might hint towards a role for TIM in circadian rhythm in humans, although more direct studies are needed to clarify this. There are excellent reviews covering the debate of whether TIM in humans has a role in circadian rhythm.^{92,93}

TIM and Human Disease

Upregulation of TIM correlates with enhanced proliferation of cancer cells.^{94,95} Overexpression of TIM is associated with increased risk of breast cancer,⁹⁶ and poor survival and prognosis in many types of cancer including lung cancer,^{97,98} skin cutaneous melanoma⁹⁹ and gliomas.¹⁰⁰

In ovarian cancer models, TIM promoted tumor progression by enhancing macrophage recruitment, however, the mechanism of this effect remains unclear.¹⁰¹ Overexpressed TIM promoted cancer metastasis in cervical cancer¹⁰² and hepatocellular carcinoma¹⁰³ by interacting with eukaryotic elongation factor 1A2 (EEF1A2), which binds to actin filaments to promote tumor cell migration.¹⁰³ In breast cancer, TIM overexpression either promoted migration and cell invasion by upregulation of MYC,¹⁰⁴ or suppressed it by binding p65 and preventing NF- κ B activation.¹⁰⁵ This discrepancy is difficult to explain given that the two studies used largely overlapping sets of breast cancer cell lines.

Additionally, TIM acts as a coactivator of estrogen receptor α , leading to stimulation of cell division and tumor growth.⁴ Consistent with this function of TIM, elevated TIM expression is associated with tamoxifen resistance in cancer cells.^{4,95}

TIM loss in colorectal cancer induced the activation of the epithelial-to-mesenchymal transition (EMT) program,¹⁰⁶ and in breast cancers higher expression of TIM was associated with epithelial-like phenotype, while its lower expression resulted in mesenchymal-like morphology,¹⁰⁵ indicating a possible role of TIM in suppressing EMT and cancer progression in some particular cases.

Interestingly, the roles of TIM in cancer progression described above are not directly related to replication or genome stability, although

TIM's role in genome stability could indirectly affect cellular proliferative status and some of the described phenotypes. However, they may also result from deregulated TIM-mediated transcription. Further studies are clearly needed to address the role of TIM in tumor development.

Increased levels of TIM also protect cancer cells from replication stress-induced as well as chemotherapy-induced DNA damage.¹⁰⁷ Upregulation of TIM is linked to cisplatin resistance of cervical cancer¹⁰⁸ and nasopharyngeal carcinoma.¹⁰⁹ In agreement with this, downregulation of TIM by microRNA-708 suppressed cell proliferation and enhanced chemosensitivity of cervical cancer cells.¹¹⁰ Despite its role in cell cycle checkpoint activation, TIM overexpression also suppressed G2/M arrest in colon cancer cells¹¹¹ or hepatocellular carcinoma through the inhibition of CHK2 phosphorylation.¹⁰³ TIM along with FANCM is critical for replication stress response at ALT telomeres, which made TIM a potential therapeutic target: co-depletion of FANCM and TIM is synthetically lethal in ALT cancers.¹¹² TIM overexpression may also protect cells against oncogene-induced senescence. TIM expression is normally downregulated during the onset of oncogene-induced or replicative senescence, and overexpression of TIM slows down these processes.¹¹³

Given the critical nature of TIM in promoting and protecting the integrity of replication, it is no surprise that pathogenic viruses conscript TIM for ensuring smooth replication of their own genomes. Kaposi's sarcoma associated herpesvirus¹¹⁴ and Epstein-Barr virus¹¹⁵ use TIM to facilitate the replication of difficult regions in their genomes, and when TIM is depleted, their episomes are rapidly lost from the infected cell. TIM may contribute to the production of antiphospholipid antibody, an antibody that contributes to systemic thrombosis, in both COVID-19 and antiphospholipid syndrome (APS) patients.¹¹⁶

Germline TIM variants are associated with defective sleep regulation and depression.¹¹⁷ A mutation in TIM caused advanced sleep phase, as it destabilized the negative regulators of the circadian clock PER2 and CRY2.⁹¹ Reduced expression and polymorphisms in TIM are associated with increased asthma risk in children.¹¹⁸ The *TIMELESS* gene is also associated with bipolar disorder, and although mechanistic details are not known, the presumed role of TIM in the circadian clock is thought to be involved.¹¹⁹

Concluding Remarks and Future Directions

The pro-tumorigenic effect of TIM overexpression and its role in protecting cancer cells against replication stress and DNA damage make it an attractive therapeutic target. Lacking any known enzymatic activities, TIM cannot be targeted by

small molecule inhibitors, however, novel approaches disrupting protein–protein interactions¹²⁰ could help specifically block particular functions of TIM without disrupting the others. Developing such targeted approaches requires a clear understanding of all the processes in various tissues that involve this essential protein. In this review we covered the key functions of TIM known to date. Many mechanistic details of these functions are still unclear and require further investigation.

The main role of TIM in cancer cells is in supporting genome stability by stabilizing replication forks and mediating the replication checkpoint activation. However, it is still unclear how the localization and stoichiometry of TIM during replication stress differ from those of TIM at the unstressed fork. FPC is stably associated with the leading edge of the replication fork and dsDNA, and this position is not easily reconciled with FPC's key function in binding ssDNA/PRA behind the fork that is required for checkpoint activation. In this review, we propose that during replication stress or at difficult-to-replicate regions, additional molecules of TIM/FPC are recruited to the replication fork to mediate its checkpoint-related function. One of the first ever described functions of TIM – coupling the helicase and the DNA polymerases at the fork – is not consistent with its location at the leading edge of the replication fork, and the multi-FPC model could resolve this contradiction. Structural, biochemical, or high-resolution imaging studies are required to test this hypothesis, and if the presence of multiple FPCs per fork is confirmed, various functions of TIM will have to be re-assessed to identify which FPC is responsible for which function.

Special attention must be paid to the functions of TIM in the absence of DNA damage or replication stress, as TIM is an essential protein, and disruption of these functions by potential therapies may lead to undesired effects on healthy tissues. Specifically, the roles of TIM in regulating apoptosis, transcription, and replication through repetitive regions have to be further described. TIM depletion resulting in apoptosis defects could be a problem for cancer therapies, so it is essential to establish the mechanistic details of the disrupted pathway. Inconsistent phenotypes associated with TIM depletion in cell culture where it leads to both S-phase delay and increased origin firing, could potentially be explained by TIM regulating transcription of some cell cycle-related genes in addition to its direct role at the replication fork. The roles of TIM in cancer progression, including cell migration and EMT, also can't be explained by its replication-related functions, and are likely linked to transcription deregulation. It is essential to identify any potential targets of TIM as a transcription factor or a transcription co-activator.

Finally, the controversial function of mammalian TIM in regulation of circadian rhythm needs to be

further addressed. As a factor involved both in DNA damage response and in the circadian rhythm, TIM is uniquely positioned to link the two processes. Studying this link could potentially allow to time genotoxic cancer therapies to specific times of the day when they are the most efficient. Further investigations of the myriad of TIM's functions will shed light on the multiple fundamental processes in the cell, as well as uncover the potential for future clinical applications.

CRediT authorship contribution statement

Sameera Vipat: Conceptualization, Writing – original draft, Writing – review & editing. **Tatiana N. Moiseeva:** Conceptualization, Visualization, Writing – review & editing, Supervision, Project administration, Funding acquisition.

DECLARATION OF COMPETING INTEREST

The authors declare that they have no known competing financial interests or personal relationships that could have appeared to influence the work reported in this paper.

Acknowledgements

This work was supported by Estonian Research Council (research grant PRG1477 to T.N.M.).

Received 1 May 2023;

Accepted 12 July 2023;

Available online 20 July 2023

Keywords:

fork protection complex;

DNA replication;

DNA damage checkpoint;

genome stability;

cancer

References

1. Benna, C., Bonaccorsi, S., Wülbeck, C., Helfrich-Förster, C., Gatti, M., Kyriacou, C.P., Costa, R., Sandrelli, F., (2010). *Drosophila timeless2* is required for chromosome stability and circadian photoreception. *Curr. Biol.* **20**, 346–352. <https://doi.org/10.1016/j.cub.2009.12.048>.
2. Gotter, A.L., Suppa, C., Emanuel, B.S., (2007). Mammalian TIMELESS and tipin are evolutionarily conserved replication fork-associated factors. *J. Mol. Biol.* **366**, 36–52. <https://doi.org/10.1016/j.jmb.2006.10.097>.
3. Shyian, M., Shore, D., (2021). Approaching protein barriers: emerging mechanisms of replication pausing in eukaryotes. *Front. Cell Dev. Biol.* **9**, 672510 <https://doi.org/10.3389/fcell.2021.672510>.

4. Magne Nde, C.B., Casas Gimeno, G., Docanto, M., Knower, K.C., Young, M.J., Buehn, J., Sayed, E., Clyne, C.D., (2018). Timeless Is a novel estrogen receptor co-activator involved in multiple signaling pathways in MCF-7 cells. *J. Mol. Biol.* **430**, 1531–1543. <https://doi.org/10.1016/j.jmb.2018.03.008>.
5. Xie, S., Mortusewicz, O., Ma, H.T., Herr, P., Poon, R.Y.C., Helleday, T., Qian, C., (2015). Timeless interacts with PARP-1 to promote homologous recombination repair. *Mol. Cell* **60**, 163–176. <https://doi.org/10.1016/j.molcel.2015.07.031>.
6. Mohanty, B.K., Bairwa, N.K., Bastia, D., (2009). Contrasting roles of checkpoint proteins as recombination modulators at Fob1- Ter complexes with or without fork arrest. *Eukaryot. Cell* **8**, 487–495. <https://doi.org/10.1128/EC.00382-08>.
7. Dheekollu, J., Wiedmer, A., Hayden, J., Speicher, D., Gotter, A.L., Yen, T., Lieberman, P.M., (2011). Timeless links replication termination to mitotic kinase activation. *PLoS One* **6**, e19596 <https://doi.org/10.1371/journal.pone.0019596>.
8. Escorcía, W., Forsburg, S.L., (2017). Destabilization of the replication fork protection complex disrupts meiotic chromosome segregation. *Mol. Biol. Cell* **28**, 2978–2997. <https://doi.org/10.1091/mbc.e17-02-0101>.
9. Inaguma, Y., Ito, H., Hara, A., Iwamoto, I., Matsumoto, A., Yamagata, T., Tabata, H., Nagata, K., (2015). Morphological characterization of mammalian Timeless in the mouse brain development. *Neurosci. Res.* **92**, 21–28. <https://doi.org/10.1016/j.neures.2014.10.017>.
10. Yoshizawa-Sugata, N., Masai, H., (2007). Human tim/timeless-interacting protein, Tipin, is required for efficient progression of S phase and DNA replication checkpoint. *J. Biol. Chem.* **282**, 2729–2740. <https://doi.org/10.1074/jbc.M605596200>.
11. Chou, D.M., Elledge, S.J., (2006). Tipin and timeless form a mutually protective complex required for genotoxic stress resistance and checkpoint function. *Proc. Natl. Acad. Sci.* **103**, 18143–18147. <https://doi.org/10.1073/pnas.0609251103>.
12. Gotter, A.L., (2003). Tipin, a novel timeless-interacting protein, is developmentally co-expressed with timeless and disrupts its self-association. *J. Mol. Biol.* **331**, 167–176. [https://doi.org/10.1016/S0022-2836\(03\)00633-8](https://doi.org/10.1016/S0022-2836(03)00633-8).
13. Holzer, S., Degliesposti, G., Kilkenny, M.L., Maslen, S.L., Matak-Vinkovic, D., Skehel, M., Pellegrini, L., (2017). Crystal structure of the N-terminal domain of human Timeless and its interaction with Tipin. *Nucleic Acids Res.* **45**, 5555–5563. <https://doi.org/10.1093/nar/gkx139>.
14. Baretic, D., Jenkyn-Bedford, M., Aria, V., Cannone, G., Skehel, M., Yeeles, J.T.P., (2020). Cryo-EM structure of the fork protection complex bound to CMG at a replication fork. *Mol. Cell* **78**, 926–940.e13. <https://doi.org/10.1016/j.molcel.2020.04.012>.
15. Jones, M.L., Baris, Y., Taylor, M.R.G., Yeeles, J.T.P., (2021). Structure of a human replisome shows the organisation and interactions of a DNA replication machine. *EMBO J.* **40**, e108819.
16. Smith-Roe, S.L., Patel, S.S., Zhou, Y., Simpson, D.A., Rao, S., Ibrahim, J.G., Cordeiro-Stone, M., Kaufmann, W. K., (2013). Separation of intra-S checkpoint protein contributions to DNA replication fork protection and genomic stability in normal human fibroblasts. *Cell Cycle* **12**, 332–345. <https://doi.org/10.4161/cc.23177>.
17. Baris, Y., Taylor, M.R.G., Aria, V., Yeeles, J.T.P., (2022). Fast and efficient DNA replication with purified human proteins. *Nature* **606**, 204–210. <https://doi.org/10.1038/s41586-022-04759-1>.
18. Lerner, L.K., Holzer, S., Kilkenny, M.L., Škivović, S., Murat, P., Schiavone, D., Eldridge, C.B., Bittleston, A., et al., (2020). Timeless couples G-quadruplex detection with processing by DDX 11 helicase during DNA replication. *EMBO J.* **39** <https://doi.org/10.15252/embj.2019104185>.
19. Mazzocchi, G., Laukkanen, M.O., Vinciguerra, M., Colangelo, T., Colantuoni, V., (2016). A timeless link between circadian patterns and disease. *Trends Mol. Med.* **22**, 68–81. <https://doi.org/10.1016/j.molmed.2015.11.007>.
20. Jumper, J., Evans, R., Pritzel, A., Green, T., Figurnov, M., Ronneberger, O., Tunyasuvunakool, K., Bates, R., et al., (2021). Highly accurate protein structure prediction with AlphaFold. *Nature* **596**, 583–589. <https://doi.org/10.1038/s41586-021-03819-2>.
21. Varadi, M., Anyango, S., Deshpande, M., Nair, S., Natassia, C., Yordanova, G., Yuan, D., Stroe, O., et al., (2022). AlphaFold protein structure database: massively expanding the structural coverage of protein-sequence space with high-accuracy models. *Nucleic Acids Res.* **50**, D439–D444. <https://doi.org/10.1093/nar/gkab1061>.
22. Young, L.M., Marzio, A., Perez-Duran, P., Reid, D.A., Meredith, D.N., Roberti, D., Star, A., Rothenberg, E., et al., (2015). TIMELESS forms a complex with PARP1 distinct from its complex with TIPIN and plays a role in the DNA damage response. *Cell Rep.* **13**, 451–459. <https://doi.org/10.1016/j.celrep.2015.09.017>.
23. Rageul, J., Park, J.J., Zeng, P.P., Lee, E.-A., Yang, J., Hwang, S., Lo, N., Weinheimer, A.S., et al., (2020). SDE2 integrates into the TIMELESS-TIPIN complex to protect stalled replication forks. *Nature Commun.* **11**, 5495. <https://doi.org/10.1038/s41467-020-19162-5>.
24. Weinheimer, A.S., Paung, Y., Rageul, J., Khan, A., Lo, N., Ho, B., Tong, M., Alphonse, S., et al., (2022). Extended DNA-binding interfaces beyond the canonical SAP domain contribute to the function of replication stress regulator SDE2 at DNA replication forks. *J. Biol. Chem.* **298**, 102268 <https://doi.org/10.1016/j.jbc.2022.102268>.
25. Cho, W.-H., Kang, Y.-H., An, Y.-Y., Tappin, I., Hurwitz, J., Lee, J.-K., (2013). Human Tim-Tipin complex affects the biochemical properties of the replicative DNA helicase and DNA polymerases. *Proc. Natl. Acad. Sci.* **110**, 2523–2527. <https://doi.org/10.1073/pnas.1222494110>.
26. Kemp, M.G., Akan, Z., Yilmaz, S., Grillo, M., Smith-Roe, S.L., Kang, T.-H., Cordeiro-Stone, M., Kaufmann, W.K., et al., (2010). Tipin-replication protein A interaction mediates Chk1 phosphorylation by ATR in response to genotoxic stress. *J. Biol. Chem.* **285**, 16562–16571. <https://doi.org/10.1074/jbc.M110.110304>.
27. Witosch, J., Wolf, E., Mizuno, N., (2014). Architecture and ssDNA interaction of the Timeless-Tipin-RPA complex. *Nucleic Acids Res.* **42**, 12912–12927. <https://doi.org/10.1093/nar/gku960>.
28. Aria, V., De Felice, M., Di Perna, R., Uno, S., Masai, H., Syväoja, J.E., van Loon, B., Hübscher, U., et al., (2013). The human Tim-Tipin complex interacts directly with DNA polymerase epsilon and stimulates its synthetic activity. *J. Biol. Chem.* **288**, 12742–12752. <https://doi.org/10.1074/jbc.M112.398073>.

29. Ünsal-Kaçmaz, K., Chastain, P.D., Qu, P.-P., Minoo, P., Cordeiro-Stone, M., Sancar, A., Kaufmann, W.K., (2007). The Human Tim/Tipin Complex Coordinates an Intra-S Checkpoint Response to UV That Slows Replication Fork Displacement. *Mol. Cell Biol.* **27**, 3131–3142. <https://doi.org/10.1128/MCB.02190-06>.
30. Smith, K.D., Fu, M.A., Brown, E.J., (2009). Tim-Tipin dysfunction creates an indispensable reliance on the ATR–Chk1 pathway for continued DNA synthesis. *J. Cell Biol.* **187**, 15–23. <https://doi.org/10.1083/jcb.200905006>.
31. Urtishak, K.A., Smith, K.D., Chanoux, R.A., Greenberg, R. A., Johnson, F.B., Brown, E.J., (2009). Timeless maintains genomic stability and suppresses sister chromatid exchange during unperturbed DNA replication. *J. Biol. Chem.* **284**, 8777–8785. <https://doi.org/10.1074/jbc.M806103200>.
32. Leman, A.R., Noguchi, C., Lee, C.Y., Noguchi, E., (2010). Human Timeless and Tipin stabilize replication forks and facilitate sister-chromatid cohesion. *J. Cell Sci.* **123**, 660–670. <https://doi.org/10.1242/jcs.057984>.
33. Xu, X., Wang, J.-T., Li, M., Liu, Y., (2016). TIMELESS suppresses the accumulation of aberrant CDC45-MCM2-7-GINS replicative helicase complexes on human chromatin. *J. Biol. Chem.* **291**, 22544–22558. <https://doi.org/10.1074/jbc.M116.719963>.
34. Lee, J., Kumagai, A., Dunphy, W.G., (2003). Claspín, a Chk1-regulatory protein, monitors DNA replication on chromatin independently of RPA, ATR, and Rad17. *Mol. Cell* **11**, 329–340. [https://doi.org/10.1016/S1097-2765\(03\)00045-5](https://doi.org/10.1016/S1097-2765(03)00045-5).
35. Li, J., Dong, J., Wang, W., Yu, D., Fan, X., Hui, Y.C., Lee, C.S.K., Lam, W.H., et al., (2023). The human pre-replication complex is an open complex. *Cell* **186**, 98–111.e21. <https://doi.org/10.1016/j.cell.2022.12.008>.
36. Moiseeva, T.N., Yin, Y., Calderon, M.J., Qian, C., Schamus-Haynes, S., Sugitani, N., Osmanbeyoglu, H. U., Rothenberg, E., et al., (2019). An ATR and CHK1 kinase signaling mechanism that limits origin firing during unperturbed DNA replication. *PNAS* **116**, 13374–13383. <https://doi.org/10.1073/pnas.1903418116>.
37. Lewis, J.S., Spenkelink, L.M., Schauer, G.D., Hill, F.R., Georgescu, R.E., O'Donnell, M.E., van Oijen, A.M., (2017). Single-molecule visualization of *Saccharomyces cerevisiae* leading-strand synthesis reveals dynamic interaction between MTC and the replisome. *Proc. Natl. Acad. Sci.* **114**, 10630–10635. <https://doi.org/10.1073/pnas.1711291114>.
38. Yeeles, J.T.P., Janska, A., Early, A., Diffley, J.F.X., (2017). How the Eukaryotic Replisome Achieves Rapid and Efficient DNA Replication. *Mol. Cell* **65**, 105–116. <https://doi.org/10.1016/j.molcel.2016.11.017>.
39. Westhorpe, R., Keszthelyi, A., Minchell, N.E., Jones, D., Baxter, J., (2020). Separable functions of Tof1/Timeless in intra-S-checkpoint signalling, replisome stability and DNA topological stress. *Nucleic Acids Res.* **48**, 12169–12187. <https://doi.org/10.1093/nar/gkaa963>.
40. Shyian, M., Albert, B., Zupan, A.M., Ivanitsa, V., Charbonnet, G., Dilg, D., Shore, D., (2020). Fork pausing complex engages topoisomerases at the replisome. *Genes Dev.* **34**, 87–98. <https://doi.org/10.1101/gad.331868.119>.
41. Schalbetter, S.A., Mansoubi, S., Chambers, A.L., Downs, J.A., Baxter, J., (2015). Fork rotation and DNA precatenation are restricted during DNA replication to prevent chromosomal instability. *Proc. Natl. Acad. Sci.* **112** <https://doi.org/10.1073/pnas.1505356112>.
42. Numata, Y., Ishihara, S., Hasegawa, N., Nozaki, N., Ishimi, Y., (2010). Interaction of human MCM2-7 proteins with TIM, TIPIN and Rb. *J. Biochem. (Tokyo)* **147**, 917–927. <https://doi.org/10.1093/jb/mvq028>.
43. Serçin, Ö., Kemp, M.G., (2011). Characterization of functional domains in human Claspín. *Cell Cycle* **10**, 1599–1606. <https://doi.org/10.4161/cc.10.10.15562>.
44. Xia, Y., Fujisawa, R., Deegan, T.D., Sonnevill, R., Labib, K.P.M., (2021). TIMELESS-TIPIN and UBXN-3 promote replisome disassembly during DNA replication termination in *Caenorhabditis elegans*. *EMBO J.* **40**, e108053.
45. Jenkyn-Bedford, M., Jones, M.L., Baris, Y., Labib, K.P.M., Cannone, G., Yeeles, J.T.P., Deegan, T.D., (2021). A conserved mechanism for regulating replisome disassembly in eukaryotes. *Nature* **600**, 743–747. <https://doi.org/10.1038/s41586-021-04145-3>.
46. Leman, A.R., Noguchi, E., (2012). Local and global functions of Timeless and Tipin in replication fork protection. *Cell Cycle* **11**, 3945–3955. <https://doi.org/10.4161/cc.21989>.
47. Dalgaard, J.Z., Godfrey, E.L., MacFarlane, R.J., Dalgaard, J.Z., Godfrey, E.L., MacFarlane, R.J., (2011). Eukaryotic Replication Barriers: How, Why and Where Forks Stall. *IntechOpen*. <https://doi.org/10.5772/20383>.
48. Voineagu, I., Narayanan, V., Lobachev, K.S., Mirkin, S.M., (2008). Replication stalling at unstable inverted repeats: Interplay between DNA hairpins and fork stabilizing proteins. *Proc. Natl. Acad. Sci.* **105**, 9936–9941. <https://doi.org/10.1073/pnas.0804510105>.
49. Hodgson, B., Calzada, A., Labib, K., (2007). Mrc1 and Tof1 Regulate DNA Replication Forks in Different Ways during Normal S Phase. *Mol. Biol. Cell* **18**, 9.
50. Krings, G., Bastia, D., (2004). *swi1* - and *swi3* -dependent and independent replication fork arrest at the ribosomal DNA of *Schizosaccharomyces pombe*. *Proc. Natl. Acad. Sci.* **101**, 14085–14090. <https://doi.org/10.1073/pnas.0406037101>.
51. Akamatsu, Y., Kobayashi, T., (2015). The human RNA polymerase I transcription terminator complex acts as a replication fork barrier that coordinates the progress of replication with rRNA transcription activity. *Mol. Cell Biol.* **35**, 1871–1881. <https://doi.org/10.1128/MCB.01521-14>.
52. Gellon, L., Kaushal, S., Cebrián, J., Lahiri, M., Mirkin, S. M., Freudenreich, C.H., (2019). Mrc1 and Tof1 prevent fragility and instability at long CAG repeats by their fork stabilizing function. *Nucleic Acids Res.* **47**, 794–805. <https://doi.org/10.1093/nar/gky1195>.
53. Razioldo, D.F., Lahue, R.S., (2008). Mrc1, Tof1 and Csm3 inhibit CAG-CTG repeat instability by at least two mechanisms. *DNA Repair* **7**, 633–640. <https://doi.org/10.1016/j.dnarep.2008.01.009>.
54. Cherng, N., Shishkin, A.A., Schlager, L.I., Tuck, R.H., Sloan, L., Matera, R., Sarkar, P.S., Ashizawa, T., Freudenreich, C.H., Mirkin, S.M., (2011). Expansions, contractions, and fragility of the spinocerebellar ataxia type 10 pentanucleotide repeat in yeast. *Proc. Natl. Acad. Sci.* **108**, 2843–2848. <https://doi.org/10.1073/pnas.1009409108>.
55. LeClere, A.R., Yang, J.K., Kirkpatrick, D.T., (2013). The role of CSM3, MRC1, and TOF1 in minisatellite stability and large loop DNA repair during meiosis in yeast. *Fungal*

- Genet. Biol.* **50**, 33–43. <https://doi.org/10.1016/j.fgb.2012.10.007>.
56. Liu, G., Chen, X., Gao, Y., Lewis, T., Barthelemy, J., Leffak, M., (2012). Altered replication in human cells promotes DMPK (CTG)_n · (CAG)_n repeat instability. *Mol. Cell Biol.* **32**, 1618–1632. <https://doi.org/10.1128/MCB.06727-11>.
 57. Leman, A.R., Dheekollu, J., Deng, Z., Lee, S.W., Das, M. M., Lieberman, P.M., Noguchi, E., (2012). Timeless preserves telomere length by promoting efficient DNA replication through human telomeres. *Cell Cycle* **11**, 2337–2347. <https://doi.org/10.4161/cc.20810>.
 58. Gadaleta, M.C., Das, M.M., Tanizawa, H., Chang, Y.-T., Noma, K., Nakamura, T.M., Noguchi, E., (2016). Swi1Timeless prevents repeat instability at fission yeast telomeres. *PLoS Genet.* **12**, e1005943.
 59. Gadaleta, M.C., González-Medina, A., Noguchi, E., (2016). Timeless protection of telomeres. *Curr. Genet.* **62**, 725–730. <https://doi.org/10.1007/s00294-016-0599-x>.
 60. Min, J., Wright, W.E., Shay, J.W., (2017). Alternative lengthening of telomeres mediated by mitotic DNA synthesis engages break-induced replication processes. *Mol. Cell Biol.* **37**, e00226–e317. <https://doi.org/10.1128/MCB.00226-17>.
 61. Bairwa, N.K., Mohanty, B.K., Stamenova, R., Curcio, M. J., Bastia, D., (2011). The intra-S phase checkpoint protein Tof1 collaborates with the helicase Rrm3 and the F-box protein Dia2 to maintain genome stability in *Saccharomyces cerevisiae*. *J. Biol. Chem.* **286**, 2445–2454. <https://doi.org/10.1074/jbc.M110.189456>.
 62. Pryce, D.W., Ramayah, S., Jaendling, A., McFarlane, R. J., (2009). Recombination at DNA replication fork barriers is not universal and is differentially regulated by Swi1. *Proc. Natl. Acad. Sci.* **106**, 4770–4775. <https://doi.org/10.1073/pnas.0807739106>.
 63. Sommariva, E., Pellny, T.K., Karahan, N., Kumar, S., Huberman, J.A., Dalgaard, J.Z., (2005). Schizosaccharomyces pombe Swi1, Swi3, and Hsk1 are components of a novel S-phase response pathway to alkylation damage. *Mol. Cell Biol.* **25**, 2770–2784. <https://doi.org/10.1128/MCB.25.7.2770-2784.2005>.
 64. Ünsal-Kaçmaz, K., Mullen, T.E., Kaufmann, W.K., Sancar, A., (2005). Coupling of human circadian and cell cycles by the timeless protein. *Mol. Cell Biol.* **25**, 3109–3116. <https://doi.org/10.1128/MCB.25.8.3109-3116.2005>.
 65. Liu, S., Bekker-Jensen, S., Mailand, N., Lukas, C., Bartek, J., Lukas, J., (2006). Claspin operates downstream of TopBP1 To Direct ATR signaling towards Chk1 activation. *Mol. Cell Biol.* **26**, 6056–6064. <https://doi.org/10.1128/MCB.00492-06>.
 66. Kang, T.-H., Leem, S.-H., (2014). Modulation of ATR-mediated DNA damage checkpoint response by cryptochrome 1. *Nucleic Acids Res.* **42**, 4427–4434. <https://doi.org/10.1093/nar/gku094>.
 67. Yang, X., Wood, P.A., Hrushesky, W.J.M., (2010). Mammalian TIMELESS Is Required for ATM-dependent CHK2 Activation and G2/M Checkpoint Control. *J. Biol. Chem.* **285**, 3030–3034. <https://doi.org/10.1074/jbc.M109.050237>.
 68. Cali, F., Bharti, S.K., Perna, R.D., Brosh Jr, R.M., Pisani, F.M., (2016). Tim/Timeless, a member of the replication fork protection complex, operates with the Warsaw breakage syndrome DNA helicase DDX11 in the same fork recovery pathway. *Nucleic Acids Res.* **44**, 705–717. <https://doi.org/10.1093/nar/gkv1112>.
 69. Yang, X.H., Shiotani, B., Classon, M., Zou, L., (2008). Chk1 and Claspin potentiate PCNA ubiquitination. *Genes Dev.* **22**, 1147–1152. <https://doi.org/10.1101/gad.1632808>.
 70. Yang, X.H., Zou, L., (2009). Dual functions of DNA replication forks in checkpoint signaling and PCNA ubiquitination. *Cell Cycle Georget. Tex.* **8**, 191–194. <https://doi.org/10.4161/cc.8.2.7357>.
 71. Cortone, G., Zheng, G., Pensieri, P., Chiappetta, V., Tatè, R., Malacaria, E., Pichierri, P., Yu, H., et al., (2018). Interaction of the Warsaw breakage syndrome DNA helicase DDX11 with the replication fork-protection factor Timeless promotes sister chromatid cohesion. *PLoS Genet.* **14**, e1007622.
 72. van Schie, J.J.M., de Lange, J., (2021). The interplay of cohesin and the replisome at processive and stressed DNA replication forks. *Cells.* **10**, 3455. <https://doi.org/10.3390/cells10123455>.
 73. Tanaka, H., Kubota, Y., Tsujimura, T., Kumano, M., Masai, H., Takisawa, H., (2009). Replisome progression complex links DNA replication to sister chromatid cohesion in *Xenopus* egg extracts. *Genes Cells* **14**, 949–963. <https://doi.org/10.1111/j.1365-2443.2009.01322.x>.
 74. Borges, V., Smith, D.J., Whitehouse, I., Uhlmann, F., (2013). An Eco1-independent sister chromatid cohesion establishment pathway in *S. cerevisiae*. *Chromosoma* **122**, 121–134. <https://doi.org/10.1007/s00412-013-0396-y>.
 75. Srinivasan, M., Fumasoni, M., Petela, N.J., Murray, A., Nasmyth, K.A., (2020). Cohesion is established during DNA replication utilising chromosome associated cohesin rings as well as those loaded de novo onto nascent DNAs. *Elife* **9**, e56611.
 76. Smith-Roe, S.L., Patel, S.S., Simpson, D.A., Zhou, Y.C., Rao, S., Ibrahim, J.G., Kaiser-Rogers, K.A., Cordeiro-Stone, M., Kaufmann, W.K., (2011). Timeless functions independently of the Tim-Tipin complex to promote sister chromatid cohesion in normal human fibroblasts. *Cell Cycle* **10**, 1618–1624. <https://doi.org/10.4161/cc.10.10.15613>.
 77. Murakami, H., Keeney, S., (2014). Temporospatial coordination of meiotic DNA replication and recombination via DDK recruitment to replisomes. *Cell* **158**, 861–873. <https://doi.org/10.1016/j.cell.2014.06.028>.
 78. Murakami, H., Keeney, S., (2014). DDK links replication and recombination in meiosis. *Cell Cycle* **13**, 3621–3622. <https://doi.org/10.4161/15384101.2014.986626>.
 79. Gotter, A.L., Manganaro, T., Weaver, D.R., Kolakowski, L. F., Possidente, B., Sriram, S., MacLaughlin, D.T., Reppert, S.M., (2000). A time-less function for mouse Timeless. *Nature Neurosci.* **3**, 755–756. <https://doi.org/10.1038/77653>.
 80. O'Reilly, L.P., Watkins, S.C., Smithgall, T.E., (2011). An unexpected role for the clock protein timeless in developmental apoptosis. *PLoS One* **6**, e17157 <https://doi.org/10.1371/journal.pone.0017157>.
 81. Yoshinaga, S.K., Peterson, C.L., Herskowitz, I., Yamamoto, K.R., (1992). Roles of SWI1, SWI2, and SWI3 proteins for transcriptional enhancement by steroid receptors. *Sci. New Ser.* **258**, 1598–1604.
 82. Doerks, T., Copley, R., Bork, P., (2001). DDT – a novel domain in different transcription and chromosome

- remodeling factors. *Trends Biochem. Sci.* **26**, 145–146. [https://doi.org/10.1016/s0968-0004\(00\)01769-2](https://doi.org/10.1016/s0968-0004(00)01769-2).
83. Barrio-Alonso, E., Lituma, P.J., Notaras, M.J., Albero, R., Boucheikioua, Y., Wayland, N., Stankovic, I.N., Jain, T., et al., (2023). Circadian protein TIMELESS regulates synaptic function and memory by modulating cAMP signaling. *Cell Rep.* **42**, 112375 <https://doi.org/10.1016/j.celrep.2023.112375>.
 84. Sehgal, A., Rothenfluh-Hilfiker, A., Hunter-Ensor, M., Chen, Y., Myers, M.P., Young, M.W., (1995). Rhythmic expression of *timeless*: a basis for promoting circadian cycles in *period* Gene autoregulation. *Science* **270**, 808–810. <https://doi.org/10.1126/science.270.5237.808>.
 85. Yang, Z., Sehgal, A., (2001). Role of molecular oscillations in generating behavioral rhythms in drosophila. *Neuron* **29**, 453–467. [https://doi.org/10.1016/S0896-6273\(01\)00218-5](https://doi.org/10.1016/S0896-6273(01)00218-5).
 86. Stone, E.F., Fulton, B.O., Ayres, J.S., Pham, L.N., Ziauddin, J., Shirasu-Hiza, M.M., (2012). The circadian clock protein timeless regulates phagocytosis of bacteria in drosophila. *PLoS Pathog.* **8**, e1002445.
 87. Stehlík, J., Závodská, R., Shimada, K., Šauman, I., Košťál, V., (2008). Photoperiodic induction of diapause requires regulated transcription of *timeless* in the larval brain of *Chymomyza costata*. *J. Biol. Rhythms* **23**, 129–139. <https://doi.org/10.1177/0748730407313364>.
 88. Engelen, E., Janssens, R.C., Yagita, K., Smits, V.A.J., van der Horst, G.T.J., Tamanini, F., (2013). Mammalian TIMELESS is involved in period determination and DNA damage-dependent phase advancing of the circadian clock. *PLoS One* **8**, e56623 <https://doi.org/10.1371/journal.pone.0056623>.
 89. Tischkau, S.A., Barnes, J.A., Lin, F.J., Myers, E.M., Barnes, J.W., Meyer-Bernstein, E.L., Hurst, W.J., Burgoon, P.W., et al., (1999). Oscillation and light induction of timeless mRNA in the mammalian circadian clock. *J. Neurosci. Off. J. Soc. Neurosci.* **19**, RC15.
 90. Barnes, J.W., Tischkau, S.A., Barnes, J.A., Mitchell, J.W., Burgoon, P.W., Hickok, J.R., Gillette, M.U., (2003). Requirement of mammalian *Timeless* for circadian rhythmicity. *Science* **302**, 439–442. <https://doi.org/10.1126/science.1086593>.
 91. Kurien, P., Hsu, P.-K., Leon, J., Wu, D., McMahon, T., Shi, G., Xu, Y., Lipzen, A., et al., (2019). TIMELESS mutation alters phase responsiveness and causes advanced sleep phase. *Proc. Natl. Acad. Sci.* **116**, 12045–12053. <https://doi.org/10.1073/pnas.1819110116>.
 92. Cai, Y.D., Chiu, J.C., (2021). *Timeless* in animal circadian clocks and beyond. *FEBS J.*, febs.16253. <https://doi.org/10.1111/febs.16253>.
 93. Gotter, A.L., (2006). A Timeless debate: resolving TIM's noncircadian roles with possible clock function. *Neuroreport* **17**, 1229–1233. <https://doi.org/10.1097/01.wnr.0000233092.90160.92>.
 94. Li, F., Zhao, C., Diao, Y., Wang, Z., Peng, J., Yang, N., Qiu, C., Kong, B., et al., (2022). MEX3A promotes the malignant progression of ovarian cancer by regulating intron retention in TIMELESS. *Cell Death Dis.* **13**, 1–13. <https://doi.org/10.1038/s41419-022-05000-7>.
 95. Mao, Y., Fu, A., Leaderer, D., Zheng, T., Chen, K., Zhu, Y., (2013). Potential cancer-related role of circadian gene TIMELESS suggested by expression profiling and in vitro analyses. *BMC Cancer* **13**, 498. <https://doi.org/10.1186/1471-2407-13-498>.
 96. Fu, A., Leaderer, D., Zheng, T., Hoffman, A.E., Stevens, R.G., Zhu, Y., (2012). Genetic and epigenetic associations of circadian gene TIMELESS and breast cancer risk. *Mol. Carcinog.* **51**, 923–929. <https://doi.org/10.1002/mc.20862>.
 97. Ye, J., Chen, J., Wang, J., Xia, Z., Jia, Y., (2022). Association of the timeless gene with prognosis and clinical characteristics of human lung cancer. *Diagnostics* **12**, 2681. <https://doi.org/10.3390/diagnostics12112681>.
 98. Yoshida, K., Sato, M., Hase, T., Elshazley, M., Yamashita, R., Usami, N., Taniguchi, T., Yokoi, K., et al., (2013). TIMELESS is overexpressed in lung cancer and its expression correlates with poor patient survival. *Cancer Sci.* **104**, 171–177. <https://doi.org/10.1111/cas.12068>.
 99. Zhao, S., Wen, S., Liu, H., Zhou, Z., Liu, Y., Zhong, J., Xie, J., (2022). High expression of TIMELESS predicts poor prognosis: a potential therapeutic target for skin cutaneous melanoma. *Front. Surg.* **9**, 917776 <https://doi.org/10.3389/fsurg.2022.917776>.
 100. Wang, F., Chen, Q., (2018). The analysis of deregulated expression of the timeless genes in gliomas. *J. Cancer Res. Ther.* **14**, S708. <https://doi.org/10.4103/0973-1482.187382>.
 101. Xing, X., Gu, F., Hua, L., Cui, X., Li, D., Wu, Z., Zhang, R., (2021). TIMELESS promotes tumor progression by enhancing macrophages recruitment in ovarian cancer. *Front. Oncol.* **11**, 732058 <https://doi.org/10.3389/fonc.2021.732058>.
 102. Zhang, W., He, W., Shi, Y., Zhao, J., Liu, S., Zhang, F., Yang, J., Xie, C., et al., (2017). Aberrant TIMELESS expression is associated with poor clinical survival and lymph node metastasis in early-stage cervical carcinoma. *Int. J. Oncol.* **50**, 173–184. <https://doi.org/10.3892/ijo.2016.3784>.
 103. Elgohary, N., Pellegrino, R., Neumann, O., Elzawahry, H. M., Saber, M.M., Zeeneldin, A.A., Geffers, R., Ehemann, V., et al., (2015). Protumorigenic role of Timeless in hepatocellular carcinoma. *Int. J. Oncol.* **46**, 597–606. <https://doi.org/10.3892/ijo.2014.2751>.
 104. Chi, L., Zou, Y., Qin, L., Ma, W., Hao, Y., Tang, Y., Luo, R., Wu, Z., (2017). TIMELESS contributes to the progression of breast cancer through activation of MYC. *Breast Cancer Res.* **19**, 53. <https://doi.org/10.1186/s13058-017-0838-1>.
 105. Li, B., Mu, L., Li, Y., Xia, K., Yang, Y., Aman, S., Ahmad, B., Li, S., Wu, H., (2021). TIMELESS inhibits breast cancer cell invasion and metastasis by down-regulating the expression of MMP9. *Cancer Cell Int.* **21**, 38. <https://doi.org/10.1186/s12935-021-01752-y>.
 106. Colangelo, T., Carbone, A., Mazzarelli, F., Cuttano, R., Dama, E., Nittoli, T., Albanesi, J., Barisciano, G., et al., (2022). Loss of circadian gene Timeless induces EMT and tumor progression in colorectal cancer via Zeb1-dependent mechanism. *Cell Death Differ.* **29**, 1552–1568. <https://doi.org/10.1038/s41418-022-00935-y>.
 107. Bianco, J.N., Bergoglio, V., Lin, Y.-L., Pillaire, M.-J., Schmitz, A.-L., Gilhodes, J., Lusque, A., Mazières, J., et al., (2019). Overexpression of Claspin and Timeless protects cancer cells from replication stress in a checkpoint-independent manner. *Nature Commun.* **10**, 910. <https://doi.org/10.1038/s41467-019-08886-8>.
 108. Zhou, J., Zhang, Y., Zou, X., Kuai, L., Wang, L., Wang, J., Shen, F., Hu, J., et al., (2020). Aberrantly expressed timeless regulates cell proliferation and cisplatin efficacy

- in cervical cancer. *Hum. Gene Ther.* **31**, 385–395. <https://doi.org/10.1089/hum.2019.080>.
109. Liu, S.-L., Lin, H.-X., Lin, C.-Y., Sun, X.-Q., Ye, L.-P., Qiu, F., Wen, W., Hua, X., et al., (2017). TIMELESS confers cisplatin resistance in nasopharyngeal carcinoma by activating the Wnt/ β -catenin signaling pathway and promoting the epithelial mesenchymal transition. *Cancer Letter* **402**, 117–130. <https://doi.org/10.1016/j.canlet.2017.05.022>.
 110. Zou, X., Zhu, C., Zhang, L., Zhang, Y., Fu, F., Chen, Y., Zhou, J., (2020). MicroRNA-708 suppresses cell proliferation and enhances chemosensitivity of cervical cancer cells to cDDP by negatively targeting timeless. *OncoTargets Ther.* **13**, 225–235. <https://doi.org/10.2147/OTT.S227015>.
 111. Neilsen, B.K., Frodyma, D.E., McCall, J.L., Fisher, K.W., Lewis, R.E., (2019). ERK-mediated TIMELESS expression suppresses G2/M arrest in colon cancer cells. *PLoS One* **14**, e0209224.
 112. Niedzwecki, B., Kambhampati, O., Granat, L., Zhang, D., (2019). The regulation of replication stress response at ALT telomeres by Timeless-1. *FASEB J.* **33**, 719.3. https://doi.org/10.1096/fasebj.2019.33.1_supplement.719.3.
 113. Shen, X., Li, M., Mao, Z., Yu, W., (2018). Loss of circadian protein TIMELESS accelerates the progression of cellular senescence. *Biochem. Biophys. Res. Commun.* **503**, 2784–2791. <https://doi.org/10.1016/j.bbrc.2018.08.040>.
 114. Dheekollu, J., Chen, H.-S., Kaye, K.M., Lieberman, P.M., (2013). Timeless-dependent DNA replication-coupled recombination promotes Kaposi's Sarcoma-associated herpesvirus episome maintenance and terminal repeat stability. *J. Virol.* **87**, 3699–3709. <https://doi.org/10.1128/JVI.02211-12>.
 115. Dheekollu, J., Lieberman, P.M., (2011). The replisome pausing factor timeless is required for episomal maintenance of latent epstein-barr virus. *J. Virol.* **85**, 5853–5863. <https://doi.org/10.1128/JVI.02425-10>.
 116. Zhang, W., Di, L., Liu, Z., Sun, Q., Wu, Y., Wang, N., Jin, M., Gao, L., et al., (2022). TIMELESS is a key gene mediating thrombogenesis in COVID-19 and antiphospholipid syndrome. *Sci. Rep.* **12**, 17248. <https://doi.org/10.1038/s41598-022-21694-3>.
 117. Utge, S.J., Soronen, P., Loukola, A., Kronholm, E., Ollila, H.M., Pirkola, S., Porkka-Heiskanen, T., Partonen, T., et al., (2010). Systematic analysis of circadian genes in a population-based sample reveals association of TIMELESS with depression and sleep disturbance. *PLoS One* **5**, e9259.
 118. Langwinski, W., Sobkowiak, P., Narozna, B., Wojsyk-Banaszak, I., Dmitrzak-Węglarz, M., Stachowiak, Z., Nowakowska, J., Bręborowicz, A., et al., (2020). Association of circadian clock TIMELESS variants and expression with asthma risk in children. *Clin. Respir. J.* **14**, 1191–1200. <https://doi.org/10.1111/crj.13260>.
 119. Carter, C.J., (2007). Multiple genes and factors associated with bipolar disorder converge on growth factor and stress activated kinase pathways controlling translation initiation: Implications for oligodendrocyte viability. *Neurochem. Int.* **50**, 461–490. <https://doi.org/10.1016/j.neuint.2006.11.009>.
 120. Lu, H., Zhou, Q., He, J., Jiang, Z., Peng, C., Tong, R., Shi, J., (2020). Recent advances in the development of protein–protein interactions modulators: mechanisms and clinical trials. *Signal Transduct. Target. Ther.* **5**, 1–23. <https://doi.org/10.1038/s41392-020-00315-3>.
 121. Nedelcheva, M.N., Roguev, A., Dolapchiev, L.B., Shevchenko, A., Taskov, H.B., Shevchenko, A., Francis Stewart, A., Stoyanov, S.S., (2005). Uncoupling of unwinding from DNA synthesis implies regulation of MCM helicase by Tof1/Mrc1/Csm3 checkpoint complex. *J. Mol. Biol.* **347**, 509–521. <https://doi.org/10.1016/j.jmb.2005.01.041>.
 122. Bando, M., Katou, Y., Komata, M., Tanaka, H., Itoh, T., Sutani, T., Shirahige, K., (2009). Csm3, Tof1, and Mrc1 form a heterotrimeric mediator complex that associates with DNA replication forks. *J. Biol. Chem.* **284**, 34355–34365. <https://doi.org/10.1074/jbc.M109.065730>.
 123. Noguchi, E., Noguchi, C., McDonald, W.H., Yates, J.R., Russell, P., (2004). Swi1 and Swi3 are components of a replication fork protection complex in fission yeast. *Mol. Cell Biol.* **24**, 8342–8355. <https://doi.org/10.1128/MCB.24.19.8342-8355.2004>.
 124. Dalgaard, J.Z., Klar, A.J.S., (2000). swi1 and swi3 perform imprinting, pausing, and termination of DNA replication in *S. pombe*. *Cell* **102**, 745–751. [https://doi.org/10.1016/S0092-8674\(00\)00063-5](https://doi.org/10.1016/S0092-8674(00)00063-5).
 125. Noguchi, C., Rapp, J.B., Skorobogatko, Y.V., Bailey, L.D., Noguchi, E., (2012). Swi1 associates with chromatin through the DDT domain and recruits Swi3 to preserve genomic integrity. *PLoS One* **7**, e43988.
 126. Katou, Y., Kanoh, Y., Bando, M., Noguchi, H., Tanaka, H., Ashikari, T., Sugimoto, K., Shirahige, K., (2003). S-phase checkpoint proteins Tof1 and Mrc1 form a stable replication-pausing complex. *Nature* **424**, 1078–1083. <https://doi.org/10.1038/nature01900>.
 127. Lo, N., Rageul, J., Kim, H., (2021). Roles of SDE2 and TIMELESS at active and stalled DNA replication forks. *Mol. Cell. Oncol.* **8**, 1855053. <https://doi.org/10.1080/23723556.2020.1855053>.
 128. Safaric, B., Chacin, E., Scherr, M.J., Rajappa, L., Gebhardt, C., Kurat, C.F., Cordes, T., Duderstadt, K.E., (2022). The fork protection complex recruits FACT to reorganize nucleosomes during replication. *Nucleic Acids Res.* **50**, 1317–1334. <https://doi.org/10.1093/nar/gkac005>.

Publication III

S. Vipat, K. Shapovalovaite, A. Morgunov, R. Harolikar, S. Vallo, T. Moiseeva, '**TIMELESS recruits the Fork Protection Complex to the replisome during DNA replication initiation in human cells**', (manuscript).

TIMELESS recruits the Fork Protection Complex to the replisome during DNA replication initiation in human cells

Sameera Vipat, Karina Shapovalovaite, Arthur Morgunov, Rohan Harolika, Sigvard Vallo, Tatiana N. Moiseeva

Abstract

TIMELESS (TIM) is an essential protein that ensures unhindered movement of the replication fork under stress or through intrinsic barriers in the genome. While its roles in the protection of stressed replication are well studied, its potential role at the step of replication initiation is less well explored. Here we use a conditional auxin-inducible degron system to study the effect of TIM depletion on replication initiation in human cells. TIM depleted cells exhibited inefficient S phase entry, and a defect in the loading of CLASPIN and TIPIN, the other two components of the Fork Protection Complex (FPC), providing the first evidence that the FPC is necessary for maintaining normal replication initiation. We further show that the FPC loads to chromatin in multiple steps, the first fraction loading concurrently with assembly of the replicative helicase and another fraction loading after DNA synthesis is initiated. Our data also show that TIM requires interaction with MCM for loading to chromatin. Using split-Turbo ID-based proximity labelling we show that there may be more than one FPC per replication fork. Our study uncovers a new role for TIM in supporting DNA replication initiation in human cells.

Introduction

The basic mechanisms of replication initiation are conserved in eukaryotes from yeast to humans [1] [2]. The assembly of the replisome begins in G1 phase of the cell cycle with origin licensing, which is loading of MCM helicase onto the origins marked by the Origin Recognition Complex (ORC). This is followed by CDK-dependent recruitment of CDC45 and GINS to MCM, leading to CMG helicase assembly. MCM is then activated by DDK- and CDK2- dependent phosphorylations, after which accessory factors and polymerase alpha (polA)-primase are recruited to the replication complex, and the full replisome is assembled. After RNA primers are synthesized by primase, PolA adds the first short stretch of DNA, after which PCNA is loaded by Replication Factor C (RFC) at the template-primer 3' end sites [3]. PCNA loading initiates polymerase delta (polD) loading [4] [5], and polD then takes over DNA synthesis from polA. As two CMG complexes start moving towards each other and bypass each other, the initial DNA synthesis on both leading and lagging strands is performed by polD [6]. Polymerase epsilon (polE) subsequently takes over the leading strand from polD [7], and after this 'polymerase switch' step, two replication forks moving in opposite directions are established.

TIM performs most of its functions bound to its obligate binding partner TIPIN, and it has been shown that depletion of one partner leads to a depletion of the other [8]. Together with CLASPIN, TIM and TIPIN, form the Fork Protection Complex (FPC), which plays a critical role in protecting the integrity of moving forks under replication stress. Some studies also consider AND-1 as a part of the FPC [9], however its position is observed in structural studies does not indicate direct interactions with the canonical FPC [10], [11] suggesting that the fork protection functions that it has [12], [12] could be performed independently of the FPC. TIM-TIPIN have been very well studied in the context of protecting replication forks from stalling when cells undergo genotoxic stress or DNA damage [13], [14]. Additionally, TIM- TIPIN are also known to support forks through several types of endogenous barrier regions in the genome [13]. During replication elongation, TIM-TIPIN have been shown to coordinate the activities of the MCM helicase and the polymerases [15], [16], [17], [18], [19]. They are believed to stimulate DNA polymerase activity and at the same time regulate MCM helicase activity [20] [17], to couple these two components of the fork together,

and this is thought to be the mechanism through which TIM-TIPIN ensure the maintenance of normal fork speed.

What roles TIM-TIPIN play in replication initiation is still poorly understood. There is conflicting evidence in this matter, with some studies reporting excessive origin firing [8] and others reporting delayed S phase entry and a reduction in S phase cell population [21], upon TIM depletion. Here, we investigate the role of TIM in replication initiation, using a conditional depletion system where TIM is tagged with a mini-auxin inducible degron (mAID) tag that allows its near-complete depletion within a short time frame [22], [23]. We show that TIM depletion causes a decrease in DNA synthesis in S phase when depleted in G1 phase, and compromised S phase entry when depleted in G2 phase. Mechanistically, TIM depletion compromises the loading of CLASPIN and TIPIN to chromatin. We also observed delayed loading of PCNA during subsequent S phase entry after TIM depletion in G2 phase.

It is currently unclear at what time during the initiation of DNA replication TIM is recruited into the replisome. It has been shown that TIM is loaded to origins at replication initiation with the same dynamics as CDC45 [24], however details of its loading timing are not well understood. In contrast, it has also been reported that TIM associates with MCM even before the beginning of S phase, which [13] may indicate that it is loaded to origins along with MCM [21]. The latter model is not consistent with TIM being located at the leading edge of the fork which would be concealed in the MCM: MCM contact in the MCM double hexamers during MCM loading, as per structural data [25]. In this study, we aimed to clarify the timing of TIM chromatin loading relative to other replication initiation proteins in synchronized cells undergoing S phase entry. We show that TIM is recruited to chromatin in multiple steps, with some TIM loading concurrently with CMG, and the rest of TIM loading upon the initiation of DNA synthesis.

Structural studies repeatedly demonstrated that TIM, TIPIN and CLASPIN are positioned at the leading edge of the replication fork, interacting with MCM and gripping DNA [10], [11], [26]. However, this position is not fully consistent with observations from biochemical studies which show that TIM directly interacts with the polymerases [17], and TIM-TIPIN bind to RPA which is loaded onto ssDNA behind the replication fork [27], [28]. We employ a split-TurboID-based proximity labelling system [29] to study the proteins in proximity of TIM at the fork and better understand TIM's position in the replisome, and the set of proteins biotinylated by the used split TurboID pairs supports the model in which there is more than one molecule of TIM per replication fork.

Using a mutant of TIM unable to interact with MCM but retaining its interactions with TIPIN and CLASPIN, we show that TIM-MCM interaction is essential for the role of TIM in the initiation of DNA replication, including supporting DNA synthesis, as well as efficient chromatin loading of TIPIN, CLASPIN and PCNA. Our study provides insights into the role of TIM in replication initiation, a process relevant in the context of carcinogenesis and anticancer chemotherapy. Our findings also shed light on other less explored facets of TIM's role, such as its position at the fork and its chromatin loading dynamics, and broaden our understanding of the complex process of replication initiation in human cells.

Results

TIM depletion compromises S phase entry and decelerates DNA synthesis

We used a mini-auxin-inducible degron (mAID) system to achieve rapid and near-complete depletion of TIMELESS, which enabled us to study its role in replication initiation in human cells. In this system, the target protein TIM is tagged with a short mAID tag using CRISPR genome modification, and additionally the F-box protein osTIR1 is stably transfected into the genome of cells [23], [30]. Our mAID system version 1 (mAID1) uses dox-inducible osTIR1 [23] while version 2 (mAID2) uses constitutively expressed osTIR1 [22], as version 2 avoids the problem of leaky degradation. In these systems, TIM is depleted to near-complete levels upon the addition of the plant hormone auxin. In the presence of the plant hormone auxin (3-IAA (indole-3-acetic acid) for mAID1 and 5-ph-IAA (5-phenyl-indole-3-acetic acid) for mAID2), the mAID

tag attached to TIM gets ubiquitylated by E3 ligase that is recruited by oTIR1, which leads to quick and efficient proteolytic degradation of TIM (16 hours for mAID1 and 3 hours for mAID2).

Two clones for mAID1- Clone 10 and Clone 28, and two clones for mAID2- Clone O3 and Clone L4 were selected, based on their ability to deplete TIM to near-complete levels. In mAID1, 16h treatment with 2 µg/ml doxycycline (dox) was used to induce oTIR1 expression. 16h treatment with 500 µM 3-IAA (aux) was used in mAID1 while 4h treatment with 1.25 µM 5-ph-IAA in mAID2 to induce TIM degradation. TIM was strongly depleted in both mAID1 and mAID2, and as expected its partner TIPIN was concurrently downregulated in mAID1 due to prolonged TIM depletion (Fig. 1A and 1B). The levels of CLASPIN were not affected by TIM depletion. mAID tagging neither caused replication stress in the clones (Fig 1A and 1B) nor affected the ability of the clones to induce the ATR replication checkpoint upon replication stress (Fig S1A and S1B).

In order to test the effect of TIM depletion on cell growth, we seeded equal numbers of Clone 10, Clone 28 or U2OS cells, and in a separate experiment, Clone O3, Clone L4 or U2OS cells, and treated them with DMSO or dox/3-IAA or 5-ph-IAA for 72 h and counted the cells every 24 h (Fig. S1E and S1F). Untreated clones grew slightly slower compared to the U2OS cells, however, the addition of dox/3-IAA or 5-ph-IAA greatly reduced the proliferation of TIM-depleted clones Clone 10, Clone 28, Clone O3 and Clone L4, which is in agreement with the essential role of TIM in human cells. Doxycycline treatment also slightly reduced the growth of U2OS cells, as has been previously observed [31], [32].

Next, in order to investigate the effect of TIM depletion on S phase entry, we depleted TIM in cells that were synchronized in G2/M using a double thymidine-nocodazole block and then allowed to enter S phase at the same time (Fig 1C). We added dox/3-IAA to mAID1 cells at the time of nocodazole addition and 5-ph-IAA to mAID2 cells at the time of release from nocodazole. Cells were collected 0h (mitosis), 3h (mid-G1 phase), 6h (beginning of S phase), and 9 h (majority of cells in S phase) following the release from nocodazole. For FACS experiments, a 30-minute pulse with nucleotide analog EdU (5-ethynyl-2'-deoxyuridine) was given to the cells before collection to label newly synthesized DNA. To study S phase entry, the percentages of cells having successfully transitioned from G1 into S phase were analyzed by dual EdU-7-AAD FACS, a technique that allows simultaneous measurement of EdU incorporation and DNA content. Quantifications of S phase cells (Fig. 1E) and G1 phase cells (Fig. S1G) showed a G1 accumulation and a significant reduction in the S phase population in clones 10 and 28 compared to U2OS, indicating that TIM depletion in G2 phase reduces the efficiency of S phase entry in the subsequent cell cycle. Additionally, DNA synthesis as measured by the level of EdU incorporation was lower in these clones compared to U2OS cells (Fig. 1F). Clones Clone O3 and Clone L4 did not show a significant reduction in the percentage of cells entering S phase (Fig. 1H) or exiting G1 phase (Fig. S1H), but did show reduced EdU incorporation compared to U2OS cells (Fig. 1I), indicating that TIM depletion in G1 phase allows for normal S phase entry but reduced DNA synthesis, the latter may be at least partly due to previously documented [16] slower fork speed upon TIM depletion. These results indicate that TIM supports replication initiation and maintains the normal speed of DNA synthesis during S phase entry.

TIM depletion leads to a defect in chromatin loading of CLASPIN and delays PCNA recruitment during origin firing

Delayed S phase entry indicates possible defects with replication initiation, we therefore aimed to determine which steps of replication initiation are affected by the absence of TIM. We synchronized clones Clone 10, Clone 28, Clone O3 Clone L4, and U2OS using the double thymidine-nocodazole block, depleted TIM and collected cells at the same timepoints as described above. To test the ability of various replication initiation proteins to be recruited to chromatin during S-phase entry in the absence of TIM, we analyzed presence of the proteins of interest in the chromatin fraction using western blot.

After prolonged TIM depletion in Clones 10 and 28, cellular levels of TIPIN were depleted (Fig. 1A, 2E). We observed a failure in the recruitment of these proteins to chromatin during S phase entry. Interestingly, we also observed a delay in the recruitment of PCNA and CLASPIN in these clones (Fig. 2A,C). CDC45 showed a delay in unloading during replication termination in the previous cell cycle, which is consistent with similar previous observations [33], attributed to the fact that TIM is required for normal replication termination. However, CDC45 chromatin loading was not affected by TIM depletion, indicating that there was no significant delay in CMG assembly, a critical step in replication initiation. After short TIM depletion in Clones O3 and L4, cellular levels of CLASPIN were unaffected by TIM depletion (Fig. 1B, 2F). However, the recruitment of CLASPIN to chromatin during S phase entry was significantly reduced. Interestingly, the recruitment of PCNA and CDC45 to chromatin was unaffected after TIM depletion in G1 (Fig. 2B,D). Our data indicated that TIM is required for the chromatin loading of CLASPIN during the initiation of DNA replication.

To confirm our findings using an alternative approach, we used an ATR inhibitor AZD6738 (ATRi) which is known to rapidly induce massive origin firing resulting in a strong recruitment of replication proteins to chromatin, MCM4 phosphorylation and an increase in EdU incorporation by replicating cells [34], [35]. We treated Clones 10 and 28, O3 and L4 or U2OS cells with DMSO or dox/3-IAA or 5-ph-IAA for 16 h or 4 h, and added DMSO or 5 μ M ATRi (AZD6738) for the last 1 h to induce origin firing. ATRi treatment caused a robust increase in EdU incorporation in untreated clones but a more modest increase in TIM depleted clones (Fig S2A). We observed significant reductions in CLASPIN and TIPIN recruitment to chromatin in response to ATRi after both prolonged TIM depletion in mAID1 clones (Fig. 2E,G) and short TIM depletion in mAID2 clones (Fig. 2F,H), while the recruitment of CDC45, GINS and POLE remained unaffected.

These data demonstrate that TIM is required for the recruitment of CLASPIN to chromatin during the initiation of DNA replication for the proper assembly of the FPC at the replication fork.

TIM loading to chromatin during origin firing occurs in multiple steps dependent on CMG assembly and on DNA synthesis

Very few studies have explored the dynamics of TIM, TIPIN or CLASPIN loading to origins during replication initiation. We therefore studied the chromatin loading of these proteins to origins relative to the loading of other replication initiation proteins using cell synchronization, to shed more light on the order of their loading.

We synchronized U2OS using the double thymidine-nocodazole block and collected cells at the following timepoints post release from nocodazole: 0h (mitosis), 2.5h (G1 phase), 4h, 5h, 6h, and 7h (most cells in S phase), and analyzed the chromatin fraction by Western blot. By 4h, CDC45 was loaded, indicative of CMG assembly. TIM, TIPIN and CLASPIN are observed to load concurrently with CMG assembly. MCM phosphorylation is observed next. PCNA is seen to begin loading starting from 4h but reaching a significantly high level by 5h (Fig. 3A,B). This is followed by polA loading, which is observed to happen by 6h. We speculate that PCNA may bind chromatin by 5h, but may actually be loaded onto DNA only after polA is available, as it has been reported that chromatin-bound PCNA does not correlate with the assembly of the replisome [36]. Overall, these data indicate that the FPC is loaded simultaneously with CMG assembly in human cells.

To identify the exact step in the cascade of origin firing when the FPC loads onto origins, we inhibited different steps of origin firing using CDK1, CDK2 or CDC7 inhibitors, which are important for S phase entry in human cells, and also used aphidicolin to block DNA synthesis by B-family DNA polymerases. We tested whether the FPC proteins could load to origins upon treatment with these inhibitors. Cell cycle analysis confirmed that these inhibitors suppress S phase entry (Fig. S3,B). We found that FPC loading is partially dependent upon CDK1, CDK2 and CDC7 activities, with FPC loading being reduced but not completely blocked by these inhibitor treatments (Fig. 3C-F). As observed previously [28], CDK1 inhibitor + CDC7

inhibitor combination treatment is the only inhibitor treatment that blocks CDC45 loading completely. Unsurprisingly, FPC loading is completely blocked by this combination treatment. These data indicate that loading of the FPC components, TIM, TIPIN and CLASPIN, is dependent upon the activities of the above tested kinases in human cells. Interestingly, FPC loading was only partially blocked by aphidicolin, which did not affect CDC45 chromatin loading. These data indicate that while DNA synthesis is required for full loading of the FPC to firing origins, CMG assembly is sufficient for partial loading. We propose that some molecules of the FPC proteins may load during the kinase-dependent steps of CMG assembly, and others may load after DNA synthesis is initiated. This observation suggests that there may be more than one molecule of the FPC present at replication forks.

Proximity labelling enabled by TIM interaction with core replication initiation proteins indicates the presence of more than one molecule of TIM per fork

There is conflicting evidence about the position of TIM at the replication fork, with structural studies finding that TIM is positioned ahead of the advancing MCM helicase [10], [11], [26], while biochemical evidence suggested that TIM interacts with the polymerases at the fork and stimulates their activities [17] [20]. To obtain some clues about the exact position of TIM at the fork, we employed a split-Turbo ID-based proximity biotin labelling strategy [29]. In this technique, two proteins are fused to two respective part of the Turbo ID enzyme (TurboN and TurboC). When these tagged proteins interact in the cell, they bring together the two inactive halves of the Turbo ID biotin ligase and reconstitute its activity, tagging proximal proteins with biotin. Biotinylated proteins can then be isolated using a streptavidin pulldown and analyzed by western blotting. To identify the best replication protein to be combined with TIM for this approach, we tagged several replication initiation proteins (MCM4, AND1, ORC6, POLE2) with TurboC and combined each of them with TurboN-TIM. TIM-ORC6 and TIM-AND-1 combinations yielded the best overall biotinylation signal (Fig. 4A, S4A). Following streptavidin pulldown, we identified TIM, TIPIN, CLASPIN, DNA polymerases alpha and epsilon, CDC45 and CHK1 among the proteins biotinylated by both of the selected pairs (Fig. 4B). These data indicate that TIM is positioned in close AND1, ORC6, as well as the identified DNA polymerases and CDC45 proteins at the fork. These biotinylation patterns do not align with the canonical position of TIM, as at this position, N-terminus of TIM is spatially too far away from ORC6 [11] (likely behind the fork working in mismatch repair) and C-terminus of AND-1, with the MCM hexamer complex in the way. Even considering the flexibility of AND1 and the lagging strand, it is difficult to reconcile the biotinylation of POLE and CDC45 by TIM positioned at the leading edge of the fork.

To explore the possibility that there could be more than one molecule of TIM per fork, we tested biotinylation using a combination of TIM-TurboC with TIM-TurboN with TurboN and TurboC fused to either the N-terminal or the C-terminal end of TIM to check if any of the combinations produced a strong biotinylation signal. TIM tagged with split-Turbo ID halves to either its N terminal or its T terminal were tested (Fig. 4C, S4B). Interestingly, TIM-TurboC produced strong biotinylation in combination with either TurboN-TIM or TIM-TurboN, indicating two molecules of TIM being positioned in proximity of each other. Analyses of proteins biotinylated by TIM-TIM combinations identified TIPIN, CLASPIN, CHK1, CDC45 and DNA polymerases alpha and epsilon, as with the previous combinations, and additionally DNA polymerase delta (Fig. 4D). Based in these data, we propose the model that there are two TIM molecules at each fork - one at the leading edge of the fork, and the other on the flexible strand, are depicted in Fig. 4E.

TIM mutant unable to interact with MCM cannot load to chromatin or rescue the replication initiation defect in TIM depleted cells

In our model, only one of the FPCs interacts with MCM. To clarify whether TIM-MCM interaction is needed for chromatin loading of TIM and its function in replication initiation, we generated and a mutant of TIM unable to interact with MCM - TIM-M*. We designed this mutant of TIM based on the data from [17]. This paper showed that the region of TIM comprising of amino acids 1-663 is sufficient for MCM interaction, but neither of the two broader regions present on either side of region 1-663 (specifically, amino acids 1-

307 or amino acids 308-1208) is sufficient for MCM interaction. We reasoned that a stretch of amino acids at the border of these two regions may be participating in MCM interaction. We deleted the amino acids 276-302 at the border of these two regions (structure shown in Fig. 5A). We also took into consideration structural data [38], [39] to ensure our deletion is not too close to the region of TIM known to be necessary for interaction with TIPIN. Phyre2 [40] and AlphaFold [41] were utilized to ensure that the amino acids chosen for deletion would cause minimal changes to the 3D structure of TIM, aiming to preserve TIM's interactions with its other partners. This mutant was confirmed to be unable to interact with MCM using co-immunoprecipitation, while the interactions with TIPIN, CLASPIN and POLE were not affected (Fig. 5B).

We reasoned that the mutant TIM-M* would not be able to load to chromatin at its canonical position, ahead of MCM at the leading edge of the fork, as it is unable to bind MCM. To test whether the TIM-M* mutant is able to load to chromatin or not, we generated a cell line expressing this mutant under the doxycycline-inducible promoter, on the background of our TIM-depleting mAID1 clones Clone 10 and Clone 28. We selected one clone on each background - Clone 10.8 and Clone 28.6, based on their ability to express TIM-M* upon addition of dox. We then titrated dox concentrations to identify the concentration of dox inducing expression of TIM-M* to levels comparable to levels of TIM-mAID-mCherry in these clones. With 72h treatment with 0.01 ug/ml dox and 12h treatment with 3-IAA, we were able to have similar levels of TIM-M* and TIM-mAID-mCherry in our clones (Fig. S5A). We used the double thymidine-nocodazole block to synchronize cells and compared the ability of TIM-M* to load to chromatin to TIM-mAID-mCherry. We found that TIM-M* is unable to load to chromatin (Fig. 6C, D). The replication initiation defect in these clones was similar to that observed in TIM depleted mAID1 clones: TIPIN, CLASPIN and PCNA were unable to load to chromatin (Fig. 6C,E), despite the presence of TIM-mAID-mCherry as well as TIPIN in the cells at normal levels (Fig. S5B). This suggests that the TIM-M* may have a dominant negative effect, sequestering other FPC components and preventing their loading to chromatin.

We next studied the ability of the TIM-M* mutant to rescue the S-phase entry defect in TIM depleted cells, using the same clones. For this experiment, we used 12h treatment with 2 ug/ml dox and 3-IAA, as these are the conditions necessary to deplete TIM-mAID-mCherry to near-complete levels in our mAID1 system (Fig. S6A). Clones Clone 10, Clone 28, Clone 10.8, Clone 28.6 and U2OS were synchronized using the double thymidine nocodazole block, and a 30-minute pulse with EdU was used before collection to label newly synthesized DNA. The ability of TIM-M*-expressing clones to rescue S phase entry was studied by comparing percentages of S phase cells, G1 phase cells and levels of EdU incorporation between TIM-depleted clones and TIM-M* mutant expressing clones. As expected, this mutant could not completely rescue the defect in S phase entry in TIM-depleted cells, despite its high levels present in the cells (Fig. 6A-C, S6B). No significant difference was observed between percentages of S and G1 phase cells and levels of EdU incorporation between TIM-depleted clone Clone 28 and TIM-M* expressing clone Clone 28.6. Surprisingly, Clone 10.8 showed a reduction in S phase population, but an increase in EdU incorporation compared to TIM-depleted clone Clone 10. It is possible that a high number of origins fire in this clone, but replication fails shortly afterwards, leading to this effect. However, this effect cannot be attributed to the presence of the TIM-M* mutant, as it was observed in only one of the two clones expressing this mutant.

Our findings suggest that TIM-MCM interaction is required for TIM recruitment to firing origins during replication initiation and to play its role in supporting replication initiation in human cells

Discussion:

In this study, we established and made use of an auxin-inducible degron (mAID) system to achieve rapid and efficient conditional depletion of TIM (Fig. 1A,B). Most previous studies of the role of TIM in replication initiation have used other strategies of TIM depletion [42], [43], [21], which are known to not be able to achieve a near-complete depletion of TIM. Here we show that TIM is required for the recruitment of TIPIN

and CLASPIN to the chromatin to assemble the Fork Protection Complex during replication initiation in human cells.

TIM depletion affects S-phase entry

We show that the absence of TIM leads to a delay in S phase entry (Fig. 1D,E,G,H,S1G,H) in human cells. This is in agreement with a previous study that showed a reduction in S phase population in TIM depleted cells compared to TIM-proficient cells [33]. A previous study reported a reduction in inter-origin distances upon TIM depletion, which is indicative of excessive origin firing [44]. Slowed forks were also reported in the absence of TIM [16]. We also observed a reduction in DNA synthesis in our system upon TIM depletion (Fig. 1F,I). TIM depletion is known to lead to a decrease in chromatin-associated cyclin E in late G1, and high levels of inhibitors p21 and p27, which suppresses CDK2 activity and delays CMG assembly [33]. We, however, did not observe a delay in CMG assembly in TIM-depleted cells, and speculate that prolonged TIM depletion in this study may have resulted in DNA damage and checkpoint activation, and therefore the delay in CMG assembly.

TIM recruits CLASPIN to chromatin during the initiation of DNA replication

TIM depletion leads to a depletion of its partner TIPIN, and since TIPIN is required to recruit CLASPIN to the fork [28] [45], [46], the reduction in TIPIN levels upon TIM depletion in both our mAID1 and mAID2 system (Fig. 1A,B,2E,F) may explain the reduced loading of CLASPIN (Fig. 2A-D). It is also possible that TIM recruits CLASPIN to origins by direct interaction, and future studies using a mutant version of TIM unable to interact with CLASPIN may clarify this question. Findings from a study that reconstituted human replication with purified proteins [19] indicate that TIM-CLASPIN interaction is crucial for leading strand replication. Taking this into account, we posit that TIM-TIPIN may promote replication initiation, by supporting the recruitment of CLASPIN to the replisome.

TIM depletion leads to a defect in PCNA chromatin loading

To our knowledge, any role of the FPC in supporting the recruitment of PCNA to the fork for replication initiation has not been previously reported. We show that when TIM/TIPIN are depleted in our mAID1 system in G2 phase of the cell cycle, PCNA recruitment to chromatin during the subsequent G1-S transition is delayed (Fig. 2A, C). It is possible that TIM's roles in maintaining the integrity of DNA during mitosis are affected by its loss in G2 phase in this system, which would cause replication stress, and lead to a delay in S phase entry and consequently PCNA loading. However, we do not observe any delay in CDC45 loading/CMG assembly, indicating that replication checkpoint is not activated. Interestingly, PCNA is seen to load normally when TIM/TIPIN are depleted in our mAID2 system later during the cell cycle, in G1 phase (Fig. 2B,D).

In both our mAID1 and mAID2 systems, the loading of TIM, TIPIN and CLASPIN are compromised. The loss of which component of the FPC may be responsible for the delay in PCNA loading during origin firing is not fully clear. An interaction of TIM with PCNA in undamaged cells has been reported [47], [48]. CLASPIN has also been shown to directly interact with PCNA in the absence of DNA damage [49], [50], via its PIP (PCNA Interacting Protein)-box motif, and this interaction is required to maintain normal speed of DNA replication [34]. However, in our mAID2 system, we observe normal PCNA loading to chromatin even when FPC loading is greatly reduced. This leads us to speculate that interaction with the FPC may not be required for PCNA loading per se, but the interaction between FPC proteins and PCNA may stabilize PCNA after it is recruited by Replication Factor C during replication initiation to maintain its appropriate levels at the fork. Further studies using a CLASPIN or TIPIN depletion system are necessary to understand whether one or all of the FPC proteins are required for normal PCNA loading.

Upon TIM depletion in G2 phase in mAID1, there is a delay but not complete abrogation of PCNA recruitment. In this case, PCNA may get loaded/stabilized at a later timepoint during replication initiation

by means of interaction with one of its numerous other PIP motif-containing partners present at the fork [3], such as CDC45 [35].

What leads to the delay in PCNA loading at the subsequent G1-S transition when TIM is depleted in G2 phase, is not clear. It has been previously reported that prolonged TIM depletion leads to an increase in the levels of replication inhibitor p21 in cells [33]. p21 is known to inhibit DNA replication through interacting with and inhibiting two distinct targets: cyclin-CDK2 kinase and PCNA [53]. In case of PCNA, p21 has been shown to act by inhibiting Replication Factor C (RFC)-catalyzed PCNA loading onto DNA [54], [55]. The above-mentioned TIM depletion study used 48 hours of siRNA-based TIM depletion and observed a reduction in CMG assembly due to the CDK2-inhibitory activity of p21. Although we did not observe any reduction in CMG assembly, likely due to lower levels of accumulated p21 than this study, it is quite possible that even a modest increase in p21 in our study could have led to its other effects in the cell. Based on this, we speculate that an increase in p21 in cells due to TIM depletion in G2 phase in our mAID1 system may have led to decreased PCNA loading onto DNA at the subsequent G1-S transition. Since in our mAID2 system TIM is depleted after completion of G2 phase and mitosis, its shorter depletion in G1 may not have led to a significant increase in p21, and thus allowed for normal PCNA loading.

TIM couples the activities of CMG helicase and DNA polymerase epsilon at replication forks [27], with a loss of TIM causing replication stress and a slow-down of replication forks. PCNA enhances the catalytic rate [56] as well as processivity [57] of DNA polymerase delta by direct interaction. DNA polymerase epsilon also requires PCNA for maximal activity [58]. Effectively, PCNA reduction may lead to decreases in the catalytic activity and/or processivity of these polymerases, further slowing down replication forks. A lack of FPC and PCNA at the forks explain the decreased fork speed upon the loss of TIM. This possibility needs to be further investigated.

Surprisingly, PCNA chromatin loading was inhibited in TIM-M* mutant (a mutant of TIM unable to interact with MCM) expressing cells, even though wild type TIM-mAID-mCherry was also present at normal levels and loaded to chromatin in these cells (Fig. 5C,E). We speculate that TIM-M* may exert a dominant negative effect, and sequesters CLASPIN and TIPIN, inhibiting their loading to chromatin.

Timing and dynamics of TIM loading during origin firing

We show that during origin firing, TIM, TIPIN and CLASPIN begin to load to chromatin after MCM loading, at the same time as CMG assembly, and before DNA polymerase alpha (Fig. 3A,B). This is consistent with the previous study that reported that TIM is recruited to origins concurrently with CDC45 [24], however this study did not investigate TIM loading in comparison to other replication initiation proteins loading.

FPC loading likely requires CMG assembly, as CDK1 and CDC7 inhibitor combination treatment abrogates both CDC45 and FPC loading (Fig. 3C-F). TIM loading is also reduced but not completely blocked upon CDK1, CDK2 or CDC7 single treatments, suggesting that TIM loading partially depends on the activities of these kinases. Interestingly, FPC loading is also partially dependent on DNA synthesis, as inhibition of DNA synthesis by aphidicolin leads to a significant reduction in FPC loading without affecting CDC45 recruitment (Fig. 3C-F). This leads us to propose that the FPC may load to chromatin in at least two steps during replication initiation: some molecules of the FPC may load at the same time as CMG assembly and the rest of the molecules may load after initial DNA synthesis. Notably, before the beginning of DNA synthesis, the two CMG complexes are next to and facing each other, and would later bypass each other head-on as DNA synthesis begins. Before the bypass, the canonical position of TIM at the leading edge of the replication fork, is not available, and yet we observe loading of TIM independent of/before DNA synthesis. It is possible that such TIM molecules load immediately after CMG bypass, as the canonical position becomes available, however our method does not allow us to resolve such closely timed events. We speculate that TIM molecules that are recruited before DNA synthesis do it through the interaction with MCM and stay on leading edge of the replication fork. After DNA synthesis begins, additional molecules of TIM/FPC load

by binding RPA on the lagging strand. TIM-TIPIN are known to interact with and be bound to each other throughout the cell cycle, however, there is evidence that TIPIN loads by binding to RPA on ssDNA, and recruits TIM to DNA, under conditions of replication stress [59]. This could be the mechanism of loading of the second molecule of TIM-TIPIN to origins; they may load on the lagging strand after ssDNA becomes available, recruited via TIPIN-RPA interaction.

Although our studies reveal that TIM, TIPIN and CLASPIN are recruited to chromatin with similar dynamics, our findings have not excluded the possibility that these proteins load concurrently but independently from one another. TIM-TIPIN loss affects CLASPIN loading, but CLASPIN loss does not affect TIM-TIPIN loading [8], suggesting that these could load independently. If CLASPIN loads after TIM loading, our method does not provide the resolution necessary to distinguish such closely timed events. Further studies using conditional depletion systems of each player (TIM, TIPIN or CLASPIN) individually will clarify this question.

Position of TIM at the replication fork

In our proximity ligation studies, we found that TIM-AND1 and TIM-ORC6 pairs biotinylate TIPIN, CLASPIN, CDC45, DNA polymerases alpha and epsilon, as well as CHK1 (Fig. 4B). Our study captures TIM-proximal proteins not specifically at replication initiation but throughout replication. AND-1 moves along with replication forks, and ORC6 is present at behind replication forks (involved in mismatch repair) [60]. CDC45 is a part of the CMG helicase, and CHK1 is possibly present interacting with CLASPIN at the RPA on the lagging strand [48]. The above findings do not align with the canonical position of TIM, even after taking into account the fact that the lagging strand is flexible. AND-1 is present at forks near CDC45, GINS and DNA polymerase epsilon [10], [11] and it is hard to imagine that TIM at its canonical position could come into close proximity with AND-1 to reconstitute a stable biotin ligase. TIM may come into proximity with ORC6 when it is present on the flexible lagging strand behind the moving fork. Two molecules of TIM in close proximity of one another at forks allowed TIM-TIM pair to biotinylate the same proteins as the TIM-AND1 and TIM-ORC6 pairs, with the addition of DNA polymerase delta (Fig. 4D). These observations support our model that there are multiple molecules of TIM present at the fork. These additional TIM molecules are presumably positioned on the lagging strand RPA-covered ssDNA, and could come close to AND-1, ORC6, leading edge FPC, and any fork components as the flexible lagging strand could allow for a change of positions (Fig.4E). It is theoretically possible that the biotinylation that we observe in case of the TIM-TIM pair could come from two TIMs situated on two distinct but close forks, or forks coming from opposite directions that merge together, however it is unlikely that such a combination would biotinylate the proteins located behind the fork, such as POLE.

Our results point towards the presence of more than one TIM molecule at each replication fork, with one molecule of TIM being at the canonical position suggested by structural studies: at the leading edge of the fork, interacting with MCM, and additional molecule(s) of TIM/FPC interacting with RPA the lagging strand.

Significance of TIM-MCM interaction for replication initiation

We next studied whether TIM interaction with MCM was required for chromatin loading of TIM in either of the two proposed positions. The mutant of TIM unable to interact with MCM could not load to chromatin during S-phase entry (Fig.5C,D) or support compensation of the absence of the endogenous TIM during S-phase entry (Fig.6A-C,S6B). One possibility is that TIM molecules would first load at the leading edge of the fork stabilized by MCM interaction, and then would jump to the lagging strand as the flexible lagging strand moves, and these would be stabilized on the lagging strand by TIPIN-RPA interaction [27], [61]. Alternatively, molecules of TIM-TIPIN may load onto the lagging strand without interaction with MCM, but via TIPIN-RPA binding. However, it is then unclear why the TIM-M* mutant failed to load, as in our TIM-M* expressing cells, TIPIN levels were normal.

It has been reported that TIM interacts with MCM throughout the cell cycle and even before the beginning of S phase [21], which led us to wonder whether TIM is loaded along with MCM during replication initiation. However, we observed that TIM is recruited to chromatin significantly later than MCM. Interestingly, TIM-M* was unable to load to chromatin during S-phase entry. We speculate that TIM loads to origins after MCM has already loaded, however TIM is stabilized and held in place at the fork by MCM interaction. Further studies are needed to clarify the mechanistic details of how exactly TIM is loaded and which player recruits TIM to the fork.

In the presence of TIM-M* mutant, CLASPIN and TIPIN could not load to chromatin during S-phase entry, although TIM-mAID-mCherry was present in the cells at normal levels and able to load to chromatin (Fig. 5C,E). We attribute this to a possible dominant negative effect of the TIM-M* mutant, which we think may sequester CLASPIN and TIPIN before the beginning of S phase and thus prevent their chromatin loading.

Perspectives

Many studies indicate that TIM, as part of the FPC, couples together the helicase activity of MCM with the activities of the polymerases by physically tethering them together [27], [16], [17]. We speculate that uncoupling of MCM and the polymerases may begin to occur very early on in the absence of TIM, and TIM's coupling activity may be important for not just replication elongation but replication initiation as well.

Loss of TIM also causes a significant fork slow-down [15]. Poorly processive polymerases due to a strong reduction in recruited PCNA, combined with uncoupled helicase-polymerases due to absence of the FPC, may lead to a catastrophic fork slow-down, as has been observed previously in the case of TIM-depleted cells [15], and this may lead to the replication initiation defect that we observe upon prolonged TIM depletion.

We show that TIM is required for CLASPIN recruitment to chromatin during replication initiation. The presence of TIM is also required in G2 phase for timely PCNA loading during the subsequent S phase. TIM, TIPIN and CLASPIN load to firing origins partially at the same time as CMG assembly, and partially after the start of DNA synthesis, and their loading requires TIM-MCM interaction.

Future studies are needed for a better understanding the role of each FPC component in replication initiation individually, as in our system, all three FPC components were absent at chromatin. Conditional depletion systems of each players would help shed light on each component's individual role. We have not answered how exactly TIM loads CLASPIN, and which regions of TIM may be responsible for this function. Mutants of TIM that do not interact with CLASPIN would help to shed light on this. A TIPIN-depletion system should help elucidate the loading defect of the TIM-M* mutant, as if TIM loads to the lagging strand via TIPIN-RPA interaction, loss of TIPIN would be expected to abrogate this loading of TIM. Detailed investigations of the defect in PCNA loading would be necessary, to understand which FPC player plays a role in supporting timely PCNA loading, and how. It is not known how TIM is loaded to DNA during replication initiation. During replication stress, it has been reported that TIM is loaded to DNA via PARP-1 interaction independent of TIPIN [62]. However, as few studies have investigated how TIM loads in the absence of stress, future efforts should focus on this. Overall, as TIM is found to be upregulated in various forms of cancer, studies that uncover its various roles in critical processes such as DNA replication initiation are very imperative in paving the way for development of future anti-cancer therapies.

Materials and methods:

Plasmids and cloning

For osTIR1 KI we used PX458-AAVS1 (a gift from Adam Karpf—Addgene plasmid # 113194) and pMK243-Tet-OsTIR1-PURO (a gift from Masato Kanemaki—Addgene plasmid # 72835) plasmids [23]. For cloning TIM gene into pUC57 vector, TIM gene was PCRed out of human cDNA using the following primers:

Tim_Sgf1_F: ATGCGATCGCCATGGACTTGCACATGATGAA and Tim_Mlu1_R: ATACGCGTGTCATCCTCATCATCCTCAA and the plasmid was verified by sequencing.

For mAID KI templates, homology arms were synthesized by Genscript in the pUC57 vector with stop codon substituted to BamHI site (5' GGATCC 3'). Insert from plasmids pMK293 (mAID-mCherry2-Hygro) (Addgene plasmid # 72831 was a gift from Masato Kanemaki) [23]. This insert was cloned into the BamHI site of the synthesized plasmid. TIM gene was then cloned into this plasmid before the mCherry-Hygro sequence, such that TIM was fused to mCherry gene and separate from hygromycin resistance gene, and flanked between the synthesized homology arms.

TIM C-terminus-targeting gRNA (ACGTGTCTATCTCTACCCCT) was expressed from pSpCas9 BB-2A-Puro (PX459) v2.0 plasmid (Genscript).

For generation of the TIM-M* mutant, the sequence corresponding to amino acids 276-302 was deleted from the TIM gene, using Gibson Assembly-based cloning. TIM-M* mutant was placed under the CMV promoter for coimmunoprecipitation experiments to achieve high overexpression, and under the doxycycline promoter for mutant cell line generation to achieve tunable expression. This plasmid also contained a neomycin (G418) resistance gene to be used as a selection marker during stable cell line generation.

Turbo ID constructs

TurboID fragments were cloned out of 3xHA-TurboID-NLS_pCDNA3 plasmid that was a gift from Alice Ting (Addgene plasmid # 107171)[63] using the following primers TurboN_F: ATACGCGTTACCCCTATGACGTCCCAGA; TurboN_R: ATGTTTAAACCAGAATCTGTTTAGCGTTCA; TurboC_F: ATGATATCGGACAGCTGGACGGCGGGAG; TurboC_R: ATGTTTAAACCTTTTCGGCAGACCGCAGAC.

Cell lines, cell culture, and transfections

U2OS (ATCC HTB-96) cells were grown in RPMI media (Capricorn Scientific, RPMI 1640 Medium, with L-Glutamine, 500 ml), supplemented with 10% FBS (GIBCO) and 1% penicillin-streptomycin (Invitrogen).

For generation of mAID1 TIM-depleting cell lines by CRISPR, as per [20] and [21], U2OS cells, having osTIR1 stably transfected under the dox promoter, were transfected with gRNA and the mAID-mCherry-hygroR KI HR templates. Growth medium was changed 8 h after transfection, 2.5 μ M DNAPK inhibitor was added for 48 h. KI cells were selected with hygromycin until the non-transfected control died, followed by single cell cloning and KI validation by PCR and western blot. Transfections were carried out using Lipofectamine 2000 (ThermoFisher), according to manufacturer's instructions. For generation of mAID2 TIM-depleting cell lines by CRISPR, U2OS-based Clone 14 F74G cells, having modified osTIR1 F74G mutant under the CMV promoter, were used, and subjected to the same procedure. The mAID tag was the same in both mAID1 and mAID2.

Primers used to validate the presence of the knock-in were as follows: TIMhtestF: CGACAATTGCTGGACAGCGAC and gtestR: GGATCCTTACTTGACAGCTC, whereas primers used to validate the absence of wt TIM allele were as follows: TIMhtestF and TIMhtestR: ATCTCCAGAGAGCTGCTGGGG.

For TIM-M*-expressing cell line generation, as per [22], mAID1 Clone 10 or Clone 28 cells were transfected with the corresponding plasmid, growth medium was changed 8 h after transfection, and KI cells were selected with G418 until the non-transfected control died, followed by single-cell cloning and KI validation by PCR and western blot. Transfections were carried out using Lipofectamine 2000 (ThermoFisher), according to manufacturer's instructions.

For validations of the knock-ins, genomic DNA was isolated using genomic DNA miniprep kit (Zymo Research, D3025).

293FT cells (ThermoFisher #R70007) were grown in DMEM media (Lonza), supplemented with 10% FBS (GIBCO) and 1% penicillin-streptomycin (Invitrogen).

Cell lysis, insoluble chromatin isolation, and western blots

Cells were lysed in 50 mM Tris-HCl (pH 7.5), 150 mM NaCl, 50 mM NaF, 1% Tween-20, 0.5% Nonidet P-40, and protease inhibitors (Pierce #A32953) for 20 min on ice. Lysates were cleared by centrifugation, and soluble protein was used for immunoprecipitation or mixed with 2X Laemmli Sample Buffer (Bio-Rad) and incubated for 7 min at 96 °C and analyzed by Western blot. For nuclease insoluble chromatin, pellets were suspended in 150 mM Hepes (pH 7.9), 1.5 mM MgCl₂, 10% glycerol, 150 mM potassium acetate, and protease inhibitors containing universal nuclease for cell lysis (ThermoFisher, 88700) and incubated for 10 min at 37 °C on the shaker. Nuclease-insoluble chromatin was pelleted by centrifugation, washed with water, and dissolved in Laemmli Sample Buffer.

For western blot analyses, proteins were separated in 8–12% SDS-polyacrylamide gels in Running buffer (25 mM Tris, 192 mM glycine, 0.1% SDS), transferred onto PVDF membrane (BioRad, #1620177) in transfer buffer (25 mM Tris, 192 mM glycine, 10% ethanol), blocked with 5% non-fat milk (BioRad, #1706404) in TBST (TBS ThermoFisher, #BP2471, 0.1% Tween-20), incubated with an appropriate dilution of the primary antibody overnight at 4 °C, washed with TBST buffer, incubated with secondary antibody for 1 h at room temperature, washed with TBST and developed using SignalFire™ Elite ECL Reagent (Cell Signaling, #12757P) and ImageQuant LAS 4000 imager (GE Healthcare). Quantification of western blots was performed using Fiji/ImageJ (version 1.53u).

Coimmunoprecipitation

293FT cells were transfected with an empty vector or N-terminally FLAG-tagged wtTIM and TIM-M* expressing constructs, using Lipofectamine 2000 as per manufacturer's instructions. 48 h later cells were lysed, and FLAG-tagged proteins were immunoprecipitated using anti-FLAG M2 affinity gel beads (Sigma-Aldrich), followed by elution with FLAG peptide.

Split Turbo ID experiments

293T cells were transfected using Lipofectamine2000, according to the instructions from the manufacturer. 48h after transfection, cells were incubated for 1h with 50uM biotin, washed with PBS, and lysed in RIPA buffer (150mM NaCl; 50mM Tris-HCl pH 7.5; 1%Triton X100; 0.1% SDS, protease inhibitors (Pierce #A32953)) on ice. After sonication using a Bioruptor sonicator (20 cycles, 30 seconds on; 30 seconds off), the lysates were cleared by centrifugation (14 000g, 15 min) and incubated with streptavidin agarose (Thermofisher) for 16h. The beads were then washed once with RIPA buffer, once with 1M NaCl, and two more times with RIPA buffer. Washed beads were then boiled with 1x Laemmli buffer (BioRad) and analyzed by western blot.

Synchronizations and chromatin loading of CMG components

In order to synchronize U2OS cells, 2 mM thymidine was added to ~25% confluent cells for 24 h. After thymidine removal, cells were washed once with warm PBS and allowed to recover in fresh medium for 5 h. Nocodazole was then added for 12 h to stop the cells in G2/M. Dox (2 ug/ml) and 3-IAA (500 uM) for mAID1 and TIM-M* FACS experiments, or 5-pH-IAA (1.25 uM) for mAID2, were added at the same time as nocodazole. 8 h later, cells were released from nocodazole, washed once with warm PBS, and incubated in pre-warmed medium with dox/aux for the indicated periods of time. For the experiments with added inhibitors, cells were released from nocodazole, washed once with warm PBS, and incubated in pre-warmed medium with 5 uM of each inhibitor for the indicated periods of time.

In order to assess the loading of the CMG components on chromatin, samples were collected by trypsinization at the indicated timepoints, pellets washed once with ice-cold PBS and kept at –80 °C and processed the next day. To obtain the nuclease-insoluble fraction, thawed pellets were resuspended in

CSK buffer (10 mM PIPES pH 7.0, 300 mM Sucrose, 100 mM NaCl, 3 mM MgCl₂, 0.5% Triton X-100, protease inhibitors (Pierce #A32953)), incubated for 5 min on ice, followed by a 5-min centrifugation (1000 × g, 4 °C). The supernatant was collected as “soluble fraction”, the pellets were washed once more with CSK buffer, digested in CSK buffer with universal nuclease for cell lysis (ThermoFisher, #88700) for 10 min at 37 °C. Samples were mixed with 2x Laemmli Sample Buffer (BioRad) and boiled for 10 min before proceeding to western blot analysis. Quantifications were performed using ImageJ and GraphPad Prism 9.

Antibodies

POLE1 (Santa Cruz, #sc-390785, 1:500), osTIR1 (MBL International, #PD048, 1:1000), GAPDH (Santa Cruz, #sc-47724, 1:1000), pCHK1 (Cell Signaling, #2360S, 1:1000), MCM4 (Cell Signaling, #3228S, 1:300), CDC45 (Santa Cruz, #sc-55569, 1:500), SLD5 (Santa Cruz, #sc-398784, 1:300), H3 (Santa Cruz, #sc-517576, 1:1000), POLE2 (Santa Cruz, #sc-398582, 1:500), PCNA (Santa Cruz, #sc-56, 1:1000), FLAG (Sigma, F3165-1MG, 1:3000), polD1 ().

Flow cytometry

For EdU FACS, cells were treated with 10 μM EdU for 30 min, trypsinized, washed with PBS, and fixed with cold 70% ethanol on ice for 30 min or at -20°C overnight. Cells were washed with PBS, and EdU staining was performed by using the EdU Click-iT kit (ThermoFisher, C10632), according to the manufacturer’s instructions. For DNA staining, we used 7-AAD (7-Aminoactinomycin D) (ThermoFisher, # A1310) or FxCycle™ PI/RNase Staining Solution (ThermoFisher, #F10797).

Flow cytometry was performed on FACSCalibur flow cytometer, and data were analyzed by using FCSalyzer software. GraphPad Prism 9 was used for statistical analyses.

References

- [1] T. N. Moiseeva and C. J. Bakkenist, “Regulation of the initiation of DNA replication in human cells,” *DNA Repair*, vol. 72, pp. 99–106, Dec. 2018, doi: 10.1016/j.dnarep.2018.09.003.
- [2] “Mechanism of Bidirectional Leading-Strand Synthesis Establishment at Eukaryotic DNA Replication Origins - ScienceDirect.” Accessed: Sep. 04, 2023. [Online]. Available: <https://www.sciencedirect.com/science/article/pii/S1097276518308797?via%3Dihub>
- [3] G.-L. Moldovan, B. Pfander, and S. Jentsch, “PCNA, the Maestro of the Replication Fork,” *Cell*, vol. 129, no. 4, pp. 665–679, May 2007, doi: 10.1016/j.cell.2007.05.003.
- [4] W. C. Drosopoulos, D. A. Vierra, C. A. Kenworthy, R. A. Coleman, and C. L. Schildkraut, “Dynamic Assembly and Disassembly of the Human DNA Polymerase δ Holoenzyme on the Genome In Vivo,” *Cell Rep.*, vol. 30, no. 5, pp. 1329-1341.e5, Feb. 2020, doi: 10.1016/j.celrep.2019.12.101.
- [5] R. E. Georgescu *et al.*, “Mechanism of asymmetric polymerase assembly at the eukaryotic replication fork,” *Nat. Struct. Mol. Biol.*, vol. 21, no. 8, Art. no. 8, Aug. 2014, doi: 10.1038/nsmb.2851.
- [6] “Evidence that DNA polymerase δ contributes to initiating leading strand DNA replication in *Saccharomyces cerevisiae* | Nature Communications.” Accessed: Sep. 04, 2023. [Online]. Available: <https://www.nature.com/articles/s41467-018-03270-4>
- [7] “CMG–Pol epsilon dynamics suggests a mechanism for the establishment of leading-strand synthesis in the eukaryotic replisome | PNAS.” Accessed: Sep. 04, 2023. [Online]. Available: <https://www.pnas.org/doi/full/10.1073/pnas.1700530114>

- [8] N. Yoshizawa-Sugata and H. Masai, "Human Tim/Timeless-interacting Protein, Tipin, Is Required for Efficient Progression of S Phase and DNA Replication Checkpoint," *J. Biol. Chem.*, vol. 282, no. 4, pp. 2729–2740, Jan. 2007, doi: 10.1074/jbc.M605596200.
- [9] J. Saldanha, J. Rageul, J. A. Patel, and H. Kim, "The Adaptive Mechanisms and Checkpoint Responses to a Stressed DNA Replication Fork," *Int. J. Mol. Sci.*, vol. 24, no. 13, Art. no. 13, Jan. 2023, doi: 10.3390/ijms241310488.
- [10] M. L. Jones, Y. Baris, M. R. Taylor, and J. T. Yeeles, "Structure of a human replisome shows the organisation and interactions of a DNA replication machine," *EMBO J.*, vol. 42, no. 22, p. e115685, Nov. 2023, doi: 10.15252/embj.2023115685.
- [11] M. Jenkyn-Bedford *et al.*, "A conserved mechanism for regulating replisome disassembly in eukaryotes," *Nature*, vol. 600, no. 7890, pp. 743–747, Dec. 2021, doi: 10.1038/s41586-021-04145-3.
- [12] T. Abe *et al.*, "AND-1 fork protection function prevents fork resection and is essential for proliferation," *Nat. Commun.*, vol. 9, no. 1, p. 3091, Aug. 2018, doi: 10.1038/s41467-018-05586-7.
- [13] S. Vipat and T. N. Moiseeva, "The TIMELESS Roles in Genome Stability and Beyond," *J. Mol. Biol.*, p. 168206, Jul. 2023, doi: 10.1016/j.jmb.2023.168206.
- [14] J. A. Patel and H. Kim, "The TIMELESS effort for timely DNA replication and protection," *Cell. Mol. Life Sci.*, vol. 80, no. 4, p. 84, Mar. 2023, doi: 10.1007/s00018-023-04738-3.
- [15] J. A. Patel, C. Zelic, J. Rageul, J. Saldanha, A. Khan, and H. Kim, "Replisome dysfunction upon inducible TIMELESS degradation synergizes with ATR inhibition to trigger replication catastrophe," *Nucleic Acids Res.*, vol. 51, no. 12, pp. 6246–6263, Jul. 2023, doi: 10.1093/nar/gkad363.
- [16] J. A. Patel, C. Zelic, J. Rageul, J. Saldanha, A. Khan, and H. Kim, "Replisome dysfunction upon inducible TIMELESS degradation synergizes with ATR inhibition to trigger replication catastrophe," *Nucleic Acids Res.*, vol. 51, no. 12, pp. 6246–6263, Jul. 2023, doi: 10.1093/nar/gkad363.
- [17] W.-H. Cho, Y.-H. Kang, Y.-Y. An, I. Tappin, J. Hurwitz, and J.-K. Lee, "Human Tim-Tipin complex affects the biochemical properties of the replicative DNA helicase and DNA polymerases," *Proc. Natl. Acad. Sci.*, vol. 110, no. 7, pp. 2523–2527, Feb. 2013, doi: 10.1073/pnas.1222494110.
- [18] J. S. Lewis *et al.*, "Single-molecule visualization of *Saccharomyces cerevisiae* leading-strand synthesis reveals dynamic interaction between MTC and the replisome," *Proc. Natl. Acad. Sci.*, vol. 114, no. 40, pp. 10630–10635, Oct. 2017, doi: 10.1073/pnas.1711291114.
- [19] Y. Baris, M. R. G. Taylor, V. Aria, and J. T. P. Yeeles, "Fast and efficient DNA replication with purified human proteins," *Nature*, vol. 606, no. 7912, Art. no. 7912, Jun. 2022, doi: 10.1038/s41586-022-04759-1.
- [20] V. Aria *et al.*, "The Human Tim-Tipin Complex Interacts Directly with DNA Polymerase ϵ and Stimulates Its Synthetic Activity," *J. Biol. Chem.*, vol. 288, no. 18, pp. 12742–12752, May 2013, doi: 10.1074/jbc.M112.398073.
- [21] X. Xu, J.-T. Wang, M. Li, and Y. Liu, "TIMELESS Suppresses the Accumulation of Aberrant CDC45-MCM2-7-GINS Replicative Helicase Complexes on Human Chromatin," *J. Biol. Chem.*, vol. 291, no. 43, p. 22544, Oct. 2016, doi: 10.1074/jbc.M116.719963.
- [22] A. Yesbolatova *et al.*, "The auxin-inducible degron 2 technology provides sharp degradation control in yeast, mammalian cells, and mice," *Nat. Commun.*, vol. 11, p. 5701, Nov. 2020, doi: 10.1038/s41467-020-19532-z.

- [23] T. Natsume, T. Kiyomitsu, Y. Saga, and M. T. Kanemaki, "Rapid Protein Depletion in Human Cells by Auxin-Inducible Degron Tagging with Short Homology Donors," *Cell Rep.*, vol. 15, no. 1, pp. 210–218, Apr. 2016, doi: 10.1016/j.celrep.2016.03.001.
- [24] A. R. Leman, C. Noguchi, C. Y. Lee, and E. Noguchi, "Human Timeless and Tipin stabilize replication forks and facilitate sister-chromatid cohesion," *J. Cell Sci.*, vol. 123, no. 5, pp. 660–670, Mar. 2010, doi: 10.1242/jcs.057984.
- [25] J. Li *et al.*, "The human pre-replication complex is an open complex," *Cell*, vol. 186, no. 1, pp. 98–111.e21, Jan. 2023, doi: 10.1016/j.cell.2022.12.008.
- [26] M. L. Jones, V. Aria, Y. Baris, and J. T. P. Yeeles, "How Pol α -primase is targeted to replisomes to prime eukaryotic DNA replication," *Mol. Cell*, vol. 83, no. 16, pp. 2911–2924.e16, Aug. 2023, doi: 10.1016/j.molcel.2023.06.035.
- [27] P. Prorok, E. Wolf, and M. C. Cardoso, "Timeless-Tipin interactions with MCM and RPA mediate DNA replication stress response," *Front. Cell Dev. Biol.*, vol. 12, p. 1346534, 2024, doi: 10.3389/fcell.2024.1346534.
- [28] M. G. Kemp *et al.*, "Tipin-Replication Protein A Interaction Mediates Chk1 Phosphorylation by ATR in Response to Genotoxic Stress," *J. Biol. Chem.*, vol. 285, no. 22, pp. 16562–16571, May 2010, doi: 10.1074/jbc.M110.110304.
- [29] K. F. Cho *et al.*, "Split-TurboID enables contact-dependent proximity labeling in cells," *bioRxiv*, p. 2020.03.11.988022, Mar. 2020, doi: 10.1101/2020.03.11.988022.
- [30] K. Nishimura, T. Fukagawa, H. Takisawa, T. Kakimoto, and M. Kanemaki, "An auxin-based degron system for the rapid depletion of proteins in nonplant cells," *Nat. Methods*, vol. 6, no. 12, Art. no. 12, Dec. 2009, doi: 10.1038/nmeth.1401.
- [31] H.-C. Chou *et al.*, "The human origin recognition complex is essential for pre-RC assembly, mitosis, and maintenance of nuclear structure," *eLife*, vol. 10, p. e61797, Feb. 2021, doi: 10.7554/eLife.61797.
- [32] S. Vipat, D. Gupta, S. Jonchhe, H. Anderspuk, E. Rothenberg, and T. N. Moiseeva, "The non-catalytic role of DNA polymerase epsilon in replication initiation in human cells," *Nat. Commun.*, vol. 13, no. 1, p. 7099, Nov. 2022, doi: 10.1038/s41467-022-34911-4.
- [33] X. Xu, J.-T. Wang, M. Li, and Y. Liu, "TIMELESS Suppresses the Accumulation of Aberrant CDC45·MCM2-7·GINS Replicative Helicase Complexes on Human Chromatin," *J. Biol. Chem.*, vol. 291, no. 43, pp. 22544–22558, Oct. 2016, doi: 10.1074/jbc.M116.719963.
- [34] "An ATR and CHK1 kinase signaling mechanism that limits origin firing during unperturbed DNA replication | PNAS." Accessed: Sep. 05, 2023. [Online]. Available: <https://www.pnas.org/doi/full/10.1073/pnas.1903418116>
- [35] "ATR kinase inhibition induces unscheduled origin firing through a Cdc7-dependent association between GINS and And-1 | Nature Communications." Accessed: Sep. 05, 2023. [Online]. Available: <https://www.nature.com/articles/s41467-017-01401-x>
- [36] G. Chhetri *et al.*, "PAF15-PCNA assembly exhaustion governs lagging strand replication and replisome integrity," Mar. 16, 2025, *bioRxiv*. doi: 10.1101/2025.03.15.641049.
- [37] J. M. Suski *et al.*, "Cdc7-independent G1/S transition revealed by targeted protein degradation," *Nature*, vol. 605, no. 7909, pp. 357–365, May 2022, doi: 10.1038/s41586-022-04698-x.

- [38] S. Holzer *et al.*, "Crystal structure of the N-terminal domain of human Timeless and its interaction with Tipin," *Nucleic Acids Res.*, vol. 45, no. 9, pp. 5555–5563, May 2017, doi: 10.1093/nar/gkx139.
- [39] M. L. Jones, Y. Baris, M. R. G. Taylor, and J. T. P. Yeeles, "Structure of a human replisome shows the organisation and interactions of a DNA replication machine," *EMBO J.*, vol. 40, no. 23, p. e108819, Dec. 2021, doi: 10.15252/embj.2021108819.
- [40] L. A. Kelley, S. Mezulis, C. M. Yates, M. N. Wass, and M. J. E. Sternberg, "The Phyre2 web portal for protein modeling, prediction and analysis," *Nat. Protoc.*, vol. 10, no. 6, pp. 845–858, Jun. 2015, doi: 10.1038/nprot.2015.053.
- [41] J. Jumper *et al.*, "Highly accurate protein structure prediction with AlphaFold," *Nature*, vol. 596, no. 7873, Art. no. 7873, Aug. 2021, doi: 10.1038/s41586-021-03819-2.
- [42] K. D. Smith, M. A. Fu, and E. J. Brown, "Tim–Tipin dysfunction creates an indispensable reliance on the ATR–Chk1 pathway for continued DNA synthesis," *J. Cell Biol.*, vol. 187, no. 1, pp. 15–23, Oct. 2009, doi: 10.1083/jcb.200905006.
- [43] A. L. Gotter, C. Suppa, and B. S. Emanuel, "Mammalian TIMELESS and Tipin are Evolutionarily Conserved Replication Fork-Associated Factors," *J. Mol. Biol.*, vol. 366, no. 1, pp. 36–52, Feb. 2007, doi: 10.1016/j.jmb.2006.10.097.
- [44] J. Rageul *et al.*, "SDE2 integrates into the TIMELESS-TIPIN complex to protect stalled replication forks," *Nat. Commun.*, vol. 11, no. 1, Art. no. 1, Oct. 2020, doi: 10.1038/s41467-020-19162-5.
- [45] A. Errico, V. Costanzo, and T. Hunt, "Tipin is required for stalled replication forks to resume DNA replication after removal of aphidicolin in *Xenopus* egg extracts," *Proc. Natl. Acad. Sci. U. S. A.*, vol. 104, no. 38, pp. 14929–14934, Sep. 2007, doi: 10.1073/pnas.0706347104.
- [46] "Separation of intra-S checkpoint protein contributions to DNA replication fork protection and genomic stability in normal human fibroblasts." Accessed: Sep. 06, 2023. [Online]. Available: <https://www.tandfonline.com/doi/epdf/10.4161/cc.23177?src=getfr>
- [47] X. H. Yang, B. Shiotani, M. Classon, and L. Zou, "Chk1 and Claspin potentiate PCNA ubiquitination," *Genes Dev.*, vol. 22, no. 9, pp. 1147–1152, May 2008, doi: 10.1101/gad.1632808.
- [48] X. H. Yang and L. Zou, "Dual Functions of DNA Replication Forks in Checkpoint Signaling and PCNA Ubiquitination," *Cell Cycle Georget. Tex.*, vol. 8, no. 2, pp. 191–194, Jan. 2009.
- [49] J.-M. Brondello, B. Ducommun, A. Fernandez, and N. J. Lamb, "Linking PCNA-dependent replication and ATR by human Claspin," *Biochem. Biophys. Res. Commun.*, vol. 354, no. 4, pp. 1028–1033, Mar. 2007, doi: 10.1016/j.bbrc.2007.01.091.
- [50] J.-M. Brondello, B. Ducommun, A. Fernandez, and N. J. Lamb, "Linking PCNA-dependent replication and ATR by human Claspin," *Biochem. Biophys. Res. Commun.*, vol. 354, no. 4, pp. 1028–1033, Mar. 2007, doi: 10.1016/j.bbrc.2007.01.091.
- [51] C.-C. Yang *et al.*, "Claspin recruits Cdc7 kinase for initiation of DNA replication in human cells," *Nat. Commun.*, vol. 7, no. 1, Art. no. 1, Jul. 2016, doi: 10.1038/ncomms12135.
- [52] A. Yadav *et al.*, "DNA replication protein Cdc45 directly interacts with PCNA via its PIP box in *Leishmania donovani* and the Cdc45 PIP box is essential for cell survival," *PLoS Pathog.*, vol. 16, no. 5, p. e1008190, May 2020, doi: 10.1371/journal.ppat.1008190.
- [53] J. Chen, P. K. Jackson, M. W. Kirschner, and A. Dutta, "Separate domains of p21 involved in the inhibition of Cdk kinase and PCNA," *Nature*, vol. 374, no. 6520, pp. 386–388, Mar. 1995, doi: 10.1038/374386a0.

- [54] V. N. Podust, L. M. Podust, F. Goubin, B. Ducommun, and U. Hübscher, "Mechanism of inhibition of proliferating cell nuclear antigen-dependent DNA synthesis by the cyclin-dependent kinase inhibitor p21," *Biochemistry*, vol. 34, no. 27, pp. 8869–8875, Jul. 1995, doi: 10.1021/bi00027a039.
- [55] S. Waga, G. J. Hannon, D. Beach, and B. Stillman, "The p21 inhibitor of cyclin-dependent kinases controls DNA replication by interaction with PCNA," *Nature*, vol. 369, no. 6481, pp. 574–578, Jun. 1994, doi: 10.1038/369574a0.
- [56] T. Mondol, J. L. Stodola, R. Galletto, and P. M. Burgers, "PCNA accelerates the nucleotide incorporation rate by DNA polymerase δ ," *Nucleic Acids Res.*, vol. 47, no. 4, pp. 1977–1986, Feb. 2019, doi: 10.1093/nar/gky1321.
- [57] X. Lu *et al.*, "Direct Interaction of Proliferating Cell Nuclear Antigen with the Small Subunit of DNA Polymerase δ^* ," *J. Biol. Chem.*, vol. 277, no. 27, pp. 24340–24345, Jul. 2002, doi: 10.1074/jbc.M200065200.
- [58] S. H. Lee, Z. Q. Pan, A. D. Kwong, P. M. Burgers, and J. Hurwitz, "Synthesis of DNA by DNA polymerase epsilon in vitro.," *J. Biol. Chem.*, vol. 266, no. 33, pp. 22707–22717, Nov. 1991, doi: 10.1016/S0021-9258(18)54626-3.
- [59] E. Noguchi, "Division of labor of the replication fork protection complex subunits in sister chromatid cohesion and Chk1 activation," *Cell Cycle*, vol. 10, no. 13, pp. 2059–2058, Jul. 2011, doi: 10.4161/cc.10.13.15805.
- [60] R. M. Jones and E. Petermann, "Replication fork dynamics and the DNA damage response," *Biochem. J.*, vol. 443, no. 1, pp. 13–26, Mar. 2012, doi: 10.1042/BJ20112100.
- [61] M. G. Kemp *et al.*, "Tipin-Replication Protein A Interaction Mediates Chk1 Phosphorylation by ATR in Response to Genotoxic Stress," *J. Biol. Chem.*, vol. 285, no. 22, pp. 16562–16571, May 2010, doi: 10.1074/jbc.M110.110304.
- [62] L. M. Young *et al.*, "TIMELESS Forms a Complex with PARP1 Distinct from Its Complex with TIPIN and Plays a Role in the DNA Damage Response," *Cell Rep.*, vol. 13, no. 3, pp. 451–459, Oct. 2015, doi: 10.1016/j.celrep.2015.09.017.
- [63] T. C. Branon *et al.*, "Efficient proximity labeling in living cells and organisms with TurboID," *Nat. Biotechnol.*, vol. 36, no. 9, pp. 880–887, Oct. 2018, doi: 10.1038/nbt.4201.

Author contributions:

TNM conceived and directed the project, performed, and analyzed some of the experiments, and reviewed and edited the manuscript. SV designed, performed, and analyzed the majority of the experiments, and wrote the manuscript, with review and editing by TNM. KS performed the proximity ligation experiments. RH, AM, and SV (author #5) performed a minority of the experiments.

Figure 1: TIM depletion compromises S phase entry and decelerates DNA synthesis

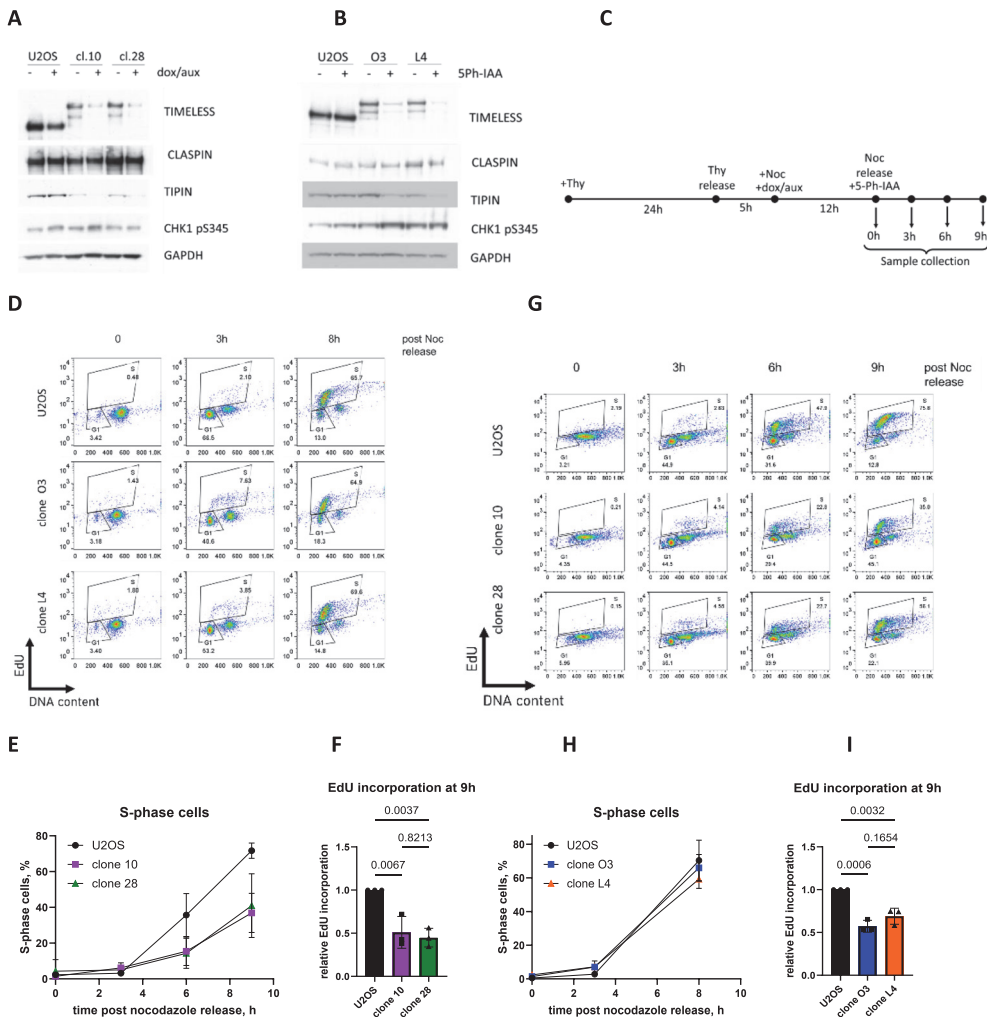
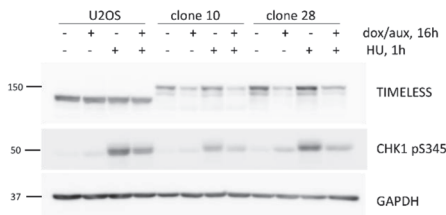


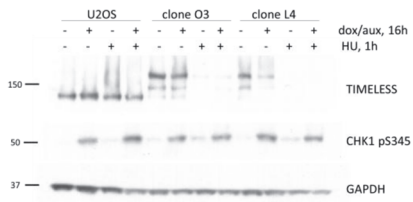
Figure 1: A-B. Wildtype U2OS, mAID1 clones Clone 10, Clone 28 or mAID2 clones Clone O3, Clone L4 were treated for 16 h with doxycycline and auxin 3-IAA, or with auxin 5-pH-IAA. Western blots of total cell lysates are shown (A,B). Synchronization timeline using the double thymidine-nocodazole block and the timepoints used for mAID1 clones (C). **D-I.** Wildtype U2OS, mAID1 clones Clone 10, Clone 28 or mAID2 clones Clone O3, Clone L4 were synchronized using the double thymidine- nocodazole block, and treated for the last 12 h with DMSO, dox /3-IAA or with 5-pH-IAA after release from nocodazole. 10 μ M EdU was added for the last 30 min of treatment. Flow cytometry plots showing EdU incorporation and DNA content (7-AAD staining) are shown (D,G). Quantification of the flow cytometry data is shown- mean + SD from n = 3 independent experiments (E,F,H,I.). EdU+ cells were quantified based on EdU signal being above G1 and G2 levels. Cells were assigned to S-phase based on DNA content of higher than 2n and being EdU positive, and to G1-phase based on DNA content of 2n and being EdU negative.

Figure S1:

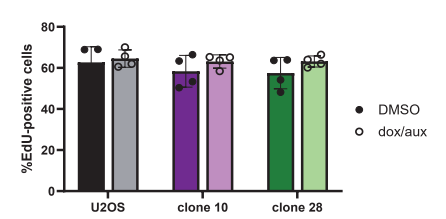
A



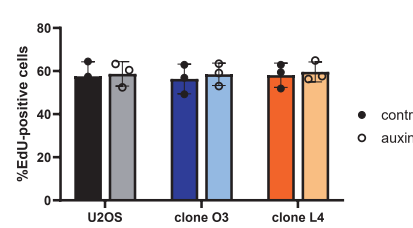
B



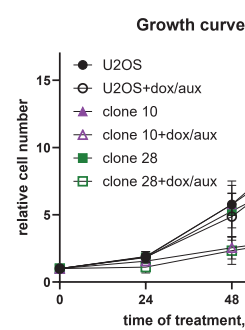
C



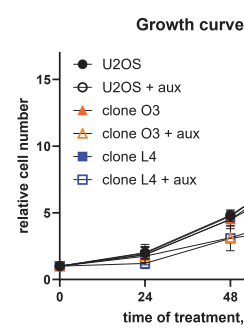
D



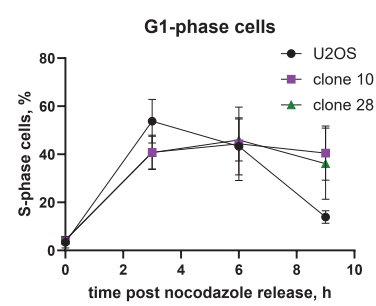
E



F



G



H

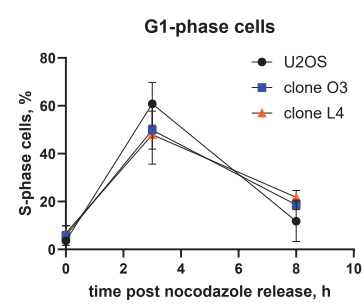
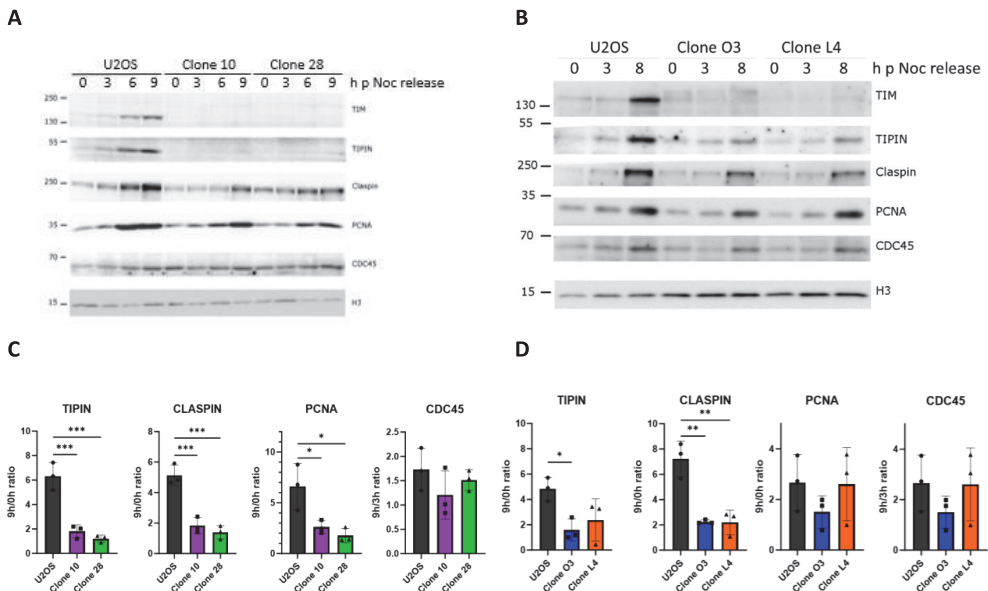


Figure S1. A-B. Wildtype U2OS, mAID1 clones Clone 10, Clone 28 or mAID2 clones Clone O3, Clone L4 were treated for 16 h with doxycycline (2 μ g/ml)/auxin 3-IAA, auxin 5-pH-IAA, or Hydroxyurea (HU) (5 mM), as indicated. Western blots of total cell lysates are shown (**A,B**). **C-D.** Wildtype U2OS, mAID1 clones Clone 10, Clone 28 or mAID2 clones Clone O3, Clone L4 were treated with DMSO, doxycycline /3-IAA or 5-pH-IAA for 16 h. 10 μ M EdU was added for the last 30 min of treatment. Quantification of the flow cytometry data is shown- mean + SD from n = 3 independent experiments (**C,D**). EdU+ cells were quantified based on EdU signal being above G1 and G2 levels. **E-F.** Equal numbers of wild-type U2OS, mAID1 clones Clone 10, Clone 28 or mAID2 clones Clone O3, Clone L4 were seeded on 60 mm dishes and treated with DMSO or dox (2 μ g/ml) /3-IAA for 72 h. Cell numbers were counted every 24 h and growth curves were plotted. The data are depicted as mean + SD from n = 3 independent experiments (**E,F**). Wildtype U2OS, mAID1 clones Clone 10, Clone 28 or mAID2 clones Clone O3, Clone L4 were synchronized using the double thymidine-nocodazole block, and treated for the last 12 h with DMSO, dox /3-IAA or with 5-pH-IAA after release from nocodazole. 10 μ M EdU was added for the last 30 min of treatment. Quantification of the flow cytometry data is shown- mean + SD from n = 3 independent experiments (**G,H**). Cells were assigned to G1-phase based on DNA content of 2n and being EdU negative.

Figure 2: TIM depletion leads to a defect in chromatin loading of CLASPIN and delays PCNA recruitment during origin firing



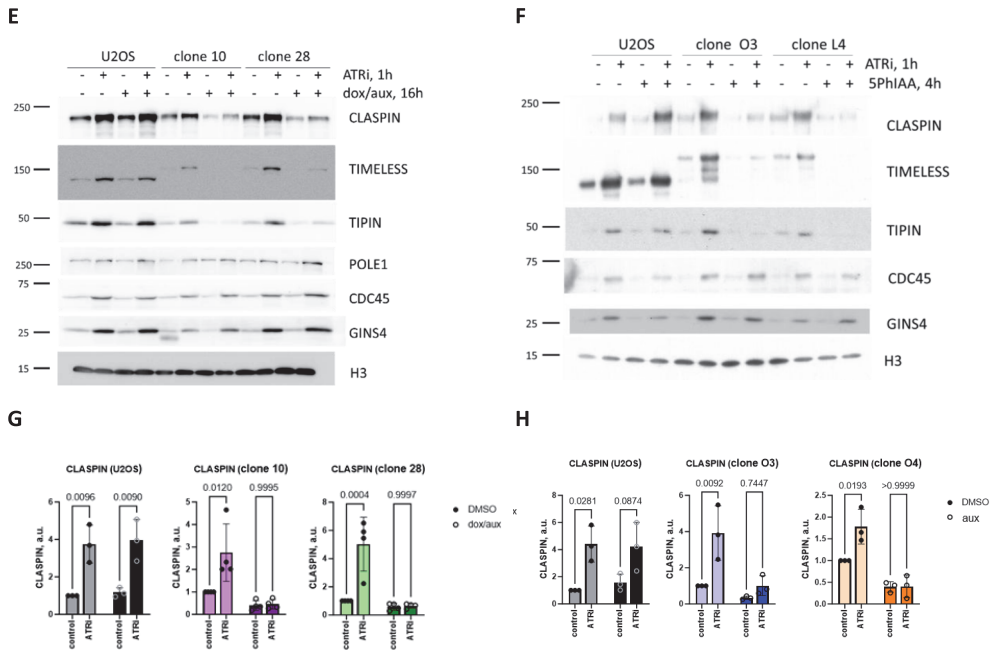


Figure 2: A-D. Wildtype U2OS, mAID1 clones Clone 10, Clone 28 or mAID2 clones Clone O3, Clone L4 were synchronized using the double thymidine- nocodazole block, and treated for the last 12 h with DMSO, dox /3-IAA or with 5-pH-IAA after release from nocodazole. Western blot analysis of the nuclease-insoluble chromatin fraction from the cells collected at the indicated timepoints is shown (A,B). Equal amounts of protein were loaded. D. Quantifications of protein loading from A,B are shown (C,D). Western blot signal intensities were quantified by ImageJ, and data were analyzed and plotted using GraphPad Prism 9. Mean + SD from 3 independent experiments is shown. **E-H.** Wildtype U2OS, mAID1 clones Clone 10, Clone 28 or mAID2 clones Clone O3, Clone L4 were treated for 16 h with doxycycline(2 ug/ml)/auxin 3-IAA, or auxin 5-pH-IAA, as indicated. 5 μ M ATRi was added to the indicated samples for 1 h, followed by cell lysis and the isolation of the insoluble chromatin fraction. Equal amounts of protein were loaded. Western blots of the insoluble chromatin fraction are shown (E,F). Quantifications of protein loading from E,F are shown (G,H). Western blot signal intensities were quantified by ImageJ, and data were analyzed and plotted using GraphPad Prism 9. Mean + SD from 3 independent experiments is shown.

Figure S2:

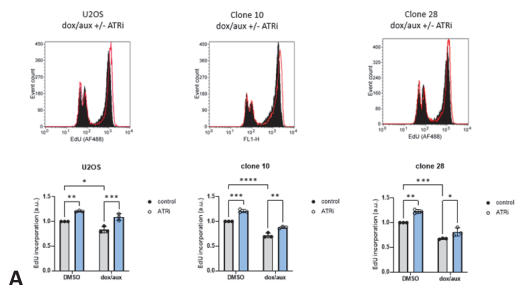
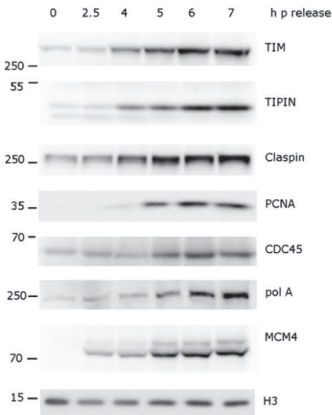


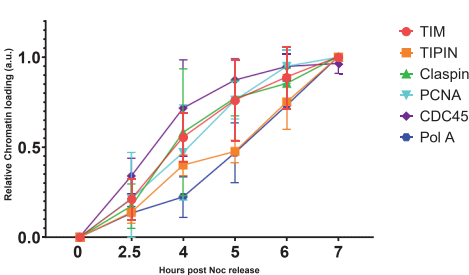
Figure S2: A. Wild-type U2OS, mAID1 clones Clone 10, Clone 28 or mAID2 clones Clone O3, Clone L4 were treated for 16 h with doxycycline(2 ug/ml)/auxin 3-IAA, or auxin 5-pH-IAA, as indicated. 5 μ M ATRi was added to the indicated samples for 1 h before harvest, and 10 μ M EdU was added for the last 30 min of treatment. Flow cytometry plots showing EdU incorporation histograms (c) and relative EdU incorporation, normalized to the samples without ATRi, are shown. Mean + SD from 3 independent experiments is shown.

Figure 3: TIM loading to chromatin during origin firing occurs in multiple steps, is dependent on CMG assembly and on DNA synthesis

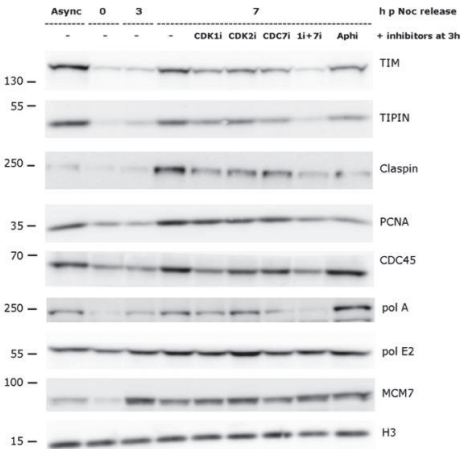
A



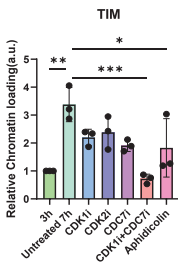
B



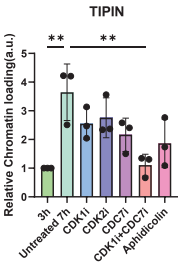
C



D



E



F

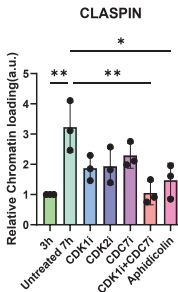


Figure 3: A-B. Wildtype U2OS cells were synchronised using the double thymidine- nocodazole. Samples were collected at the indicated timepoints post nocodazole release. Western blot analysis of the nuclease-insoluble chromatin fraction from the cells collected at the indicated timepoints is shown (A). Equal amounts of protein were loaded. Quantifications of protein loading from A are shown (B). Western blot signal intensities were quantified by ImageJ, and data were analyzed and plotted using GraphPad Prism 9. Mean + SD from 3 independent experiments is shown. **C-F.** Wildtype U2OS cells were synchronised using the double thymidine- nocodazole block. 3h post nocodazole release, the indicated inhibitors were added at 5 μ M. Samples were collected at the indicated timepoints post nocodazole release. Western blot analysis of the nuclease-insoluble chromatin fraction from the cells is shown (C). Equal amounts of protein were loaded. Quantifications of protein loading from C are shown (D-F). Western blot signal intensities were quantified by ImageJ, and data were analyzed and plotted using GraphPad Prism 9. Mean + SD from 3 independent experiments is shown.

Figure S3:

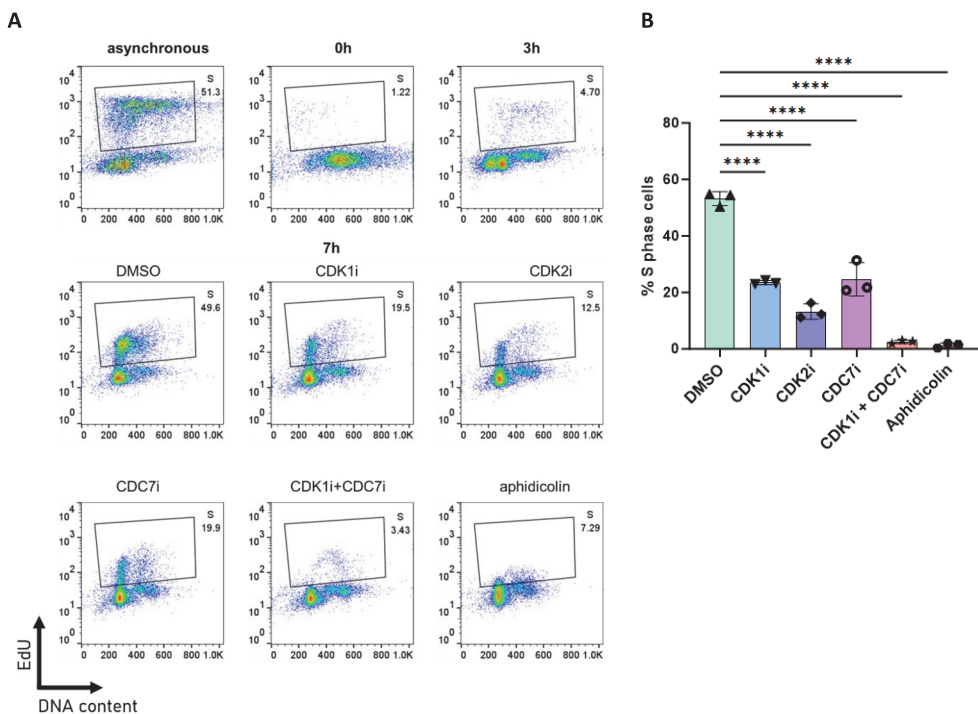
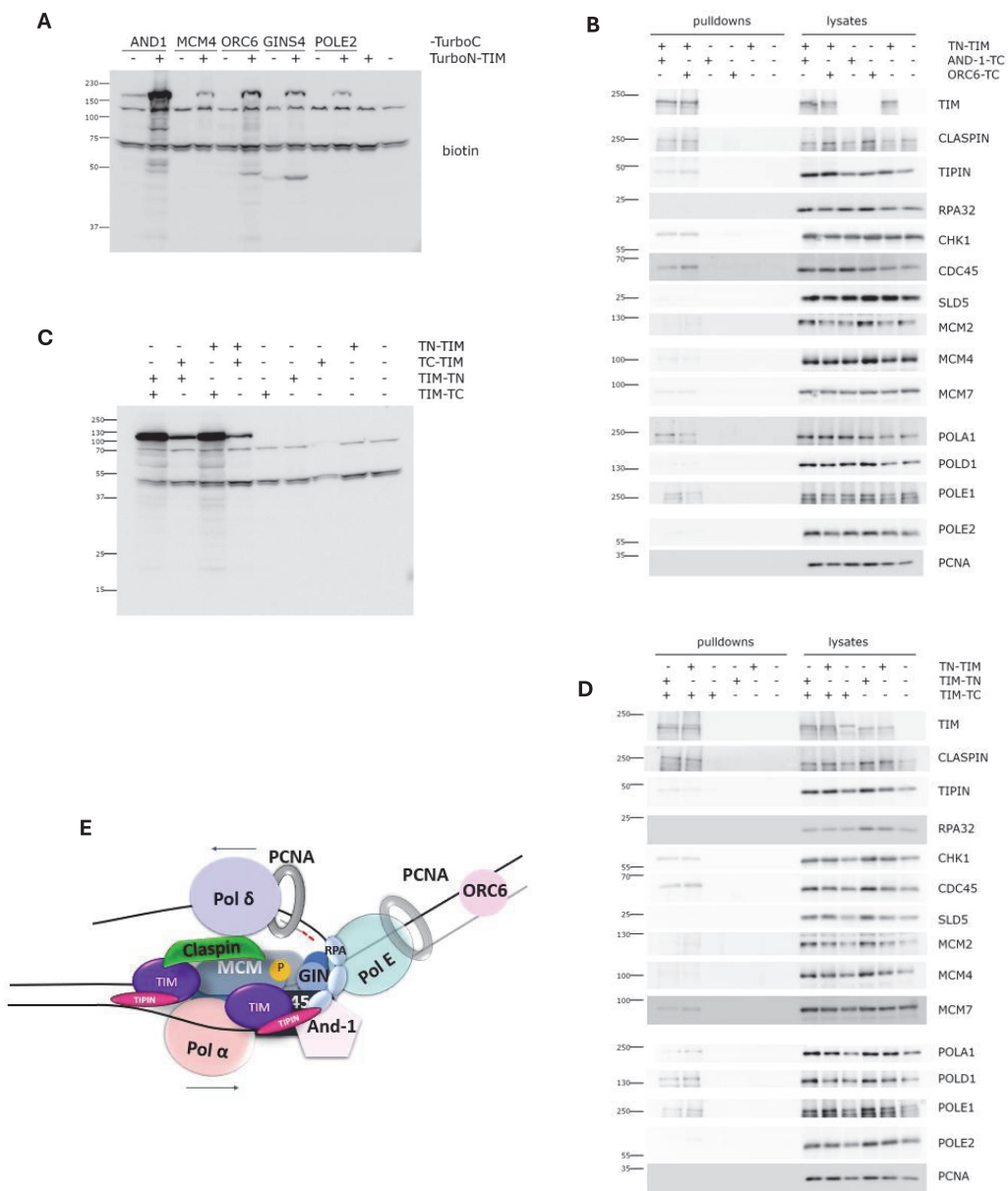


Figure S3. A-B. Wildtype U2OS cells were synchronised using the double thymidine- nocodazole block. 3h post nocodazole release, the indicated inhibitors were added at 5 μ M. Samples were collected at the indicated timepoints post nocodazole release. 10 μ M EdU was added for the last 30 min of treatment. Plots (A) and quantification (B) of the flow cytometry data is shown- mean + SD from n = 3 independent experiments. EdU+ cells were quantified based on EdU signal being above G1 and G2 levels. Cells were assigned to S-phase based on DNA content of higher than 2n and being EdU positive.

Figure 4: Proximity labelling enabled by TIM interaction with core initiation proteins indicates the presence of more than one molecule of TIM per fork



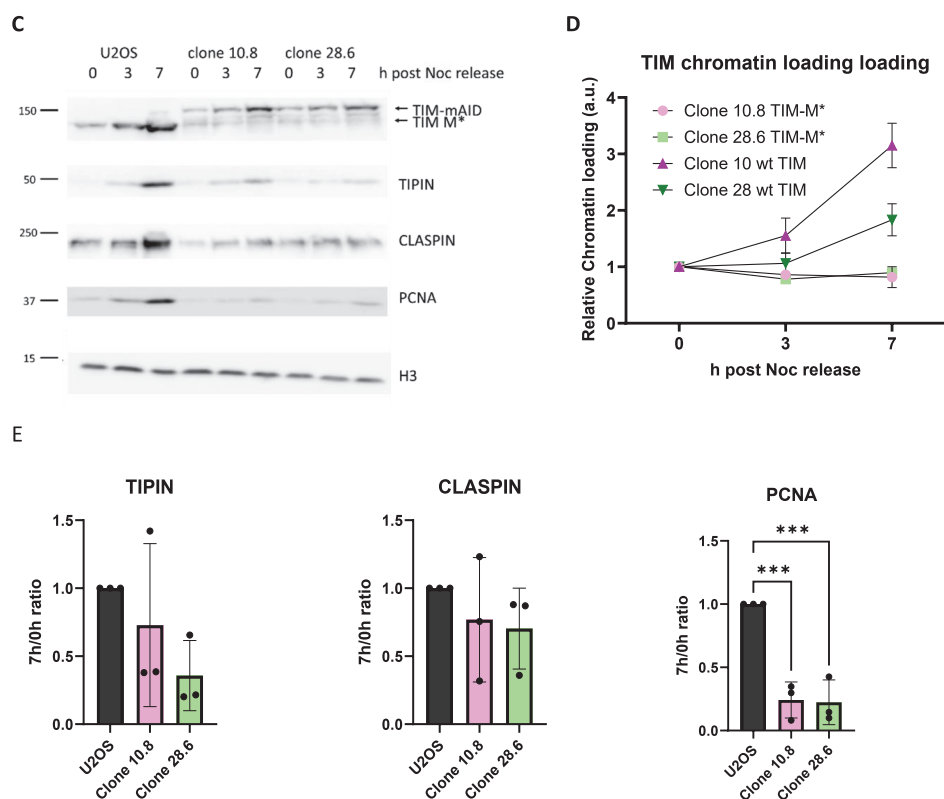
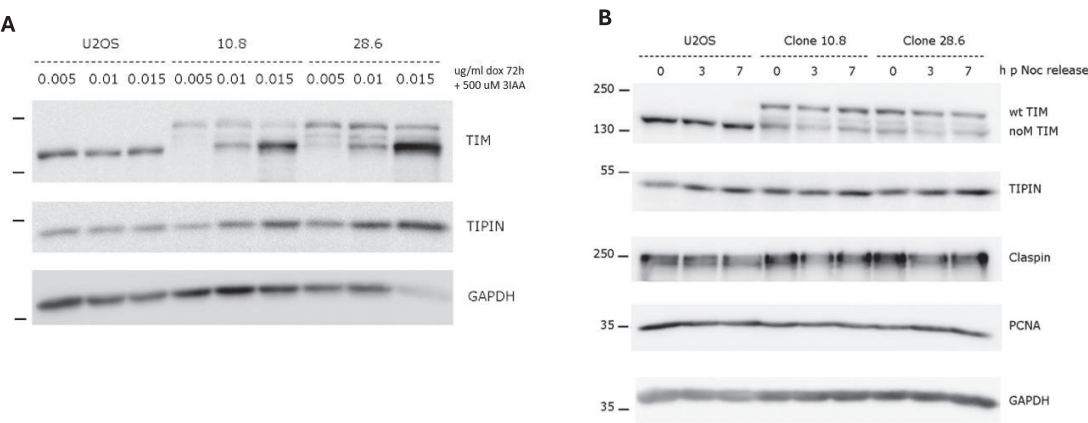


Figure 5: **A.** The deleted fragment in TIM-M* mutant designed based on the 3D structure 7PLO from PDB [11], and biochemical study [17] is shown. **B.** 293FT cells were transfected with an empty vector or the constructs shown, fused to FLAG tags at their N-termini. 48 h later cells were lysed, and FLAG-tagged proteins were immunoprecipitated using M2 agarose beads, followed by elution with FLAG peptide. Western blots of the eluted protein and input samples are shown (**B**). **C-E.** Wildtype U2OS, mAID1 clones Clone 10 and Clone 28, and TIM-M*-expressing clones Clone 10.8 and Clone 28.6 were synchronised using the double thymidine- nocodazole block and treated for the last 72 h with 0.01 ug/ml doxycycline and for the last 12 h with dox/3-IAA. Western blot analysis of the nuclease-insoluble chromatin fraction from the cells collected at the indicated timepoints is shown (**C**). Equal amounts of protein were loaded. Quantifications of indicated proteins loading from **C** are shown (**D,E**). Western blot signal intensities were quantified by ImageJ, and data were analyzed and plotted using GraphPad Prism 9. Mean + SD from 3 independent experiments is shown.

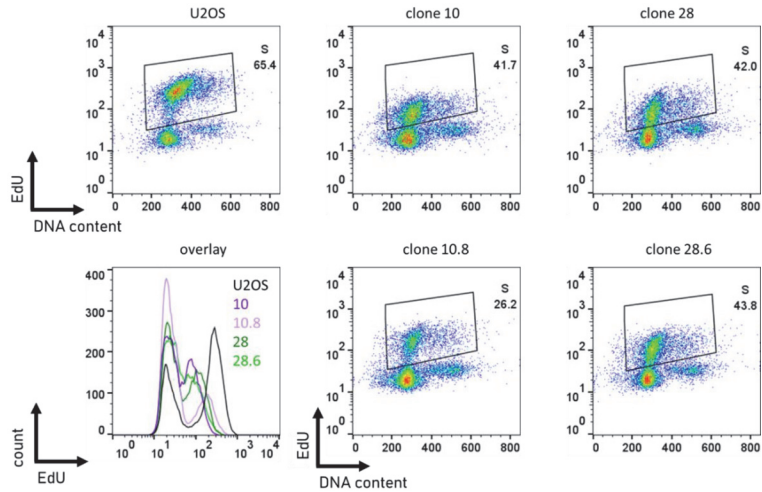
Figure S5:



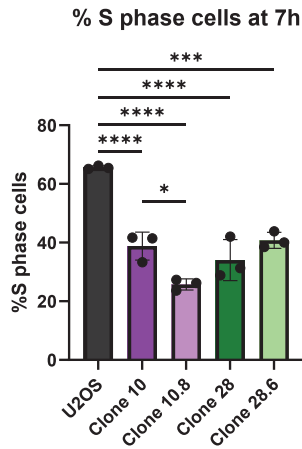
FigureS5: A. Wildtype U2OS, mAID1 clones Clone 10 and Clone 28, and TIM-M*-expressing clones Clone 10.8 and Clone 28.6 were treated for 72 h with the indicated concentrations of doxycycline and for the last 12 hours with 3-IAA. Western blots of total cell lysates are shown (A). Equal amounts of protein were loaded. **B.** Wildtype U2OS, mAID1 clones Clone 10 and Clone 28, and TIM-M*-expressing clones Clone 10.8 and Clone 28.6 were synchronised using the double thymidine- nocodazole block and treated for the last 72 h with 0.01 ug/ml doxycycline and for the last 12 h with dox/3-IAA. Western blot soluble fraction from the cells collected at the indicated timepoints is shown (B). Equal amounts of proteins were loaded.

Figure 6: TIM mutant unable to interact with MCM cannot rescue the initiation defect in TIM depleted cells

A



B



C

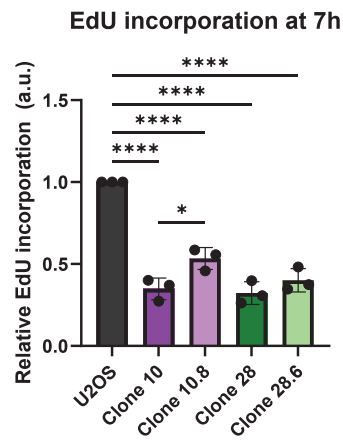
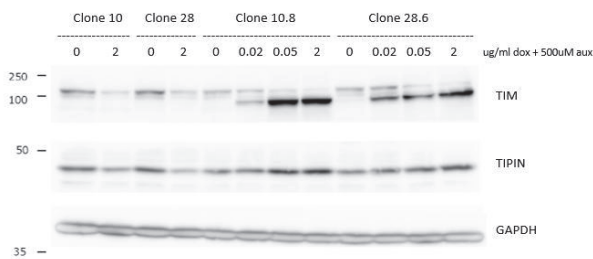


Figure 6. A-C. Wild-type U2OS, mAID1 clones Clone 10 and Clone 28, and TIM-M^{*}-expressing clones Clone 10.8 and Clone 28.6 were treated for the last 72 h with 2 ug/ml doxycycline and for the last 12 h with 3-IAA. 10 μ M EdU was added for the last 30 min of treatment. Flow cytometry plots and histograms showing EdU incorporation and DNA content (7-AAD staining) are shown (A). Quantifications of % S phase cells (B) and relative EdU incorporation (C), from A are shown with mean + SD plotted from n = 3 independent experiments. EdU+ cells were quantified based on EdU signal being above G1 and G2 levels. Cells were assigned to S-phase based on DNA content of higher than 2n and being EdU positive, and to G1-phase based on DNA content of 2n and being EdU negative.

Figure S6:

A



B

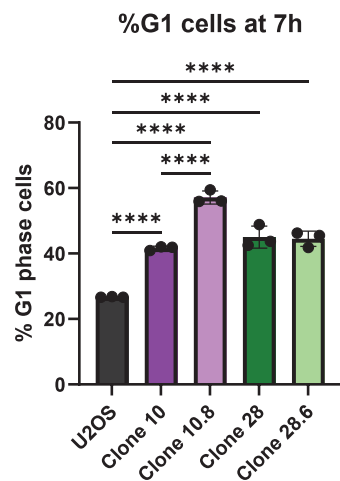
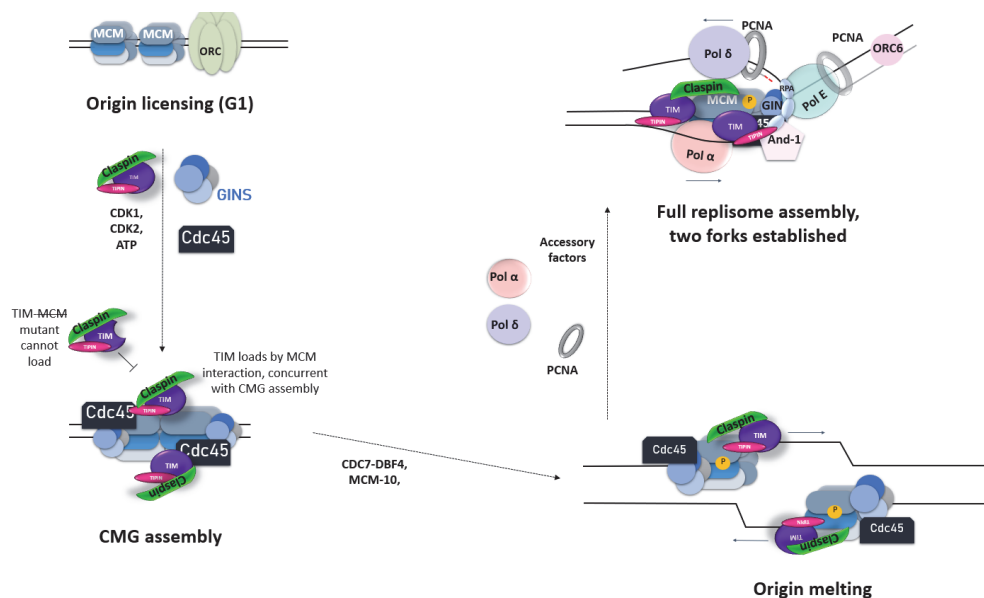


Figure S6: A. Wild-type U2OS, mAID1 clones Clone 10 and Clone 28, and TIM-M*-expressing clones Clone 10.8 and Clone 28.6 were treated for 16 h with the indicated concentrations of doxycycline and 3-IAA. Western blot analysis of the soluble fraction from the cells collected at the indicated timepoints is shown (A). Equal amounts of protein were loaded. **B.** Wild-type U2OS, mAID1 clones Clone 10 and Clone 28, and TIM-M*-expressing clones Clone 10.8 and Clone 28.6 were treated for the last 72 h with 2 ug/ml doxycycline and for the last 12 h with 3-IAA. 10 μ M EdU was added for the last 30 min of treatment. Flow cytometry plots showing G1-phase cells are shown (B) with mean + SD plotted from n = 3 independent experiments. Cells were assigned to G1-phase based on DNA content of 2n and being EdU negative.

Figure 7: Proposed model of TIM dynamics at the replication fork



Curriculum vitae

Personal data

Name: Sameera Anant Vipat
Date of birth: 25/12/1991
Place of birth: Pune, India
Email: sameera.vipat@gmail.com

Education

2021– Tallinn University of Technology, Estonia, PhD Gene Technology
2016–2018 University of California, Davis, USA, MS Microbiology
2012–2014 National Institute of Virology, India, MSc Virology
2009–2012 Abasaheb Garware College, under the aegis of Savitribai Phule
Pune University, India, BSc Microbiology

Conferences and presentations

2025 Tallinn University of Technology symposium: “Winter Seminar in Gene Sciences”, Jäeneda, Estonia, **oral presentation**
2024 EMBL Symposium: “DNA replication: from basic biology to disease”, EMBL Heidelberg, Germany, **poster presentation**

Supervision

2023–2024 **Artur Morgunov**, BSc, “Effect of TIMELESS protein overexpression on DNA replication in human cells”
2021 **Sigvard Vållo**, BSc, “Optimizing proximity labeling split-TurboID system to identify novel DNA replication initiation factors in human cells”

Publications

Sherry L. Haller, Chorong Park, Ryan C. Bruneau, Dewi Megawati, Chi Zhang, **Sameera Vipat**, Chen Peng, Tatiana G. Senkevich, Greg Brennan, Loubna Tazi, Stefan Rothenburg (2024). **Host species-specific activity of the poxvirus PKR inhibitors E3 and K3 mediate host range function.** Journal of Virology, vol. 98, no. 11, pp. e01331-24, Oct. 2024, doi: 10.1128/jvi.01331-24.

Sameera Vipat, Tatiana N. Moiseeva (2024). **The TIMELESS roles in genome stability and beyond.** Journal of Molecular Biology, vol. 436, no. 1, p. 168206, Jan. 2024, doi: 10.1016/j.jmb.2023.168206.

Sameera Vipat*, Dipika Gupta*, Sagun Jonchhe*, Hele Anderspuk, Eli Rothenberg & Tatiana N. Moiseeva (2022). **The non-catalytic role of DNA polymerase epsilon in replication initiation in human cells.** Nature Communications, vol. 13, no. 1, p. 7099, Nov. 2022, doi: 10.1038/s41467-022-34911-4.

Sameera Vipat*, Greg Brennan*, Chorong Park, Sherry L Haller, Stefan Rothenburg (2020). **Rapid, seamless generation of recombinant poxviruses using host range and visual selection.** Journal of Visualized Experiments, JoVE, no. 159, p. 10.3791/61049, May 2020, doi: 10.3791/61049.

*Contributed equally

Elulookirjeldus

Isikuandmed

Nimi: Sameera Anant Vipat
Sünniaeg: 25/12/1991
Sünnikoht: Pune, India
E-post: sameera.vipat@gmail.com

Hariduskäik

2021– Tallinna Tehnikaülikool, doktoriõpingud
2016–2018 Kalifornia Ülikool, Davis, USA, magistrikraad (mikrobioloogia)
2012–2014 India Rahvuslik Viroloogiainstituut, magistrikraad (viroloogia)
2009–2012 Abasaheb Garware Kolledž, Savitribai Phule Pune Ülikool, India, bakalaureusekraad (mikrobioloogia)

Konverentsid ja esinemised

2025 Tallinna Tehnikaülikooli sümpoosion: “Winter Seminar in Gene Sciences 2025”, **suuline ettekanne**
2024 EMBL sümpoosion: “DNA replication: from basic biology to disease”, EMBL Heidelberg, Saksamaa, **stendiettekanne**

Lõputööde juhendamine

2023–2024 **Artur Morgunov**, BSc, “TIMELESS valgu üleekspressiooni efekt DNA replikatsioonile inimrakkudes”
2021 **Sigvard Vållo**, BSc, “Proksimaalse märgistamise süsteemi split-TurboID kasutamine, et identifitseerida uusi DNA replikatsiooni initsiatsiooni faktoreid inimrakkudes”

Publikatsioonid

Sherry L. Haller, Chorong Park, Ryan C. Bruneau, Dewi Megawati, Chi Zhang, **Sameera Vipat**, Chen Peng, Tatiana G. Senkevich, Greg Brennan, Loubna Tazi, Stefan Rothenburg (2024). **Host species-specific activity of the poxvirus PKR inhibitors E3 and K3 mediate host range function**. Journal of Virology, vol. 98, no. 11, pp. e01331-24, Oct. 2024, doi: 10.1128/jvi.01331-24.

Sameera Vipat, Tatiana N. Moiseeva (2024). **The TIMELESS roles in genome stability and beyond**. Journal of Molecular Biology, vol. 436, no. 1, p. 168206, Jan. 2024, doi: 10.1016/j.jmb.2023.168206.

Sameera Vipat*, Dipika Gupta*, Sagun Jonchhe*, Hele Anderspuk, Eli Rothenberg & Tatiana N. Moiseeva (2022). **The non-catalytic role of DNA polymerase epsilon in replication initiation in human cells**. Nature Communications, vol. 13, no. 1, p. 7099, Nov. 2022, doi: 10.1038/s41467-022-34911-4.

Sameera Vipat*, Greg Brennan*, Chorong Park, Sherry L Haller, Stefan Rothenburg (2020). **Rapid, seamless generation of recombinant poxviruses using host range and visual selection**. Journal of Visualized Experiments, JoVE, no. 159, p. 10.3791/61049, May 2020, doi: 10.3791/61049.

* Panustasid võrdselt

ISSN 2585-6901 (PDF)
ISBN 978-9916-80-310-3 (PDF)